UNIVERSITÉ DE MONTRÉAL

MINING WASTEWATER TREATMENT BY SLAG FILTERS

DOMINIQUE CLAVEAU-MALLET

DÉPARTEMENT DES GÉNIES CIVIL, GÉOLOGIQUE ET DES MINES

ÉCOLE POLYTECHNIQUE DE MONTRÉAL

MÉMOIRE PRÉSENTÉ EN VUE DE L'OBTENTION

DU DIPLÔME DE MAÎTRISE ÈS SCIENCES APPLIQUÉES

(GÉNIE CIVIL)

JUIN 2012

© Dominique Claveau-Mallet, 2012.

UNIVERSITÉ DE MONTRÉAL

ÉCOLE POLYTECHNIQUE DE MONTRÉAL

Ce mémoire intitulé:

MINING WASTEWATER TREATMENT BY SLAG FILTERS

présenté par : CLAVEAU-MALLET Dominique

en vue de l'obtention du diplôme de : Maîtrise ès sciences appliquées

a été dûment accepté par le jury d'examen constitué de :

M. COURCELLES Benoît, Ph. D., président

M. COMEAU Yves, Ph. D., membre et directeur de recherche

M. WALLACE Scott, Ph. D., membre et codirecteur de recherche

Mme POTVIN Estelle, Ph. D., membre

ACKNOWLEDGEMENTS

Thank you to my director Yves Comeau for his trust in me and his constant presence.

Thank you to laboratory technicians who helped me in this project: Denis Bouchard for technical support and phosphorus analysis, Manon Leduc for metals analysis, Marie Ferland for fluoride analysis and preparation of feeding solutions, Yvéric Rousseau for the preparation of figures 4.2, 4.4 and 4.7 and Jean-Philippe Massé for the X-ray diffraction analysis support and for transmission electronic microscopy analysis.

Thank you to my codirector Scott Wallace, from Naturally Wallace Consulting, for his presence all along the project and for his precious advices. Thank you to professionals from Shaw Environmental, who realized the preliminary feasibility study related to this project, especially to Ernie Stine, who provided a preliminary list of slag suppliers. Thank you to all slag suppliers who sent samples. Thank you to Judy Lissick, from Naturally Wallace Consulting, for her technical support in the slag samples shipment.

Thank you to Aurore Bordier, intern at École Polytechnique during the summer and fall 2011, who sampled and took care of my experiments during my maternity leave.

A special thank you to professor Kalle Kirsimäe, to Riho Mõtlep and Martin Liira, from the Department of Geology from the University of Tartu, Estonia, for the oxide composition analysis of slag.

Thank you to the Natural Sciences and Engineering Research Council of Canada, to the *Fonds québécois de recherche sur la nature et les technologies*, to Naturally Wallace Consulting, to the *Société de recherche en aquaculture continentale*, to the *Réseau aquaculture Québec*, to Arcelor Mittal and to Harsco Materials for the funding of this project.

Thank you to Mathieu Bélisle for the exceptional support that enabled me to realize this project, and to my baby Rosanne who was nice when I was writing my master thesis.

RÉSUMÉ

Les deux objectifs de ce projet étaient de proposer un système de traitement par filtres à scories du lixiviat de la mine Joplin, Missouri et de proposer un modèle préliminaire des mécanismes de rétention du phosphore dans les filtres à scories. Trois phases expérimentales ont été réalisées : essais individuels en flacon, essais séquentiels en flacon et essais en colonnes. Les essais individuels en flacon ont été utilisés pour comparer la performance de traitement de 10 scories et 1 apatite et pour choisir les meilleurs matériaux parmi ceux-ci. Les essais séquentiels en flacon ont été utilisés pour comparer les performances de traitement de quelques séquences de filtres. Finalement, les essais en colonnes ont été utilisés pour caractériser la performance d'enlèvement et la longévité d'un filtre soumis à des conditions d'alimentation contrôlées. Durant les essais en colonnes, l'effet de la composition de l'affluent, du temps de rétention hydraulique des vides et de la séquence de filtre a été mesuré. Certains essais en colonnes ont été opérés spécifiquement pour étudier les mécanismes d'enlèvement du phosphore.

Le modèle proposé est défini par les étapes suivantes : 1) la dissolution cinétique des scories est représentée par la dissolution de CaO, 2) un fort pH dans le filtre cause la précipitation du phosphore et la croissance de cristaux, 3) la rétention des cristaux est causée par filtration, décantation et densification, 4) la diminution du volume de réaction (et du temps de réaction) disponible est causée par l'accumulation de cristaux et autres particules dans les vides, 5) le pH dans le filtre diminue avec le temps si le temps de réaction est trop court (ce qui résulte en une diminution de l'efficacité d'enlèvement). Une nouvelle approche pour définir les performances des filtres à scories est proposée. La capacité de rétention à saturation est exprimée en mg P / mL de vides.

Le système proposé pour traiter le lixiviat de la mine Joplin est composé de deux filtres successifs de scories EAF Fort Smith opérés à un temps de rétention hydraulique des vides total de 34 h. Après 179 jours d'opération, les performances de traitement des deux filtres ont été de 99.9 %, 85.3 %, 98.0 % et 99.3 % pour le phosphore, le fluor, le manganèse et le zinc, respectivement.

ABSTRACT

The two objectives of this project were to propose a slag filters treatment system for the leachate of the Joplin mine, Missouri, and propose a preliminary model for phosphorus removal mechanisms in slag filters. Three experimental phases were realized: individual batch tests, sequential batch tests and column tests. Individual batch tests were used to compare the treatment performance of 10 slags and 1 apatite and to select the best materials from this list. Sequential batch tests were used to compare the treatment performance of several filter sequences. Finally, column tests were used to characterize the removal performance and longevity of controlled filters. During column tests, the effect of influent composition, void hydraulic retention time and filter sequences was measured. Some column tests were operated especially for the study of phosphorus removal mechanisms.

The proposed model is expressed by the following steps: 1) the rate limiting dissolution of slag is represented by the dissolution of CaO, 2) a high pH in the slag filter results in phosphorus precipitation and crystal growth, 3) crystal retention takes place by filtration, settling and growth densification, 4) the decrease in available reaction volume is caused by crystal and other particulate matter accumulation (and an associated decrease in available reaction time), and 5) the pH decreases in the filter over time if the reaction time is too short (which results in a reduced removal efficiency). A new approach to define filter performance is proposed. Saturation retention capacity is expressed in units of mg P/ mL voids.

The proposed system for the treatment of the Joplin mine leachate is composed of two successive Fort Smith EAF slag filters operated at a total void hydraulic retention time of 34 hours. After 179 days of operation, the treatment performance of this system was 99.9 %, 85.3 %, 98.0 % et 99.3 % for phosphorus, fluoride, manganese and zinc respectively.

CONDENSÉ EN FRANÇAIS

Les sites miniers abandonnés ont des impacts significatifs sur l'environnement. La dégradation des paysages s'ajoute à la pollution directe des cours d'eau avoisinants par les lixiviats miniers. Dans ce projet, on s'intéresse à une mine de gypse abandonnée située à Joplin, au Missouri. De fortes concentrations de plusieurs contaminants (phosphore, fluor et métaux) étaient présentes dans le cours d'eau récepteur. Ce site a été restauré par la mise en place d'une station d'épuration chimique, qui est toujours en opération. Le lixiviat minier est collecté et traité à la chaux pour précipiter les contaminants. Cependant, ce système ne répond plus aux exigences de rejet les plus récentes. Le Gouvernement du Missouri a décidé d'investir dans une nouvelle technologie de traitement qui serait économique et plus efficace que le système actuel. Dans une analyse préliminaire, les filtres à scories d'aciérie, qui sont un résidu de production de l'industrie de l'acier, ont été choisis pour répondre à ce défi. L'École Polytechnique a été mandatée via ce projet de maîtrise pour mettre en œuvre la première partie du projet de mise à niveau.

Objectif 1 : Proposer, à partir d'essais en laboratoire, un filtre à scories pour le traitement du lixiviat minier Joplin. Le système proposé doit être économique et répondre aux nouvelles exigences de rejet.

Une deuxième problématique a été abordée. Le traitement du phosphore par les filtres à scories est bien connu, mais les performances sont variables d'une étude à l'autre. À ce jour, il n'existe pas d'outils de prédiction de performance pour les filtres à scories. Une compréhension globale et une conceptualisation des phénomènes impliqués dans les filtres à scories sont nécessaires pour développer de tels outils de prédiction.

Objectif 2 : Proposer un modèle préliminaire des mécanismes d'enlèvement du phosphore dans les filtres à scories.

Le programme expérimental a comporté trois phases : les essais individuels en flacon, les essais séquentiels en flacon et les essais en colonnes. Trois eaux minières synthétiques, représentant les concentrations minimales, moyennes et maximales retrouvées sur le site, ont été reconstituées au laboratoire à partir de sels chimiques. Dix types de scories (neuf en provenance des États-Unis et une en provenance du Québec) et un type d'apatite (en provenance de la Floride) ont été testés.

Les essais individuels en flacon sont des essais comparatifs utilisés pour dresser une liste de scories par potentiel de traitement. 35 g de scories ont été mis en contact dans 700 mL d'eau usée, puis mis en rotation à 170 rpm et 20°C pour une durée de 2 jours. La concentration résiduelle des contaminants a été mesurée après 24 h et 48 h. Les essais ont été réalisés en duplicatas dans deux types d'eau (concentration minimale et concentration maximale).

Un essai séquentiel en flacon est une version modifiée de l'essai individuel. Après 24 h de réaction avec un premier type de scorie, la solution est filtrée à 0,45 microns puis mise en contact avec 35 g d'un deuxième type de scorie pour 24 h supplémentaires. La concentration des contaminants est mesurée après chaque tranche de 24 h. Les résultats des séquences sont ensuite comparés avec ceux des essais individuels. Seules les scories sélectionnées à partir de l'étape précédente sont testées en duplicata. Les essais sont réalisés dans un seul type d'eau (concentration maximale).

La configuration des essais en colonnes est déterminée sur la base des résultats des deux étapes précédentes. Neuf essais sont réalisés avec des paramètres variables (séquence de filtres, type de scorie et débit d'alimentation). Trois types de scories sont testés (les scories EAF de Blytheville, EAF de Contrecoeur et EAF de Fort Smith). Différents temps de rétention hydraulique sont testés (1.5 h à 19 h). Les séquences testées sont : scories Contrecoeur seules, scories Fort Smith seules, scories Blytheville seules et scories Fort Smith suivies de scories Blytheville. Les colonnes étaient faites de plastique PVC transparent et avaient une longueur de 17 cm et un diamètre de 15 cm. L'effluent des colonnes a été échantillonné deux fois par semaine pour le suivi des paramètres (pH, Ca, P, Mn, Zn, Al, F). Les essais en colonnes ont duré de 30 à 630 jours, la plupart d'entre eux ayant duré de 150 à 200 jours. Les précipités formés dans les colonnes ont été échantillonnés à la fin des essais et caractérisés par diffraction aux rayons X (détermination de la composition et de la taille) et par microscope électronique à transmission (étude de la forme et de l'organisation des précipités). Des essais de toxicité ont été réalisés sur les scories utilisées dans les essais en colonnes.

Les résultats des essais individuels en flacon ont indiqué que trois scories se sont démarquées pour leur capacité à monter le pH et à traiter le phosphore (scories BOF d'Indiana Harbor East, scories EAF de Fort Smith, scories BOF de Cleveland). Les scories EAF de Blytheville ont été les plus efficaces pour traiter le fluor, mais leur efficacité a diminué lorsque

l'eau à traiter était trop concentrée (faible capacité à monter le pH des scories). Cette observation a déterminé le choix des séquences à tester lors des essais séquentiels en flacon. Peut-on augmenter la capacité de traitement du fluor des scories EAF Blytheville par un filtre préliminaire de scories à forte capacité de hausse du pH?

Les résultats des essais séquentiels en flacon ont indiqué que la séquence Fort Smith – Blytheville a permis d'augmenter la capacité de traitement globale de la chaîne de traitement. On a observé d'abord une forte montée du pH, ensuite un bon traitement de tous les contaminants, en particulier le fluor. Les scories EAF de Fort Smith et EAF de Blytheville ont été sélectionnées pour les essais en colonnes. Les scories BOF Cleveland étaient trop friables et les scories BOF d'Indiana Harbor East étaient moins efficaces que les scories EAF de Fort Smith. Les scories EAF de Contrecoeur ont été testées en colonnes pour étudier les mécanismes d'enlèvement du phosphore parce que leur comportement avait été bien caractérisé lors d'études antérieures à Polytechnique. Les essais de toxicité réalisés sur ces trois scories ont montré qu'elles étaient sécuritaires pour l'environnement parce que leur relargage dans l'eau distillée résultait en des concentrations en dessous des seuils de performance cibles pour une variété de contaminants (cuivre, fer, plomb, nickel, zinc).

Un modèle préliminaire des mécanismes d'enlèvement du phosphore a été proposé. Il est défini par les étapes suivantes : 1) la dissolution cinétique des scories est représentée par la dissolution de CaO, 2) un fort pH dans le filtre cause la précipitation du phosphore et la croissance de cristaux, 3) la rétention des cristaux est causée par filtration, décantation et densification, 4) la diminution du volume de réaction (et du temps de réaction) disponible est causée par l'accumulation de cristaux et autres particules dans les vides, 5) le pH dans le filtre diminue avec le temps si le temps de réaction est trop court (ce qui résulte en une diminution de l'efficacité d'enlèvement). L'organisation des cristaux dans un filtre à scories détermine sa capacité de rétention du phosphore. Une organisation compacte des cristaux augmente la capacité de rétention du filtre. Une nouvelle approche pour définir les performances des filtres à scories est proposée. La capacité de rétention à saturation est exprimée en mg P / mL de vides.

Les résultats des essais en colonnes applicables à la mine Joplin ont indiqué que la meilleure performance de traitement a été obtenue par deux filtres successifs composés de scories EAF Blytheville. Ce système a atteint des abattements de 98.8 %, 94.8 %, 94.4 % et 98.6 % pour

le phosphore, le fluor, le manganèse et le zinc, respectivement, après 169 jours d'opération. Cependant, l'efficacité du premier filtre a diminué après 30 jours d'opération, limitant son utilisation à long terme. Le système composé de deux filtres successifs Fort Smith a été moins efficace pour le traitement du fluor, mais la capacité maximale de traitement du premier filtre a été conservée durant 70 jours. Après 179 jours d'opération, les performances de traitement des deux filtres ont été de 99.9 %, 85.3 %, 98.0 % et 99.3 % pour le phosphore, le fluor, le manganèse et le zinc respectivement. Ainsi, le système recommandé est composé de deux filtres successifs de scories EAF Fort Smith opérés à un temps de rétention hydraulique des vides total de 34 h.

Un fort lien entre le pH de l'effluent et la concentration en phosphore a été observé. La composition de l'eau usée a eu une influence sur l'enlèvement du fluor. L'abattement moyen à pleine capacité a été de 10% en eau faiblement concentrée et de 85% en eau fortement concentrée dans les filtres Fort Smith. L'enlèvement du fluor est augmenté lorsque le ratio fluor/phosphore est bas, favorisant la précipitation de fluoroapatite. L'efficacité d'enlèvement des métaux était liée au pH de façon semblable au phosphore. L'abattement moyen à pleine capacité des scories Blytheville et Fort Smith était de 75% pour le manganèse et supérieur à 90% pour le zinc. Le manganèse n'était pas traité si le pH était plus bas que 6.

La comparaison des résultats avec les exigences de rejets a indiqué que le système retenu ne répond pas à la cible de rejet visée en phosphore total. En effet, la concentration de phosphore à l'effluent du système en pleine capacité se situe en moyenne entre 0.01 et 0.1 mg P/L alors que la cible était de 0.0005 mg P/L. Cependant, l'efficacité de traitement des filtres à scories est comparable à celle de technologies complexes et coûteuses, par exemple les membranes. Considérant la simplicité économique des filtres à scories, leur performance d'enlèvement du phosphore pourrait être acceptée. La cible de performance du fluor n'a pas été atteinte. L'exigence de rejet était de 2 µg/L tandis que la concentration à l'effluent des filtres se situait entre 2 et 7 mg/L. Cependant, de telles concentrations sont très basses si on les compare à des effluents traités d'autres types d'eaux usées contenant du fluor. Elles sont du même ordre de grandeur que la recommandation du Canada pour le fluor dans l'eau potable. De plus, l'enlèvement du fluor était considéré comme un objectif secondaire, la priorité étant le traitement du phosphore. Considérant les circonstances précédentes, les performances de traitement du fluor des filtres à scories semblent acceptables puisque 99,9% du phosphore et 85,3% du fluor ont été

abattu, respectivement. Les exigences de rejet pour l'enlèvement des métaux étudiés ont été atteintes. La concentration à l'effluent du système proposé était de 0,2 à 1 mg/L d'aluminium et de 0,01 à 0,03 mg/L de zinc. Les exigences de rejet étaient de 187 mg/L pour l'aluminium et de 0,042 mg/L pour le zinc.

La croissance de cristaux dans les filtres a été étudiée avec la détermination de la taille des cristaux. Une interprétation qualitative des taux de croissance d'apatite dans les filtres amont a indiqué que ceux-ci sont dépendants de la composition de l'eau usée. Plus la concentration en phosphore est élevée, plus le taux de croissance est rapide. Les courbes taille de cristaux – temps se développaient en forme d'éventail. Cette observation suggère que de nouveaux cristaux sont continuellement formés pendant que les cristaux déjà en place continuent de croître, résultant en une distribution de tailles de cristaux, les noyaux les plus vieux étant les plus gros. La composition d'hydroxyapatite des cristaux a été observée très tôt. L'hydroxyapatite était la principale phase minéralogique après 30 jours. Ainsi, les phosphates de calcium précurseurs à l'hydroxyapatite, qui sont soit des solides amorphes ou des phases minéralogiques instables, ont été assez rapidement transformés en hydroxyapatite.

La formation de calcite a été observée dans les filtres alimentés avec de l'eau usée contenant du carbone inorganique. La formation de calcite est compétitive à la formation d'hydroxyapatite. Les cristaux de calcite étaient systématiquement plus gros que les cristaux d'hydroxyapatite. La calcite occupe de l'espace qui n'est plus disponible pour la formation et la croissance d'hydroxyapatite. L'augmentation du temps de rétention hydraulique des vides a favorisé la précipitation de calcite, ce qui souligne l'importance de l'optimisation du temps de rétention hydraulique. Un long temps de rétention hydraulique favorise la précipitation compacte et augmente la capacité de rétention de cristaux, mais la proportion de calcite dans les cristaux est plus grande. La présence de calcite dans les interstices est également favorisée par le contact direct du filtre avec l'atmosphère.

L'utilisation de filtres à scories EAF Fort Smith est recommandée pour le traitement du lixiviat minier à Joplin. Les résultats de cette étude indiquent que deux filtres successifs Fort Smith ayant un temps de rétention hydraulique total de 34 heures ont été très efficaces durant au moins 172 jours. La longévité du système peut être augmentée en ajoutant des filtres successifs. L'utilisation des scories EAF Blytheville n'est pas recommandée parce que sa longévité est trop

courte, même si sa capacité de traitement du fluor est plus grande que celle des scories Fort Smith. En prévision de futurs essais en colonnes et pilote à la mine, certaines recommandations additionnelles ont été formulées : l'utilisation d'un lixiviat minier réel, la réalisation d'essais en colonnes en réplicata, l'utilisation de scories provenant de différentes piles de production, le suivi de tous les métaux incluant les métaux lourds, l'utilisation de mélanges de scories Fort Smith avec une petite quantité de scories Blytheville et l'optimisation du temps de rétention hydraulique et de la longévité par rapport aux coûts d'installation et de remplacement.

Des recommandations pour améliorer le modèle des mécanismes d'enlèvement du phosphore dans les filtres à scories ont été formulées. La caractérisation précise de la cinétique de dissolution des scories est nécessaire, tout comme une étude approfondie des caractéristiques des cristaux, incluant leur forme, leur organisation, ainsi que les phénomènes de nucléation et croissance. Le modèle doit être complété par des notions de perméabilité et de diffusion dans les médias granulaires. Tous les phénomènes impliqués dans les filtres à scories doivent être réunis dans un modèle numérique qui permette de prédire les performances des filtres.

TABLE OF CONTENTS

AKNOWLEDGEMENTS III

RÉSUMÉ IV

ABSTRACT V

CONDENSÉ EN FRANÇAIS VI

TABLE OF CONTENTS XII

LIST OF TABLES XV

LIST OF FIGURES XVI

ACRONYMS AND SYMBOLS XIX

LIST OF APPENCIDES XX

INTRODUCTION 1

CHAPTER 1 LITERATURE REVIEW 4

1.1 The mining leachate treatment challenge 4

1.2 What is slag ? 5

1.3 Wastewater treatment by slag 5

1.3.1 Phosphorus treatment 6

1.3.2 Fluoride and metals treatment 7

1.4 Phosphorus removal mechanisms in slag filters and proposed models 8

1.4.1 Models based on chemical equilibria 10

1.4.2 Models based on chemical kinetics 11

1.4.3 Summary of prediction tools for slag processes 13

CHAPTER 2 MATERIALS AND METHODS 14

2.1 Reconstituted wastewater and tested media 14

2.2 Individual batch tests 17

2.3 Sequential batch tests 18
2.4 Column tests 19
2.4.1 Experimental setup 19
2.4.2 Experimental protocol 20
2.5 Analytical determinations 21
2.5.1 Water samples 21
2.5.2 Crystal samples 22
2.6 Toxicity tests 22
CHAPTER 3 RESULTS 23
3.1 Individual batch tests 23
3.2 Sequential batch tests 24
3.3 Column tests 25
3.3.1 Column set 1 25
3.3.2 Column set 2 28
3.3.3 Precipitate characterization 29
3.4 Toxicity tests 32
CHAPTER 4 MODEL OF PHOSPHORUS PRECIPITATION AND CRYSTAL FORMATION IN ELECTRIC ARC FURNACE STEEL SLAG FILTERS (ARTICLE) 34
4.1 Introduction 34
4.2 Materials and methods 36
4.2.1 Reactive media and reconstituted effluent 36
4.2.2 Column tests 36
4.2.3 Analytical determinations 37
4.3 Results 37
4.4 Discussion 41

4.4.1 Slag dissolution and role of pH 41

4.4.2 Water velocity and crystal behavior in the filter 42

4.4.3 Proposed conceptual model 44

4.4.4 Parameters that influence crystal accumulation and organization 46

4.4.5 A new approach for the expression of phosphorus retention capacity 47

4.4.6 Practical recommendations 48

CHAPTER 5 TREATMENT PERFORMANCE OF SLAG FILTERS 50

5.1 Selection of media and treatment sequences 50

5.2 Efficiency and longevity of filters 51

5.2.1 Phosphorus removal 52

5.2.2 Fluoride removal 54

5.2.3 Metals removal 57

5.2.4 Performance goals 57

5.2.5 Crystal growth 58

CONCLUSION AND RECOMMENDATIONS 63

REFERENCES 68

APPENDICES 73

LIST OF TABLES

Table 1.1 : Comparison of prediction tools efficiency for different treatment slag processes 13

Table 2.1 : Average composition of the reconstituted effluents 15

Table 2.2 : Tested slags and apatites 16

Table 2.3 : Chemical composition of tested slags 17

Table 2.4 : Mineralogical composition of slags 17

Table 2.5 : Summary of column tests parameters 20

Table 2.6 : Joplin performance goals, acceptable effluent limits and maximum TCLP concentrations for a non toxic media (Environmental Health and Satefy Online, 2008) 22

Table 3.1 : Qualitative comparison of individual batch tests using WW 1. Significant observations are highlighted.....23

Table 3.2 : Qualitative comparison of individual batch tests using WW 3. Significant observations are highlighted.....23

Table 3.3 : Qualitative comparison of sequential batch tests 25

Table 3.4 : Precipitate sampling and characterization.....30

Table 5.1 : Contaminant retention for Joplin column tests 51

Table A.1: Individual batch tests results (tests in WW 1).....73

Table A.2: Individual batch tests results (tests in WW 1).....74

Table A.3: Individual batch tests results (tests in WW 3).....75

Table A.4: Individual batch tests results (tests in WW 3).....76

LIST OF FIGURES

Figure 2.1 : Origin of tested materials. (map: http://litlink.ket.org/stations/stationshome.aspl)....16

Figure 2.2 : Individual batch tests experimental setup....18

Figure 2.3 : Sequential batch tests experimental setup....18

Figure 2.4 : Column tests experimental setup....19

Figure 2.5 : Example of a 3-liter column filled with slag. 20

Figure 3.1 : Sequential batch tests results 24

Figure 3.2 : pH monitoring of column effluents, set 1....25

Figure 3.3 : Calcium monitoring of column effluents, set 1 26

Figure 3.4: ortho-phosphates monitoring of column effluents, set 1 26

Figure 3.5: Fluoride monitoring of column effluents, set 1 27

Figure 3.6: Manganese monitoring of column effluents, set 1....27

Figure 3.7: Zinc monitoring of column effluents, set 1 28

Figure 3.8: Aluminum monitoring of column effluents, set 1 28

Figure 3.9 : pH and calcium monitoring of column effluents, set 2 28

Figure 3.10 : ortho-phosphates and fluoride monitoring of column effluents, set 2....29

Figure 3.11 : Manganese and zinc monitoring of column effluents, set 2 29

Figure 3.12 : Theoretical diffractograms of HAP and calcite 31

Figure 3.13 : Comparison of HAP / calcite proportions in XRD diffractograms based on intensity of two characteristic peaks. No calcite visible and HAP predominant (A); HAP predominant and calcite present (B); calcite predominant and HAP present (C) 31

Figure 3.14 : Results of toxicity tests in distilled water for major compounds (A), iron (B) and trace compounds (C) 32

Figure 3.15 : Results of toxicity tests in acetic acid for trace compounds (A), major compounds (B) and calcium (C)....32

Figure 4.1 : Relationship between effluent pH and normalized effluent o-PO_4 (influent [o-PO_4] = 26 ± 2 mg P/L) 38

Figure 4.2 : Phosphorus removal efficiency at different HRTV expressed in traditional mg P / g slag (A) and newly proposed mg P / mL voids (B). The duration of the experiment is indicated besides the last data point presented.....39

Figure 4.3 : Progression of the precipitate bed within the HRT_V = 16.3 h column. The position of the reaction front was determined visually 40

Figure 4.4 : Photo of white crystals (>95% apatite confirmed by X-ray diffraction) formed on cavity wall (A); TEM photo of apatite crystal aggregate (B); TEM photo of acicular apatite crystals (C); TEM photo of a crystal seed with fibrous aspect (D).....40

Figure 4.5 : Effect of water velocity on phosphorus retention capacity 42

Figure 4.6 : Crystal growth observed in filters (three data points for three different filters). Mean crystal size was determined by XRD and V_w stands for water velocity 43

Figure 4.7 : Conceptual representation of a compact (left) and a loose (right) crystal organization in a slag filter. The mass of apatite crystals in the filter is considered identical in both filters 45

Figure 5.1 : Column tests experimental setup.....52

Figure 5.2 (suite): Relationship between effluent o-PO_4 concentration and pH ([A] in logarithm scale, [B] in arithmetic scale).....54

Figure 5.3 : Relationship between fluoride and pH in column effluent.....55

Figure 5.4 : Effluent concentrations of an efficient slag filter (two successive Fort Smith EAF slag filters operated at total HRT_V of 34 h) compared with Joplin project performance goals, actual effluent concentrations of the lime treatment plant and selected regulations.....58

Figure 5.5 : Relationship between calcium and pH at columns' effluent. Ca, inlet refers to the initial concentration in WW (WW 1, 2 or 3). Ca, outlet refers to the concentration at each column's effluent.....59

Figure 5.6 : Hydroxyapatite growth in upstream filters.....60

Figure 5.7 : Comparison of HAP and calcite crystal sizes. For each point, sizes are computed from the same diffractogram. The height of the sample in the column is given at the right of each point (cm) 62

Figure B.1 : Phosphorus retention capacities of upstream filters (set 1 only) 77

Figure B.2 : Fluoride retention capacities of upstream filters 77

Figure B.3 : Manganese retention capacities of upstream filters 78

Figure B.4 : Zinc retention capacities of upstream filters 78

Figure B.5 : Aluminum retention capacities of upstream filters 79

ACRONYMS AND SYMBOLS

Acronyms:

ANC curves	Acid neutralizing capacity curves
ASTM	American Society for Testing and Materials
EAF	Electric arc furnace
FAP	Fluoroapatite
HAP	Hydroxyapatite
HRT_V	Void hydraulic retention time
MDDEP	Ministère du développement durable, de l'environnement et des parcs du Québec
NSA	National Slag Association
TCLP	Toxicity characteristic leaching procedure
TEM	Transmission electronic microscope
USEPA	United States Environmental Protection Agency
WW	Wastewater
XRD	X-Ray diffraction

Symbols:

m_{media}	mass of the slag media in a column, g
Q_{av}	average influent flowrate in a column, mL/min
V_c	volume of a column, mL
V_{void}	void volume in a column, mL
ρ_s	slag density, g/cm^3

LIST OF APPENCIDES

APPENDIX A INDIVIDUAL BATCH TEST RESULTS 73

APPENDIX B RETENTION CAPACITY OF FILTERS 77

INTRODUCTION

Context and objectives

Abandoned mining sites have a significant impact on the environment. Major alterations on the landscape are added to direct pollution of surrounding water streams by mining leachates. In this project, the focus of the investigation was an abandoned gypsum mining site located in Joplin, Missouri. High concentrations of various contaminants (phosphorus, fluoride and metals) were present in nearby water streams. This site was previously managed by the implementation of a chemical treatment plant, which is currently in operation. The mining leachate is collected and treated with lime addition, which precipitates contaminants. However, this system does not meet the latest discharge regulations. In particular, the presence of phosphorus at the treatment plant effluent is a major concern because it favours eutrophication even at very low concentrations. Implementing an economical technology that both reduces phosphorus concentrations enough to avoid eutrophication and removes typical heavy metals present in the mining leachates is a challenge.

The Missouri Trust decided to invest in a new treatment plan that would be economical and more efficient than the existing treatment plant. In that context, two engineering firms and one institution were hired to conduct that project: Shaw Environmental, Naturally Wallace Consulting and Polytechnique Montréal. In a preliminary analysis, steel slag filters were selected as promising treatment systems for this specific application. Polytechnique Montréal was mandated via this master project to conduct the first part of the project.

Objective 1: Propose, on the basis of lab-scale tests, a slag filter treatment system suitable for the treatment of the Joplin mining leachate. The proposed system has to meet new discharge criteria and be economical.

The hypothesis of this objective is that a correctly optimized slag filter is more efficient and economical than the existing chemical treatment plant. Filter parameters that need to be optimized are: slag type, hydraulic retention time and filter sequences.

A second problem was addressed in that master thesis project. Phosphorus treatment by slag filters is a well documented issue, but performances are variable between different studies. To this day, no efficient performance prediction tools exist for slag filters and the performance

has to be assessed by pilot tests. A global understanding and conceptualization of involved phenomena in slag filters is needed to develop such prediction tools.

Objective 2: Propose a preliminary model of phosphorus removal mechanisms in steel slag filters.

A new hypothesis has been formulated: a model based on crystal formation and accumulation in slag filters improves the actual understanding of phosphorus removal mechanisms and leads to more reliable prediction tools.

Content of this master thesis

In the literature review section, a summary of slag applications for wastewater treatment is presented, including phosphorus treatment, fluoride treatment and metal treatments. A synthesis of involved mechanisms in slag filters and actual prediction tools follow. Two chapters are devoted to the methodology and results. Several paragraphs of Chapters 1 and 2 were reproduced from the article «Steel slag filtration for extensive treatment of mining wastewater», presented at the 2011 WEFTEC congress[1].

The discussion is divided in two chapters. The first one is the reproduction of the article «Model of phosphorus precipitation and crystal formation in electric arc furnace steel slag», published in *Environmental Science and Technology* in 2012. In this chapter, a preliminary model for phosphorus removal mechanisms is presented. The second discussion chapter addresses the need for a new treatment plan at the Joplin mining site and adds complementary information to the preliminary model. Finally, recommendations for the implementation of pilot tests at the Joplin mine and for the refinement of the phosphorus retention mechanisms model are given in the last section.

The article presented in this master thesis[2] played a major role in the evolution of this project. It provides answers to the second objective formulated above. The ideas leading to the

---

[1] Claveau-Mallet, Dominique; Wallace, Scott and Comeau, Yves. (2011). Steel slag filtration for extensive treatment of mining wastewater. Paper presented at the WEFTEC congress, Los Angeles, California, October 15-19.

[2] Claveau-Mallet, Dominique; Wallace, Scott and Comeau, Yves. (2012). Model of phosphorus precipitation and crystal formation in electric arc furnace. *Environmental Science and Technology*, 46(3), p. 1465-1470.

article are presented in the literature review (Chapter 1). The methodology and results presented in the article are also presented and explained in Chapter 2 and Chapter 3, which are more complete and detailed.

CHAPTER 1 LITERATURE REVIEW

1.1 The mining leachate treatment challenge

Mining operations can have major impact on the environment, indirectly also affecting human health. In particular, site closure is a determinant step to limit long-term damage caused by mining leachates. Mining residual tailings are stocked in piles that can reach large dimensions. If rain and surface water are not well controlled, they may become contaminated while flowing in piles and being discharged in natural systems. Even if many modern mining companies take the responsibility to restore the site after the mine life, old orphan mining sites still exist and create contamination from mining leachates.

A frequent problem related to mining leachates is acid mine drainage. Sulphidic minerals contained in tailings react with air and water to form sulphuric acid (Demers et al., 2011). This reaction is fed by tailings during decades before the acidification process is extinguished. This acid leachate favours the dissolution of metals contained in the tailings, including heavy metals.

Mining leachates are controlled by two main technologies: passive covers or treatment of the leachate. These two technologies are fundamentally different. The purpose of passive covers is to limit interactions between the environment (water and air) and the tailings. In other words, passive covers minimize the leachate generation process. Multilayer soil covers were used in lab scale and full-scale applications to control acid mine drainage by limiting oxygen diffusion and water infiltration in tailings (Aubertin et al., 1996; Mbonimpa et al., 2003).

If passive covers are interesting treatment solutions, it is sometimes preferable for economic or technical reasons to accept the leachate formation and treat it before it is discharged in the environment. Treatment reactors may be chemical or biological systems. As an exemple, acid mine drainage can be treated by sulphate reducing bacteria, which cause precipitation of heavy metals as sulfur minerals (Neculita, Zagury & Bussière, 2007).

The Joplin gypsum mine leachate has a particular composition. It contains typical high concentration of sulfates, but its pH is neutral. As a consequence, common and heavy metals are present, but in lower concentrations than what is seen in average acid mine drainage. The leachate contains high concentration of phosphorus (up to 110 mg P/L). In this specific case, phosphorus removal is a priority to avoid eutrophication of downstream water streams. The

Missouri Trust, the authority responsible for the Joplin site restoration, chose to investigate the treatment of the mine leachate with a reactive slag filter and to prioritize on phosphorus removal.

1.2 What is slag ?

Slag is a waste material produced in iron and steel mills. When the original ore is melted, metallic and non metallic components are separated. The artificial lava floating over melted iron is recovered and cooled, resulting in slag. Different varieties of slag exist, depending on the metallurgical process it comes from. Two main types of slag are identified by the American National Slag Association (NSA): blast furnace slag and steel slag (NSA, 2009). Blast furnace slag is produced from iron mills, where iron ore, flux stone (calcium rich stone) and coke react in a blast furnace. Its main components are silica oxides, alumina, lime and magnesia. Steel slag is produced from basic oxygen furnace (BOF slag) or electric arc furnace (EAF slag), where iron and scrap are processed with lime. Its main components are calcium silicates, aluminoferrites and oxides of calcium, iron, magnesium and manganese. Three types of slag shapes are produced (air cooled, expanded or granulated). Cooling processes determine the porosity and crystalline fraction of slag. Finally, crushing and/or sieving result in different slag grain size, from powder to coarse aggregates.

Slag is used in numerous applications. Depending of its properties, it is used for pavements, concrete, bituminous pavements, railroad ballasts, roofing aggregates, mineral wool insulation, floor fill, highway base, agricultural liming, unpaved parking or roads and wastewater treatment (NSA, 2009). When slag is used for an environmental purpose, its leaching behavior has to be carefully tested and certified as environmentally safe. Leaching of heavy metals is a crucial concern. However, data concerning slag indicate that many slags in North America are considered non hazardous waste and can be safely used (Proctor et al., 2000).

1.3 Wastewater treatment by slag

There are two different manners to use slag for wastewater treatment. Powdered or small sized slag can be a sorbent in a completely mixed system (jar tests, adsorption isotherms) or granular slag may constitute the media in a filter. Both systems have their advantages and limitations. Granular filters are simple, economical and extensive compared to sorption systems that involve maintenance and complexity (continuous feeding with slag media, energy need for

mixing, sludge disposal, need of a settling or filtration unit). On the other side, sorption systems are more reliable than granular filters because they do not clog and treatment performances are easily determined by adsorption isotherms.

In the literature, treatment performances are presented with both concepts: adsorption isotherms or filter performance (removal efficiency). However, these two approaches are often used without distinction even if they are fundamentally different. Authors of recent literature reviews outline the difficulty to correlate treatment performances between different studies when both methodologies are employed (Chazarenc et al., 2008; Vohla et al., 2001). Adsorption isotherms have been used to predict the treatment performance of filters, but this prediction method was shown to lead to incorrect results (Chazarenc et al., 2008; Drizo et al., 2002). In this study, the filter approach is used, as we were interested in extensive treatment systems. Preliminary adsorption jar-tests are used for comparative purposes.

1.3.1 Phosphorus treatment

Phosphorus is the principal contaminant treated by slag, as confirmed by the many studies devoted to that topic (Chazarenc et al., 2008; Vohla et al., 2001). The treatment performances of slag for phosphorus removal have been studied using short-term batch tests, column tests or field-scale tests. Short-term batch tests remain the most well documented approach (Chazarenc et al., 2008), but focus will be given to column and field-scale filters in the next paragraphs.

Different types of wastewater have been treated in recent slag column or field-scale applications. Baker, Blowes and Ptacek (1998) operated slag columns during 4 years and achieved 90% phosphorus removal with hydraulic retention time of voids (HRT_V) of 0.9 day. Smyth et al. (2002) used slag in soil to intercept a contaminant plume from a septic tank. He monitored his system with piezometry during 2 years. He reached a phosphorus concentration of 0.05 mg P/L at the outlet. He also performed column tests for 8 years with an outlet phosphorus concentration of 0.3 mg P/L after that period. Chazarenc, Brisson and Comeau (2007) tested slag columns at the outlet of constructed wetlands. They reported 75% phosphorus removal in one year of operation. Koiv et al. (2010) reported efficient phosphorus removal from pre-treated domestic wastewater and landfill leachates. In New-Zealand, slag filters were operated for more than 5 years as post-treatment of domestic wastewater treatment ponds (Pratt & Shilton, 2010).

Recently, a pilot slag filter in a fish farm resulted in more than 97% phosphorus removal from the sludge in several months of operation (Brient, 2012).

Some specific properties of slag filters have been addressed in recent studies. Regeneration of slag filters after drying was shown to be possible by Drizo et al. (2002), who increased her column retention capacity from 1.35 to 2.35 mg P / g of slag with this process. The hydraulic retention time of slag filters has a direct impact on their removal performances (Liira et al., 2009; Shilton et al., 2005). Some authors highlighted important differences between short term tests and pilot tests performance results. Shilton et al. (2005) reported that full-scale tests gave higher removal performances than similar tests conducted in columns, possibly because of the influence of algae. Pratt and Shilton (2010) suggested that short-term batch tests are not suitable to characterize performances of slag filters even if phosphorus is treated by adsorption, because long-term slag alteration creates new adsorption sites. The major difficulties related with slag filters are clogging and decline of efficiency after 6 months (Chazarenc et al., 2008). Finally, the formation of hydroxyapatite was observed by many authors when the effluent pH of filters is high (Chazarenc et al., 2008; Vohla et al., 2011).

1.3.1.1 Phosphorus recovery

Phosphorus in wastewater is a contaminant, but it is also a nutrient. Phosphorus recovery from wastewater is possible by precipitation of phosphate phases, which have economical value for the fertilization industry. Phosphorus is generally recovered in a dedicated process, mainly fluidised beds involving chemical additives (Valsami-Jones, 2001). Phosphorus is precipitated and recovered on seeds. Steel slag filters offer promising phosphorus recovery applications because phosphorus precipitation in stable phases occur within these filters. A used filter that includes both phosphorus and calcium source could be used directly as a fertilizer.

1.3.2 Fluoride and metals treatment

As presented in a preceding section, wastewater treatment by slag involves two main applications: adsorption batch processes and filters. While both approaches have been studied for phosphorus removal, fluoride was mainly treated with batch processes. Fluoride removal from drinking water was studied by adsorption on various media such as coal fly ash or natural mud (Chen et al., 2010; Lu, Wang & Ban, 2010; Xue & Ma, 2009). Adsorption on slag was also used

for wastewaters with higher fluoride concentration (Huang, Shih & Chang, 2011; Xu et al., 2011). Fluoride removal by precipitation (mainly as CaF_2) was tested with chemical additives such as CaF_2 or CaF_2-$Al(OH)_3$ seeds (Yan et al., 2001) or in fluidized bed of silica sand (Aldaco, Irabien & Luis, 2005). Several specific industrial wastewaters (semiconductor manufacturers and electronic industries) contain both high fluoride and phosphorus, which reduces the removal efficiency of fluoride by CaF_2 formation (Warmadewanthi & Liu, 2009). Some authors reported selective precipitation of phosphorus or fluoride from wastewater (Grzmil & Wronkowski, 2006; Warmadewanthi & Liu, 2009; Yang et al., 2001). All these processes for fluoride removal were efficient, but involved the continuous addition of chemicals and the production of chemical sludge that was expensive to manage and required significant maintenance.

The use of slag for the treatment of metals was well documented in a recent critical review (Zhou & Haynes, 2010). Slag was mainly studied as an adsorbent in single-metal contaminant batch tests and characterized with Langmuir or Freundlich equations (Beh et al., 2010; Huifen et al., 2011; Sheng-Yu et al., 2009; Wang & Lin, 2010). Slag columns were operated for metal removal with a resulting arsenic effluent concentration of 0.003 mg/L (Smyth et al., 2002). Low concentrations of metals (Cu, Mg, Mn, Ni, Zn) in domestic wastewater were removed with slag filters (Renman et al., 2009).

Metal removal with slag may be compared with chemical precipitation of metals. Most of heavy metal hydroxides have minimum solubility between pH of 9 and 12 (Metcalf & Eddy, 2003), which is the typical pH range of an efficient slag filter.

1.4 Phosphorus removal mechanisms in slag filters and proposed models

In the beginning of this chapter, a major problem concerning prediction tools for treatment performances of slag was outlined. Three different methodologies – batch tests, column tests and pilot tests – were indistinctly used to explain two different phenomena – adsorption and precipitation. Moreover, the limit between adsorption and precipitation/crystallization is not clear. Adsorption is the first step of every nucleation seed formation. The relative importance of adsorption and precipitation depends on pH. Adsorption dominates at low pH and precipitation at high pH (Baker, Blowes & Ptacek, 1998). The complexity of systems (water composition, presence of nucleation seeds, hydraulics, etc.) makes the situation difficult to generalize, so that adsorption may occur as much as precipitation. Slag itself adds complexity to the situation: their

composition are so different depending on the natural ore, type of furnace, type of cooling process and used additives that there is no direct relationship between slag type and removal efficiency. In general, blast furnace slags are more efficient than steel slags (Vohla, 2011).

In this master thesis framework, the focus was be given to prediction tools for alkaline slag filters. These are defined as a fixed granular media that increases the pH of the water that flows through it. Such a filter involves seven phenomena :

- **Diffusion.** Dissolved ions from the slag surface migrate in the water via diffusion. Diffusion may be slowed by the presence of accumulated matter.
- **Adsorption.** Adsorption is the adhesion of free ions or molecules in the solution on a solid particle. Adsorption is controlled by surface energy, may be reversible and may be influenced by inhibitors. Adsorbed ions or molecules may be bound to adsorption sites by week or strong chemical links.
- **Nucleation.** Nucleation is the amorphous formation of a solid phase nucleus. It may occur on a pre-existing surface or freely in a solution. The nucleation rate is dependent on many factors (catalytic pre-existing surfaces, adsorbed ions on these pre-existing surfaces, composition of water, etc.)
- **Crystal growth**. Crystal growth is the progressive formation of organized solid phases. Crystal growth is a surface phenomenon as free ions join pre-existing crystal or nucleus. Crystal growth rate is generally different from nucleation rate and it also depends on environmental factors (geometry and composition of pre-existing crystal or seeds, adsorbed ions on these pre-existing surfaces, composition of water, etc.)
- **Crystal reorganisation**. Pre-existing solid phases (amorphous seeds or crystals) may reorganise and transform into a more stable phase.
- **Filtration**. Filtration occurs in slag filters because direct nucleation within the solution is possible. Newly formed seeds are either retained by slag particles or other fixed crystals and seeds. They also may be washed out if hydrodynamic conditions favour it. Wastewater suspended solids containing organic matter may also be retained by direct filtration, increasing the rate of filter clogging.

- **Settling**. If water velocity, turbulence conditions and crystal size allow it, crystals may settle within the filter.

The term «precipitation» is a general one that includes both nucleation and crystal growth. Existing prediction tools are based on one or more of these phenomena, but not necessarily all of them. In the next lines, these prediction tools are shortly presented. They are divided in two main categories which are models based on chemical equilibria, and models based on chemical kinetics.

1.4.1 Models based on chemical equilibria

Models based on chemical equilibria assume that the system has reached steady state conditions. The major problem with these models is that the rate of kinetic reactions is very important in precipitation processes. When precipitation occurs, the final chemical species present in a given solution are often better described by kinetics and not by equilibrium (Valsami-Jones, 2001). This is especially true when we are dealing with geological reactions (transformation of gypsum to anhydrite, formation of calcite, etc.).

1.4.1.1 Adsorption capacity of slag (mg P / g of slag)

This is the main ratio currently used to characterize the treatment performance of slag. Its principle is simple: the slag has a maximum retention capacity that is reached after all its adsorption sites are occupied. This value is simply determined by classical adsorption isotherms in batch tests. However, it considers only adsorption among the seven involved phenomena. This is why adsorption isotherms from batch tests are unreliable for the prediction of slag filter performance (Drizo et al., 2002).

1.4.1.2 Phosphorus fractionation

This method is used to characterize the phosphorus potential for reuse as a fertilizer (Drizo et al., 2002; Pratt & Shilton, 2010). It describes the proportion of phosphorus bound to different ions (calcium solids, iron-bound, etc.) This method is not a direct prediction tool for performance, but it provides information about phosphorus reactions in slag filters.

1.4.2 Models based on chemical kinetics

Models based on chemical kinetics consider reaction rates, which is essential for a better understanding of the seven phenomena involved in slag filter treatment. They are more complicated than models based on equilibrium, but they give more realistic predictions. Unfortunately, the several existing models based on kinetics explain only a part of what happens in slag filters.

1.4.2.1 Studies of slag behavior

Slag particles are directly responsible for adsorption and filtration, and they modify the water composition, which leads to precipitation mechanisms. Microscopic photography of slag surfaces was performed by some authors (Koiv et al., 2010; Pratt & Shilton, 2010), allowing qualitative description of the interaction between slag surfaces and crystal formation. An alteration of slag surfaces over time was reported by Bowden et al. (2009), highlighting that crystal formation processes change with time.

Slag leaching of calcium and hydroxides within the wastewater is responsible for precipitation mechanisms (Claveau-Mallet, Wallace & Comeau, 2012). pH-rise kinetics was studied in batch tests and modeled with classical kinetic models, such as the intra-particle diffusion or the pseudo-second-order model (Chazarenc et al., 2008). Acid neutralizing capacity curves (ANC curves) were proposed to describe the slag potential for pH rise (Kostura, Kulveitova & Leko, 2005). This author related ANC curves to the successive dissolution of different mineralogical phases within slag. ANC curves are promising tools to predict the long-term capacity of slag to increase pH, but still don’t consider kinetics.

1.4.2.2 Studies of hydroxyapatite formation and growth

Studies concerning hydroxyapatite (HAP) formation and growth are numerous. Needs from different applied science branches (wastewater treatment, mineralogy and crystallography, biomedical, ceramics) have resulted in various results, often presented with different approaches. HAP is known to be the final crystallographic phase of other metastable calcium phosphates as monetite, octacalcium phosphate, tricalcium phosphate or amorphous calcium phosphate (Valsami-Jones, 2001). Two nucleation processes are possible: homogenous - directly from aqueous species - or heterogenous - on surfaces or seeds (Valsami-Jones, 2001). These nucleation

processes have great importance in phosphorus recovery from fluidized beds, where heterogeneous nucleation must be favoured. HAP formation was observed in supersaturated solutions because ionic association effects limit the contribution of aqueous species to saturation (Baker et al., 1998; Valsami-Jones, 2001).

The water composition affects HAP formation. HAP nucleation and growth rates are influenced by major ions concentration as calcium, hydroxides and phosphorus (Tsuru et al., 2001). Metallic ions may catalyze or inhibit nucleation or growth of HAP (Lundager Madsen, 2008) and also affect crystal shapes. Carbonates are growth inhibitors because they attach to growth surfaces (Valsami-Jones, 2001) or contribute to calcium carbonate formation, as competitive processes (Liira et al., 2009). HAP precipitation was diminished in water with low concentration of phosphorus (Koiv et al., 2010).

The transformation of HAP into fluoroapatite (FAP) by ionic migration of fluoride ions into the apatite structure has been theoretically demonstrated (Jay, Rushton & Grimes, 2012). These authors showed that fluoride migration is possible only over 1100 K, suggesting that HAP cannot transform to FAP at ambient environmental temperatures.

1.4.3 Summary of prediction tools for slag processes

A summary of prediction tools for three different slag processes in presented in Table 1.1. An emphasis is given to the last column which describes alkaline reactive filters.

Table 1.1 : Comparison of prediction tools efficiency for different treatment slag processes

Process	**Adsorption batch process**	**Reactive filters - low pH**	**Reactive filters - high pH**
Example	Activated carbon	Melter slag for P removal (Pratt & Shilton, 2010). Full-scale filters installed at a WW treatment plant. Filters reached 75% P removal after 5 years of operation.	EAF steel slag for P removal (Baker et al., 1998). Columns fed with artificial WW (3.3 mg P/L) during 1500 pore volumes (4 years). Achieved >90% P removal.
Involved phenomena	Adsorption	Principally adsorption. Precipitation and filtration are possible but have little influence	Adsorption, nucleation, crystal growth, crystal reorganization, filtration
Performance prediction with batch tests	Applicable: conditions are similar to the process	Poor prediction results. Adsorption sites may be changed after a long time (media alteration, hydraulics)	Poor prediction results. Batch tests do not consider filtration and crystal behavior (growth and organization). Completely mixed batch tests are not representative of a complex flow in a porous media
Performance prediction with column tests	Not applicable	Applicable if field conditions are respected (filter geometry and HRT_V, feeding variability, presence of algae and sun, etc.)	
Performance prediction with numeric modelling	Many simple adsorption isotherms are applicable (Freundlich, Langmuir, etc.)		See the recommendation section for the presentation of research needs in this thesis to develop such a model

Table 1.1 shows how prediction of slag processes performance may be challenging. Phosphorus removal is achieved by different phenomenon depending if water is neutral or alkaline, and the difference between these two environments is not well defined. Complex long-term field conditions as slag alteration or alga presence may modify the slag capacity for treatment. Finally, numerical modelling is currently used only for adsorption batch processes.

CHAPTER 2 MATERIALS AND METHODS

The experimental program included three parts: individual batch tests, sequential batch tests and column tests. Individual batch tests were used to compare the treatment potential of different media and select the most efficient media. Sequential batch tests are a slightly modified version of the individual batch tests, where different treatment sequences of slag are compared. Finally, column tests are used to characterize the treatment performances and longevity of lab-scale slag filters. Column tests were divided in two sets. The first set of tests was conducted with the best media and sequences selected from the first two parts. The second set of tests was used to develop a preliminary model for phosphorus removal mechanisms. A detailed description of the three experimental phases is given below, preceded by the description of the reconstituted wastewater (WW) and media used in the experimental program. The subsequent section describes analytical determinations used in the three parts of the experimental program. The last section describes toxicity tests that were performed on the media used in column tests.

The present chapter includes the methodology section described in the article of Chapter 4, which corresponds to the second set of column tests.

2.1 Reconstituted wastewater and tested media

Tests were conducted with three reconstituted mine effluents, WW 1, 2 and 3 representing, respectively, the minimum, mean and maximum concentrations observed at the Joplin site. WW 1 and 3 were used in the first set of column tests and WW 2 was used in the second set. These effluents were prepared using laboratory-grade salts (e.g. KH_2PO_4, $CaCl_2$, $MnSO_4$, etc.) dissolved in tap water for WW 1 and 3 and distilled water for WW 2. Salts were individually dissolved then mixed together. pH was adjusted to the field value with H_2SO_4 5N for WW 1 and 3 and with NaOH 6N for WW 2. The solution was left to rest for at least 24 h to reach equilibrium (a small amount of precipitate formed during the mixing of individually dissolved salts) and settled. The supernatant was used in all tests. A sample of the initial solution was filtered and used for analytical characterization. The average composition of the reconstituted effluents is shown in Table 2.1.

Table 2.1 : Average composition of the reconstituted effluents

Component	Units	WW 1	WW 2	WW 3
pH	-	6.92	6.52	5.67
Na	mg/L	154	146	311
Ca	mg/L	32	149	177
K	mg/L	17	52	132
Mg	mg/L	16	8	17
Al	mg/L	1.7	0	8.2
Mn	mg/L	0.24	0.71	0.83
Zn	mg/L	0.20	0.52	3.3
SO_4	mg S/L	201	134	317
Cl	mg/L	25	197	265
o-PO_4	mg P/L	11	26	107
F	mg/L	9	7	37

One type of apatite, nine types of slag from the United States and one type of slag from Quebec were tested (Table 2.2 and Figure 2.1). All slag samples were sieved to 5-10 mm, washed and air dried before utilization. The utilization of 5-10 mm slag was based on previous studies that compared the efficiency of coarse, 5-10 mm and fine grained slag (Anjab, 2009). 5-10 mm slag was shown to be an optimum compromise between reactive surfaces and hydraulic efficiency. Some slag samples had to be crushed to achieve 5-10 mm because of the original size of the material (slags #2, 3, 4, 8 and 9). The apatite sample was tested in batch tests without initial washing and sieving (5-20 mm). The chemical composition of tested slags is presented in Table 2.3. These analyses were performed by Acme Analytical Laboratories (Vancouver, BC) with ICP-emission spectrometry preceded by a $LiBO_2/Li_2B_4O_7$ fusion and dilute nitric digestion. The mineralogical composition of slags used in column tests is presented in Table 2.4. Mineralogical composition was determined by X-ray diffraction (XRD) analysis in the Geology Department of Tartu University, Estonia.

Table 2.2 : Tested slags and apatites

#	Slag/Steel compagny	Media	Type	Location
1	Harsco Metals	Slag	EAF	Blytheville, Arkansas
2	Phoenix Services	Slag	ACBF	Indiana Harbor East, Indiana
3	Phoenix Services	Slag	BOF	Indiana Harbor East, Indiana
4	Granite City Slag LLC	Slag	BF	Granite City, Illinois
5	Levy	Slag	EAF	Decatur (Trinity), Alabama
6	MultiServ	Slag	EAF	Contrecoeur, Quebec
7	Tube City	Slag	EAF	Fort Smith, Arkansas
8	Charleston Mill Service	Slag	EAF	Charleston, South Carolina
9	Golden Triangle Mill Service	Slag	EAF	Columbus, Mississippi
10	Stein	Slag	BOF	Cleveland, Ohio (Arcelor Mittal)
Ap1	Cargill	Apatite	Sedimentary	Florida (Cargill)

Note: ACBF: air cooled blast furnace slag; BF; blast furnace slag; BOF: basic oxygen furnace slag; EAF: electric arc furnace slag.

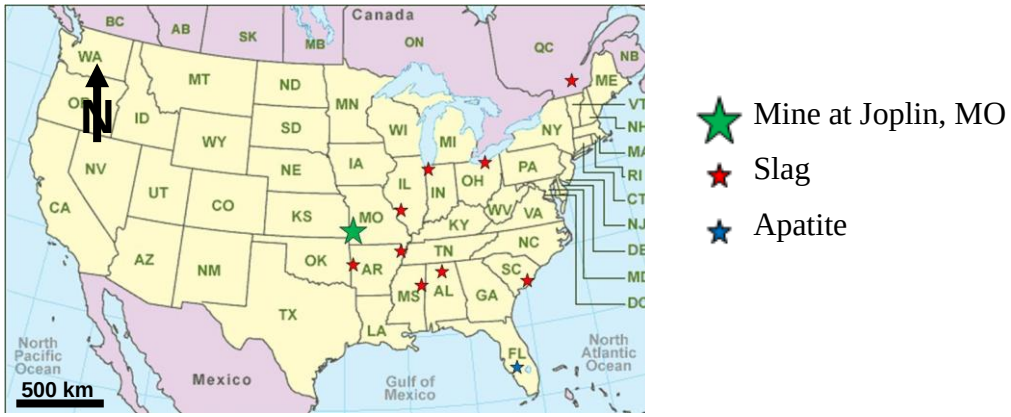

Figure 2.1 : Origin of tested materials. (map: http://litlink.ket.org/stations/stationshome.aspl)

Table 2.3 : Chemical composition of tested slags

Slag ID		**DL**	**1**	**2**	**3**	**4**	**5**	**6**	**7**	**8**	**9**	**10**
SiO_2	%	0.01	10.94	37.45	11.95	40.12	10.68	15.92	14.49	11.57	12.22	16.28
Al_2O_3	%	0.01	11.87	11.59	4.42	8.33	4.60	6.03	7.69	6.17	5.91	5.14
Fe_2O_3	%	0.04	29.50	0.69	35.18	0.76	42.48	33.08	25.20	40.45	35.67	18.21
MgO	%	0.01	10.27	13.48	8.30	12.47	10.42	12.07	14.66	12.66	12.77	10.19
CaO	%	0.01	31.67	34.85	37.25	36.76	28.10	30.16	28.75	27.00	28.32	40.60
Na_2O	%	0.01	0.06	0.46	0.05	0.23	0.03	0.08	0.06	0.04	0.02	0.05
K_2O	%	0.01	0.03	0.65	0.04	0.45	0.01	0.01	<0.01	0.01	<0.01	0.03
TiO_2	%	0.01	0.50	0.49	0.60	0.33	0.47	0.99	0.37	0.51	0.53	0.44
P_2O_5	%	0.01	0.48	<0.01	0.68	0.01	0.60	0.28	0.31	0.59	0.52	0.47
MnO	%	0.01	3.29	0.49	3.18	0.61	4.18	2.37	7.96	3.18	5.36	3.88
Cr_2O_3	%	0.002	0.675	0.006	0.185	0.011	0.858	0.578	1.094	0.887	1.179	0.406
Ba	ppm	5	455	760	516	355	430	392	436	606	443	75
Ni	ppm	20	<20	<20	<20	<20	<20	<20	103	<20	<20	24
Sr	ppm	2	301	455	173	416	255	223	267	305	348	184
Zr	ppm	5	194	187	497	194	111	255	1011	117	91	204
Y	ppm	3	27	69	5	37	17	44	8	23	9	8
Nb	ppm	5	182	6	238	30	239	109	180	216	429	93
Sc	ppm	1	6	15	2	9	5	180	2	6	2	2
Total	%		99.4	100.3	102.0	100.2	102.5	101.7	100.8	103.8	102.6	95.8

Note: 1% equals 10 000 ppm. DL for detection limit.

Table 2.4 : Mineralogical composition of slags

Slag ID		**1**	**6**	**7**
		Proportion (%)		
Merwinite	$Ca_3Mg(SiO_4)_2$	9.2 ± 0.3	4.6 ± 0.2	3.9 ± 0.2
Wuesitite	FeO	30.8 ± 0.2	45.5 ± 0.2	42 ± 0.2
C2S, beta	Ca_2SiO_4	26 ± 0.3	23.8 ± 0.2	29.2 ± 0.2
C4AF	$Ca_2Fe_{0.28}Al_{1.72}O_5$	3.5 ± 0.1	1.5 ± 0.1	3.5 ± 0.1
Mayenite	$Ca_{12}Al_{14}O_{33}$	4.7 ± 0.1	0.6 ± 0.1	2.7 ± 0.1
Gehlenite	$Ca_2Al(Si,Al)_2O_7$	2.1 ± 0.1	4.9 ± 0.1	0.9 ± 0.1
Periclase	MgO	3.2 ± 0.2	0.7 ± 0.1	3.3 ± 0.1
Akermanite	$Ca_2MgSi_2O_7$	2 ± 0.1	1.3 ± 0.1	1.7 ± 0.1
Magnesioferrite	$MgFe_2O_4$	14.9 ±0.1	5.6 ± 0.1	5.1 ± 0.1
Bredigite	$Ca_{14}Mg_2(SiO_4)_8$	3 ± 0.2	11.4 ± 0.2	7.3 ± 0.2
Spinel, submagnesian	$MgAl_2O_4$	0.5 ± 0.1	-	-
Quartz	SiO_2	-	-	0.4 ± 0.06
Total		99.9	99.9	100.0

2.2 Individual batch tests

Individual batch tests are short-term tests used to establish a comparative list of media in terms of treatment efficiency. A 35 g media sample was placed in a 1000 mL Erlenmeyer flask

containing 700 mL of WW. The Erlenmeyer flask was shaken for 48 hours at 20°C and 170 rpm. Samples were taken after 0, 24 and 48 hours and filtered for the determination of P, F, Al, Mn, Zn and pH. WW 1 and 3 were tested for each media. A blank test containing the WW without media was conducted with each test group (7 tests including one blank sample conducted at the same time). Tests were run in duplicates. The experimental setup is shown in Figure 2.2.

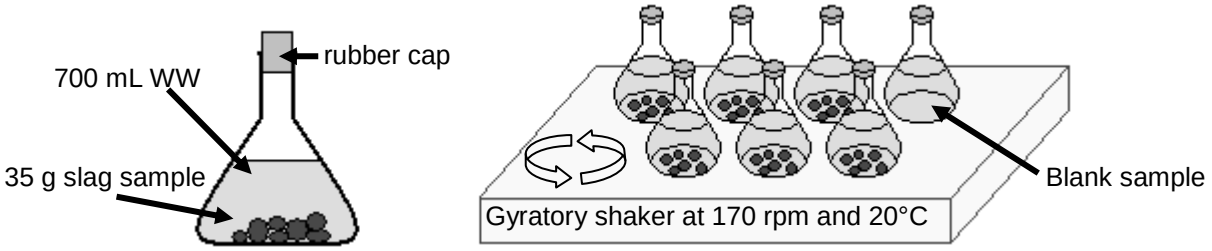

Figure 2.2 : Individual batch tests experimental setup

2.3 Sequential batch tests

In sequential batch tests, different treatment sequences were tested. A 24 h individual batch test was performed with a first media and then the solution was filtered and used for a second individual batch test of 24 h with a second media. The treatment performance of a two-media sequence (24 h with first media and 24 h with second media) was compared with the treatment performance of a single-media system (48 h of the same media, as tested in individual batch tests). A blank test without media was conducted with each test group. Tests were run in duplicates. WW 3 only was used in sequential batch tests. The tested sequences and WW were chosen on the basis of individual batch tests results. This explanation is presented in section 5.1. The experimental setup is shown in Figure 2.3.

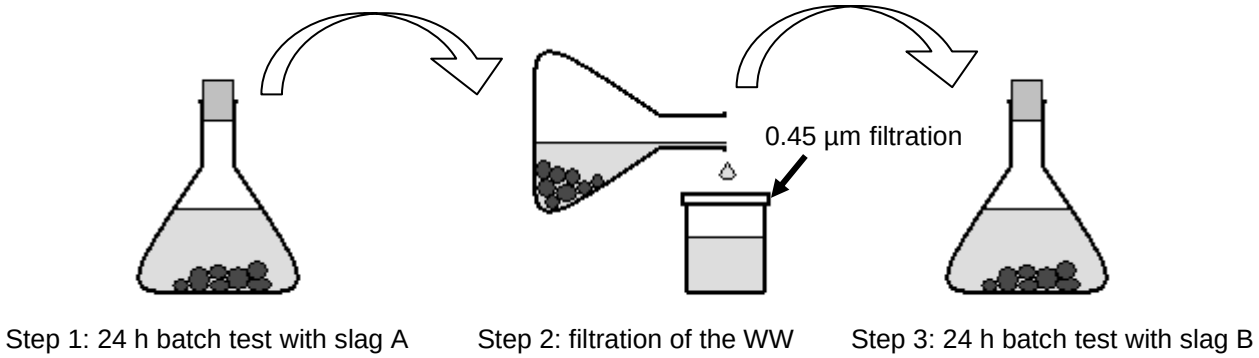

Figure 2.3 : Sequential batch tests experimental setup

2.4 Column tests

2.4.1 Experimental setup

Column tests were performed using transparent plastic columns (17 cm long and 15 cm in diameter) fed continually with a peristaltic pump from the bottom center (upflow) with the effluent coming out from the top center. Set 1 was performed using WW 1 and WW 3. Slags #1 and #7 were selected for set 1 (choose explained in section 5.1). Set 2 was performed with WW 2 and slag #6. The experimental setup is shown in Figure 2.4 and summarized in Table 2.5. A column filled with slag is shown in Figure 2.5. HRT_V were chosen on the basis of previous studies experimented at Polytechnique Montreal (Anjab, 2009).

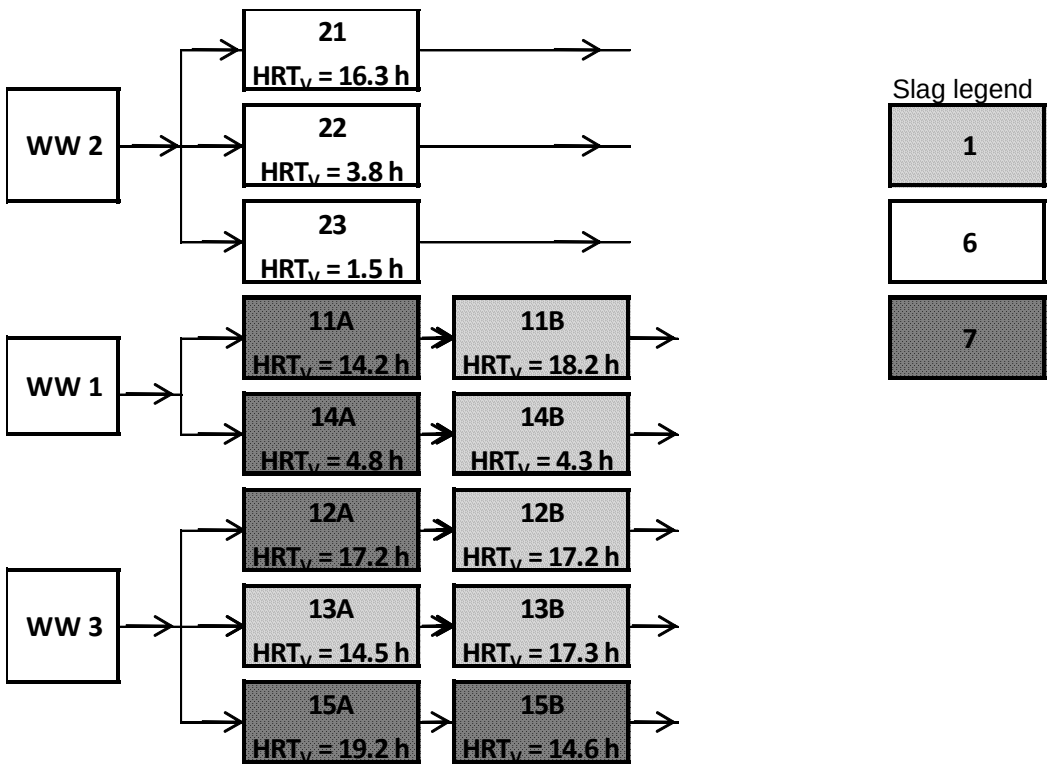

Figure 2.4 : Column tests experimental setup

Table 2.5 : Summary of column tests parameters

	ID	Media	Feeding WW	Q_{av} mL/min	HRT_V h	Test duration d
Set 1	11A	7	1	1.89	14.2	162
	11B	1			18.2	
	12A	7	3	1.95	17.2	222
	12B	1			17.2	
	13A	1	3	1.94	14.5	169
	13B	1			17.3	
	14A	7	1	7.72	4.8	145
	14B	1			4.3	
	15A	7	3	1.94	19.2	179
	15B	7			14.6	
Set 2	21	6	2	1.86	16.3	630
	22	6	2	6.75	3.8	152
	23	6	2	20.86	1.5	30

Note: Q_{av} = average inflow

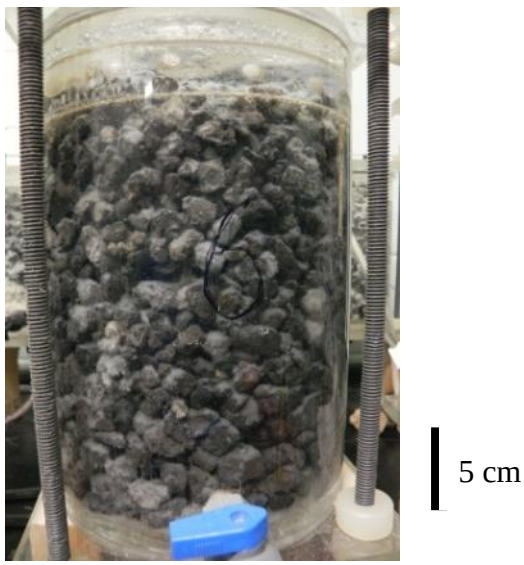

Figure 2.5 : Example of a 3-liter column filled with slag.

2.4.2 Experimental protocol

Columns were filled with washed and 105°C-dried 5-10 mm slag. The HRT_V for each column was computed following a weight procedure utilized in permeability tests (ASTM, 2006; Chapuis, Baass & Davenne, 1989) :

$$HRT_V = \frac{V_{void}}{Q_{av}} \tag{2.1}$$

$$V_{void} = V_c - \frac{m_{media}}{\rho_s} \tag{2.2}$$

Q_{av} is indicated in Table 2.5 for each column and the density of the slag (ρ_s, g/cm^3) is estimated at 3.6 g/cm^3. The volume of the column (V_c, mL) is determined by difference between the weight of the column filled with water and the weight of the empty column. The mass of dry slag in the column (m_{media}, g) is determined by the difference between the weight of the column filled with dry slag and the weight of the empty column. The volume of voids (V_{void}, mL) is the effective volume used for the calculation of the HRT_V.

The effluent of each column was collected twice or once a week for pH, P, F, Ca, Mn, Zn and Al determination. pH was measured in the next half-hour following sampling to minimize interference with the atmosphere.

At the end of tests, columns were opened and precipitates were sampled. Precipitates were picked off with a metal spatula and absorbent paper was put over it to remove water. The resulting precipitate (having a paste aspect) was dried at room temperature.

2.5 Analytical determinations

2.5.1 Water samples

pH was determined on water samples in the next half-hour following sampling, using a 4-point calibration (pH = 4, 7, 10 and 12). Water samples were acidified with H_2SO_4 5N or HNO_3 6N prior to subsequent tests. Orthophosphates were determined using a Lachat Quikchem 8500 flow injection analyser, using the ascorbic acid method (APHA et al., 2005). Analyses of metals were conducted with a AAnalyst 200 flame atomic absorption apparatus, using a standard mass spectrometry method (Centre d'expertise en analyse environmentale du Québec, 2006). Analyses of sulfates were conducted with the turbidimetric method (APHA et al., 2005). Fluoride concentration was determined using a Cole-Parmer epoxy combined probe filled with KCl 3M.

2.5.2 Crystal samples

Analytical procedure for XRD (including determination of crystal size) and transmission electronic microscopy (TEM) are presented in section 4.2.2 (methodology section of the article).

2.6 Toxicity tests

Toxicity tests were performed to assess the environmental safety of slag. A slightly modified version of the toxicity characteristic leaching procedure (TCLP) from the United States Environmental Protection Agency (USEPA) was used (USEPA, 1992). A 35 g slag sample was placed in a 1000 mL Erlenmeyer flask filled with 700 mL of extraction fluid. The Erlenmeyer was mixed for 24 h, after which metal concentrations are determined. Samples were tested in duplicates and the higher concentrations were kept. Two extraction fluids were tested: distilled water and acetic acid (TCLP extraction solution #2). Toxicity tests results were compared with the Joplin performance goals and TCLP criteria for a media to be considered a non hazardous waste, presented in Table 2.6. Phosphorus treatment was the principal objective. The other performance goals were secondary.

Table 2.6 : Joplin performance goals, acceptable effluent limits and maximum TCLP concentrations for a non toxic media (Environmental Health and Satefy Online, 2008)

Parameter	Units	Effluent limits	Performance goals	TCLP limit
Al	mg/L	373	187	
Cd	µg/L	0.8	0.4	1000
Cu	µg/L	10.4	5.2	
Fe	mg/L	1	0.5	
Pb	µg/L	6.5	3.3	5000
Ni	µg/L	79	39	
Zn	µg/L	84	42	
NH_4	mg N /L	2.5	1.3	
SO_4	mg S/L	0.4	0.2	
F	µg/L	4	2	
Total P	µg P/L		0.5	

Note: this table does not include all the organic and inorganic contaminants analyzed in the TCLP procedure

CHAPTER 3 RESULTS

3.1 Individual batch tests

Results of individual batch tests are summarized and qualitatively compared in Table 3.1 and Table 3.2. Significant observations are highlighted in these Tables. Detailed results from individual batch tests are presented in **Erreur ! Source du renvoi introuvable.**.

Table 3.1 : Qualitative comparison of individual batch tests using WW 1. Significant observations are highlighted

Slag ID	pH rise at 48 h	[P] at 24 h	[F] at 48 h	[Mn] at 48 h	[Zn] at 24 h
#1	pH over 11	[P] = 0	[F] < 1 mg/L	[Mn] < 0.05 mg/L, but slags #2 and #4 showed leaching after t = 24 h	Similar treatment results: [Zn] < 0.01 mg/L
#2	pH ~ 9	low	Similar treatment results: [F] = 5-9 mg/L		
#3	pH over 11	[P] = 0			
#4	pH ~ 9	[P]= 8-11 mg P/L			
#5	pH ~ 11	[P] < 1 mg P/L			
#6	pH ~ 10	[P]= 4-6 mg P/L			
#7	pH over 11	[P] = 0			
#8	pH ~ 10	[P]= 4-6 mg P/L			
#9					
#10	pH over 11	[P] = 0			
#ap1	no pH rise	[P]= 8-11 mg P/L			

Table 3.2 : Qualitative comparison of individual batch tests using WW 3. Significant observations are highlighted

Slag ID	pH rise at 48 h	[P] at 24 h	[F] at 48 h	[Mn] at 48 h	[Zn] at 24 h	[Al] at 48 h
#1	pH < 9	[P] = 80-110 mg P/L	[F] = 10-15 mg/L	[Mn] < 0.4 mg/L, but slags #2 and #4 showed leaching at t = 24 h	Similar treatment results: [Zn] = 0	Similar treatment results: [Al] < 0.5 mg/L
#2						
#3	pH ~ 11	[P] < 80 mg P/L	[F] = 18-25 mg/L			
#4	pH < 9	[P] = 80-110 mg P/L	[F] = 10-15 mg/L			
#5			[F] = 18-25 mg/L			
#6						
#7	pH ~ 11	[P] < 80 mg P/L				
#8	pH < 9	[P] = 80-110 mg P/L				
#9						
#10	pH ~ 12	[P] = 0				
#ap1	no pH rise	[P] = 80-110 mg P/L	[F] = 10-15 mg/L	close to initial value		

Individual batch tests results indicate that removal of phosphorus and metal is strongly linked with pH rise. Three slags (#3, #7 and #10) had a strong capacity to increase the pH in both types of WW. The pH rise was slower in the concentrated WW (WW 3) for all slags, resulting in a lower phosphorus removal capacity. Slag #1 had the highest fluoride removal capacity in WW 1, but its capacity was weakened in a concentrated WW. Slags #2 and #4 showed manganese leaching in both types of WW. Sedimentary apatite was not efficient for pH rise or phosphorus removal, but was efficient for fluoride removal.

3.2 Sequential batch tests

Results of sequential batch tests are presented in Figure 3.1 and summarized in Table 3.3.

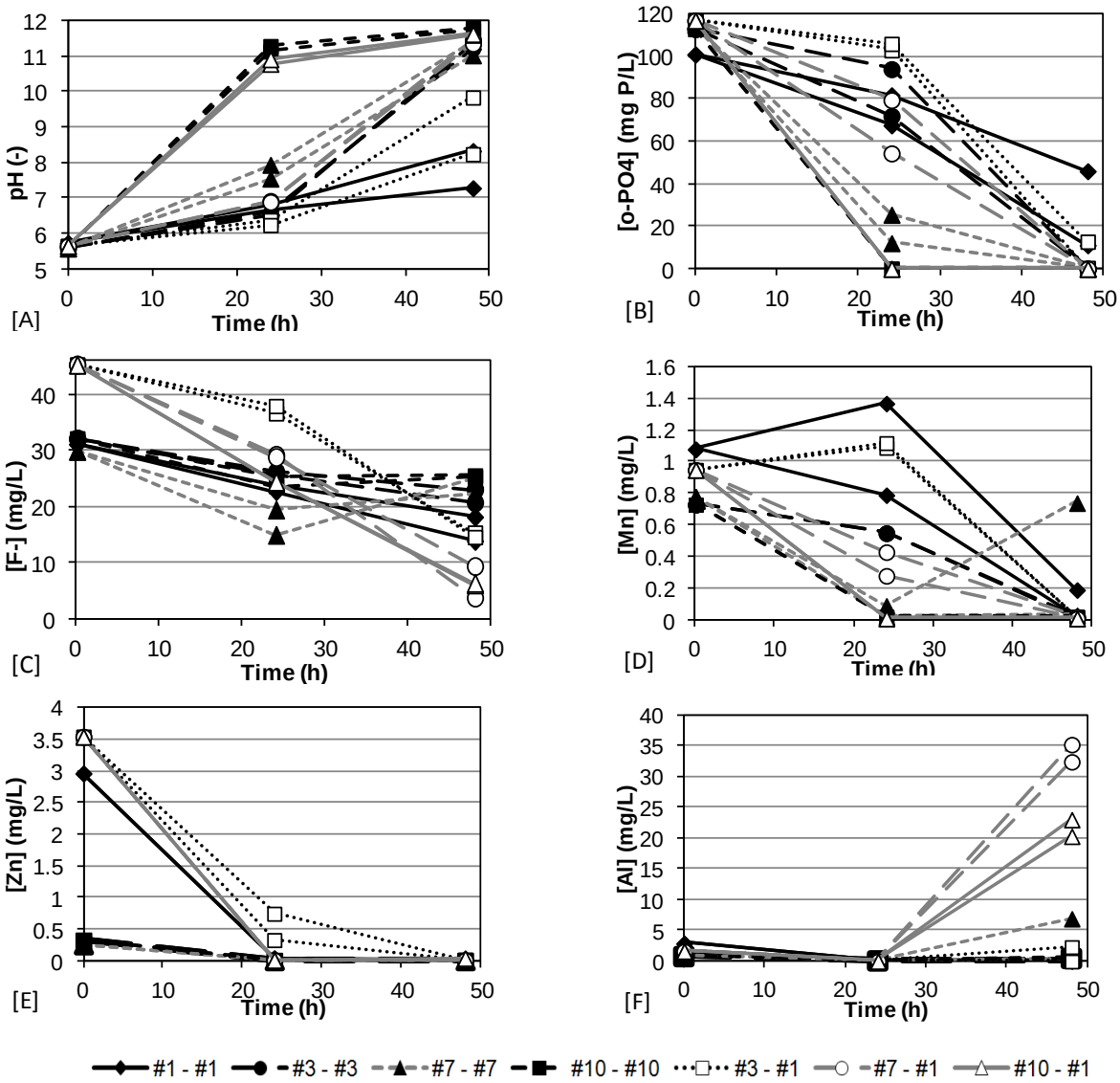

Figure 3.1 : Sequential batch tests results

Table 3.3 : Qualitative comparison of sequential batch tests

Sequence ID	pH rise at 48 h	[P] at 24 h	[F] at 48 h	Mn removal	[Zn] at 24 h	Al removal
#1-#1	pH = 8	[P] = 50-110 mg P/L	[F] = 12-25 mg/L	similar treatment results	[Zn] = 0	Similar treatment results, with Al leaching of sequences #7-#7, #7-#1 and #10-#1 (up to 35 mg/L)
#3-#3	pH = 11					
#7-#7		[P] < 30 mg P/L				
#10-#10		[P] = 0				
#3-#1	pH < 9	[P] = 50-110 mg P/L			[Zn] < 1 mg/L	
#7-#1	pH = 11		**[F] < 10 mg/L**		[Zn] = 0	
#10-#1		[P] = 0				

The pH rise capacity of all tested sequences (#3-#1, #7-#1, #10-#1) was better than using only slag #1, corresponding in a better phosphorus removal in sequences. The fluoride removal ability of slag #1 was increased by using upstream slag. The fluoride removal efficiency was better for the tested sequences than for slag #1 alone.

3.3 Column tests

3.3.1 Column set 1

Results of the first set of column tests are presented in Figure 3.2 to Figure 3.8. In these figures, upstream columns are presented on the left (panel A) and downstream columns are presented on the right (panel B).

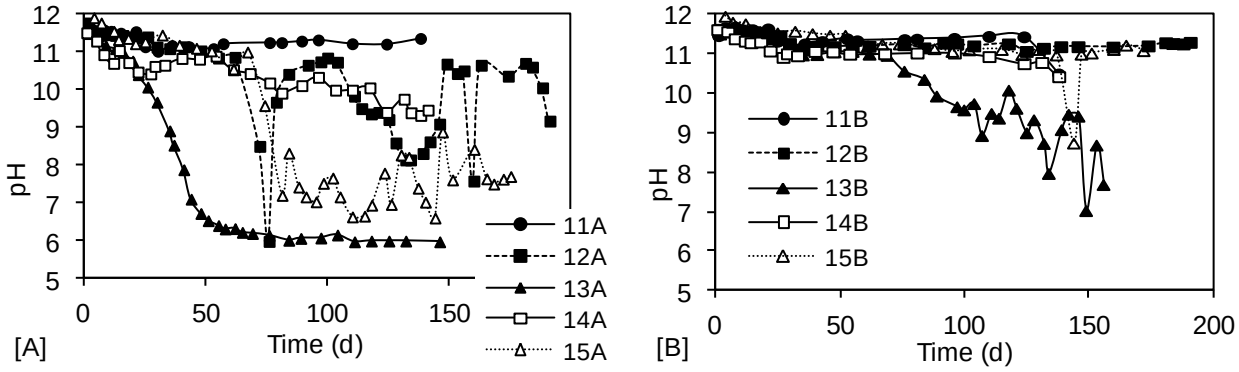

Figure 3.2 : pH monitoring of column effluents, set 1

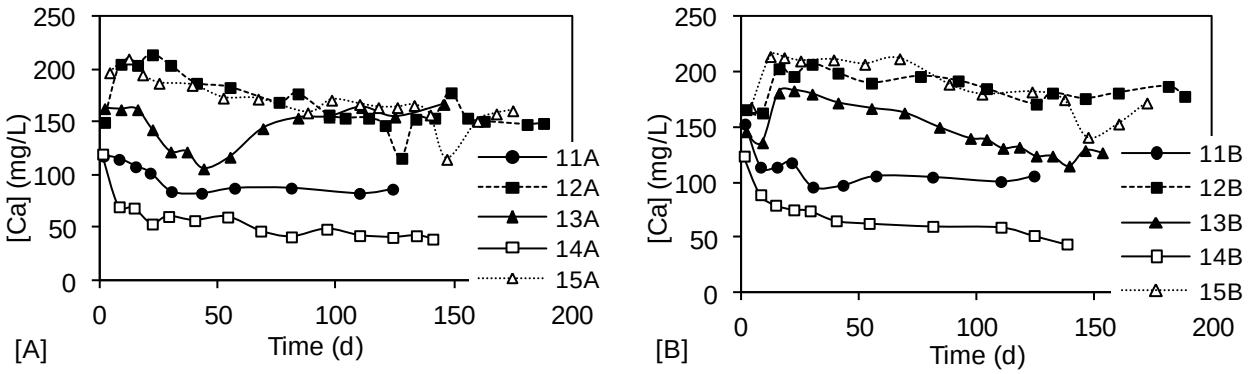

Figure 3.3 : Calcium monitoring of column effluents, set 1

In general, removal of all contaminants was related to high pH and calcium concentrations. Several head columns had a pH drop during the experiment. The pH drop of EAF slag from Blytheville was observed sooner than the pH drop of EAF slag from Fort Smith. Downstream columns all had an effluent pH over 11, except column 13B which had a pH drop after 70 days of operation.

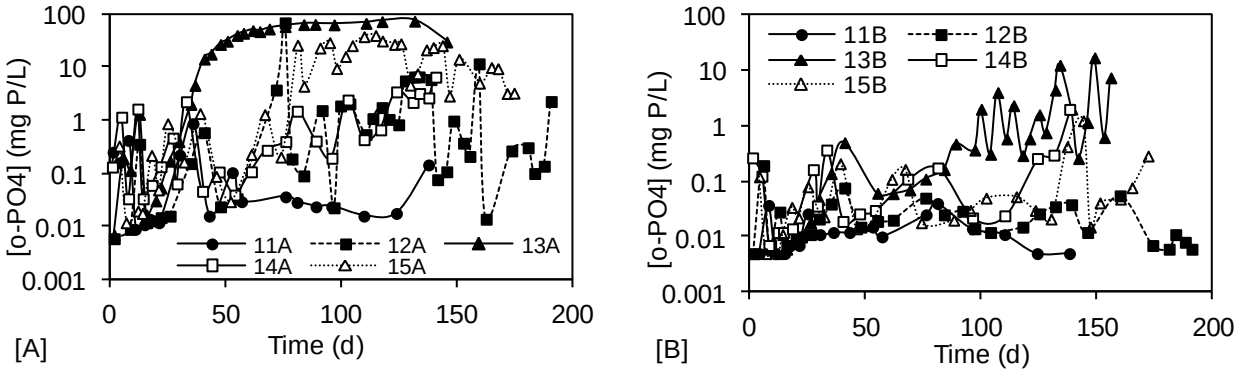

Figure 3.4: ortho-phosphates monitoring of column effluents, set 1

Phosphorus concentration was between 0.01 and 1 mg P/L when the effluent pH was over 10 independly of slag type. In general, downstream filters polished the upstream filters' effluent to concentrations between 0.01 and 0.1 mg P/L. Phosphorus removal efficiency was greatly affected by the loss of effluent high pH in columns 13A, 13B and 15A.

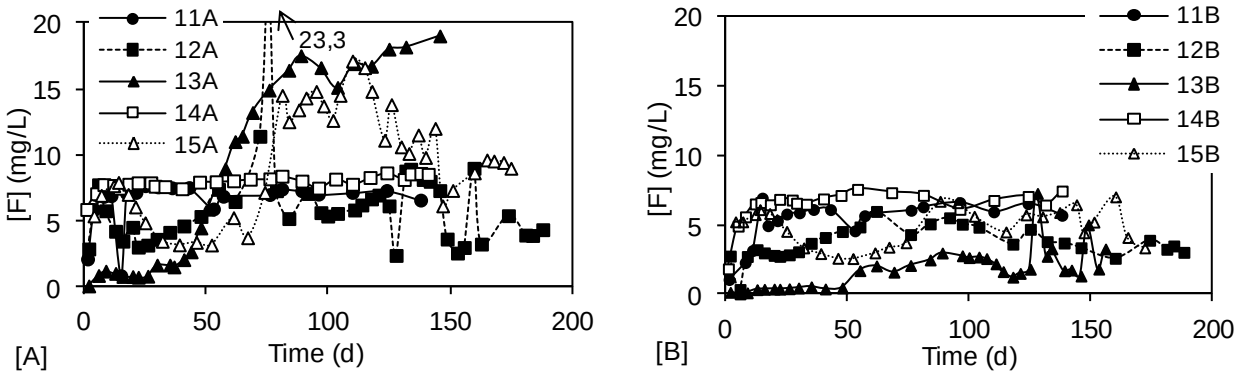

Figure 3.5: Fluoride monitoring of column effluents, set 1

Fluoride removal performance was low in WW 1 (initial concentration of 10 mg/L, treated concentration of 7 mg/L) and high in WW 3 (initial concentration of 40 mg/L, t treated concentration of 4 mg/L). Blytheville slag provided significant fluoride removal in WW 3 (<1 mg/L, column 13A) compared to Fort Smith slag (4 mg/L, column 12A). Fluoride removal was diminuished by high pH loss in column 13A and 15A. Downstream filters reduced of approximatly 1 mg/L the upstream filters' effluent concentration.

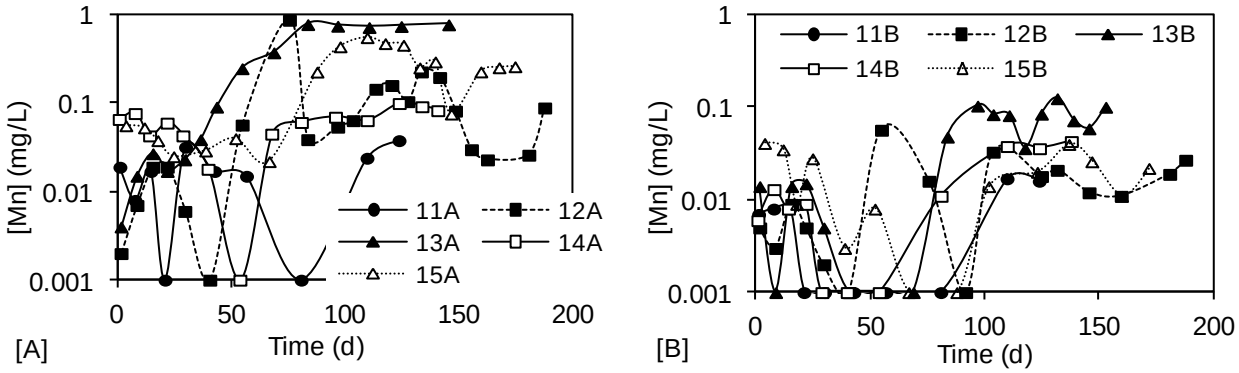

Figure 3.6: Manganese monitoring of column effluents, set 1

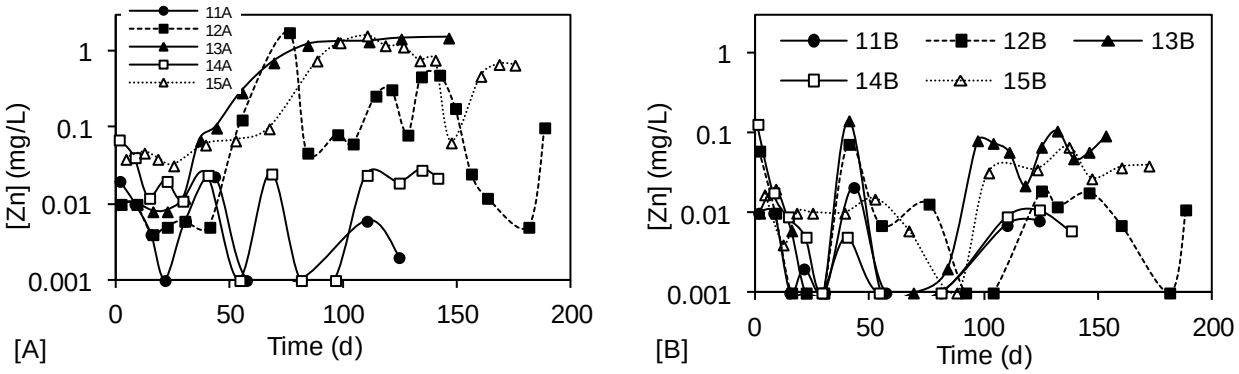

Figure 3.7: Zinc monitoring of column effluents, set 1

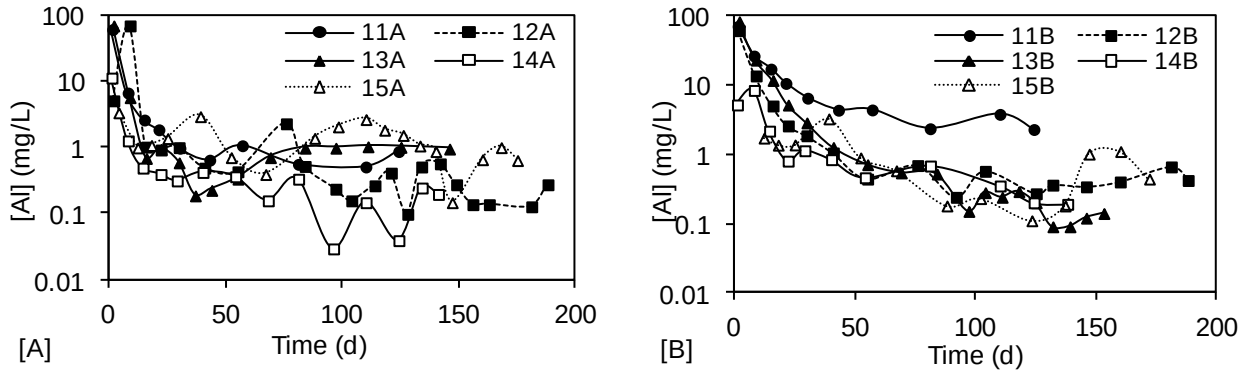

Figure 3.8: Aluminum monitoring of column effluents, set 1

Manganese and Zinc removal was affected by high pH loss in columns 13A and 15A. This relationship was not observed for aluminum, whose concentration was in general below 1 mg/L. However, initial leaching of aluminum was observed for all columns at the beginning of operation. When the pH was over 10, the manganese concentration was below 0.1 mg/L and the zinc concentration was below 0.5 mg/L.

3.3.2 Column set 2

Results of the second set of column tests are presented in Figure 3.9 to Figure 3.11.

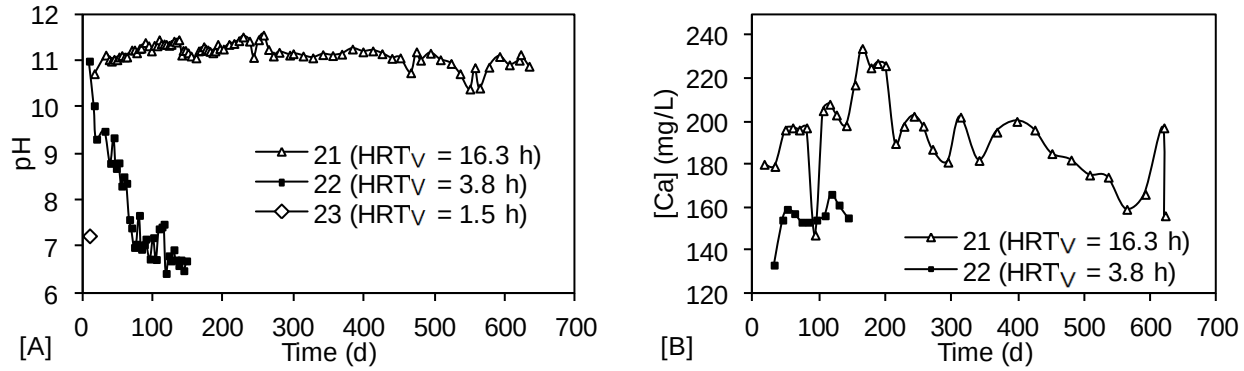

Figure 3.9 : pH and calcium monitoring of column effluents, set 2

The pH effluent was at 11 at the beginning of the test, after which a pH drop was observed in two columns. The pH drop appeared sooner when the column's HRT_V was shorter. No pH drop was observed in column 21. High pH at effluent was related to high calcium concentration.

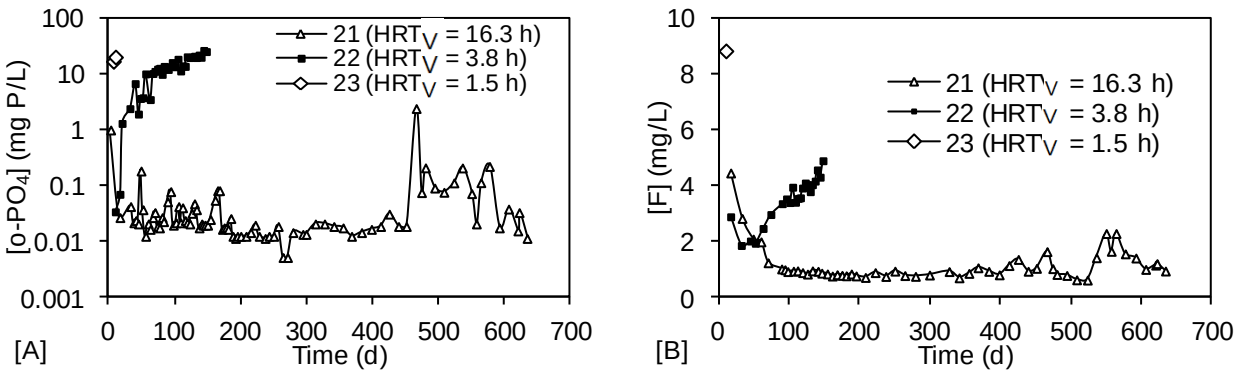

Figure 3.10 : ortho-phosphates and fluoride monitoring of column effluents, set 2

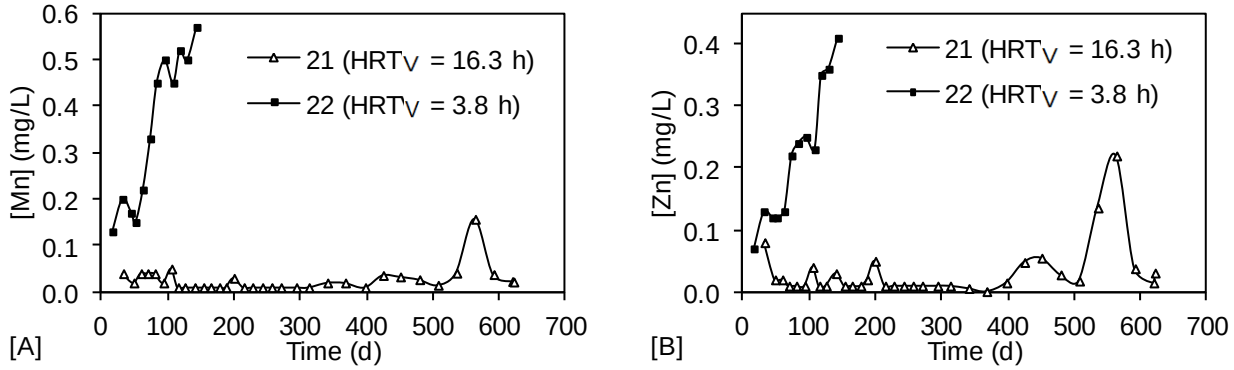

Figure 3.11 : Manganese and zinc monitoring of column effluents, set 2

Phosphorus, fluoride and metals were removed efficiently when the pH was over 10, as was observed in set 1. Phosphorus concentration was between 0.01 and 1 mg P/L when the effluent pH was over 10. Fluoride removal increased with time in column 21. The fluoride concentration at the effluent of this column was 4 mg/L in the first operation days and it decreased to 1 mg/L after 100 days of operation. Manganese and zinc concentration was below 0.2 mg/L when the pH was over 10 (column 21).

3.3.3 Precipitate characterization

A summary of precipitate characterization data is presented in Table 3.4. XRD theoretical diffractograms of HAP and calcite are shown in Figure 3.12. A new parameter was created to compare the proportions of HAP and calcite within sample: the HAP/$CaCO_3$ ratio. It was defined as the ratio between the intensity of the HAP peak at position $2\theta = 25.9°$ and the intensity of the calcite peak at position $2\theta = 29.5°$ (Figure 3.13). It is important to note that this parameter does

not allow to determine the quantitative proportion of HAP and calcite in the sample, but it is a method to qualitatively compare the amount of calcite in each sample.

Table 3.4 : Precipitate sampling and characterization

Column ID	**Sampling location in column**	**Sampling time**	**HAP/$CaCO_3$ ratio***	**HAP mean crystal size by XRD**	**$CaCO_3$ mean crystal size by XRD**
		d		**Å**	**Å**
11A	top	162	0.64	158	-
12A	top	222	2.56	334	-
12A	top	222	n. a.	345	-
12A	5 cm below top	222	n. a.	523	-
12A	mid-height	222	n. a.	450	-
12A	5 cm above bottom	222	n. a.	320	-
12A	bottom	222	n. a.	477	714
12B	top	222	n. a.	599	310
12B	bottom	222	0.590	187	2650
13A	top	169	n. a.	536	-
13A	5 cm above bottom	169	n. a.	652	-
13A	bottom	169	n. a.	579	-
14A	top	145	0.18	195	1125
14A	bottom	145	0.58	217	1911
14B	top	145	0.302	205	>max**
14B	bottom	145	0.273	190	3159
15A	top	179	n. a.	322	-
15A	top	179	n. a.	354	-
15A	mid-height	179	n. a.	418	-
15A	bottom	179	n. a.	402	-
15B	top	179	0.596	237	2220
15B	bottom	179	2.40	362	883
21	top	419	n. a.	580	-
21	bottom	438	n. a.	860	-
21	bottom	630	n. a.	735	-
22	bottom	148	n. a.	410	-
23	bottom	20	n. a.	230	-

*defined as the ratio of the intensity of the HAP peak at position $2\theta = 25.9°$ and the intensity of the calcite peak at position $2\theta = 29.5°$

** the crystal size is greater than the validity range of the Scherrer equation

Note: n.a.: not available

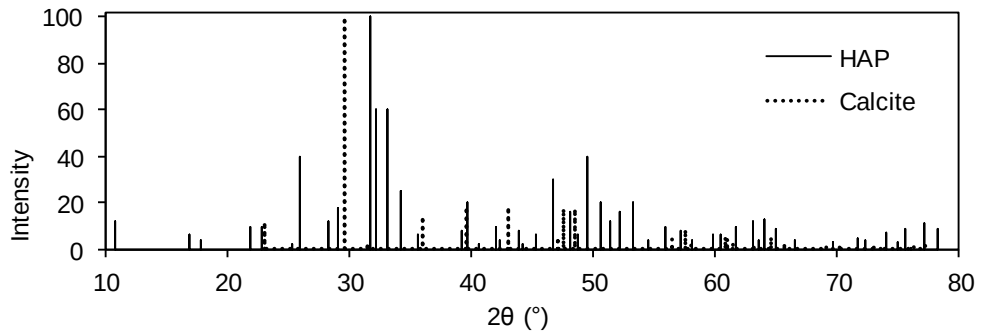

Figure 3.12 : Theoretical diffractograms of HAP and calcite

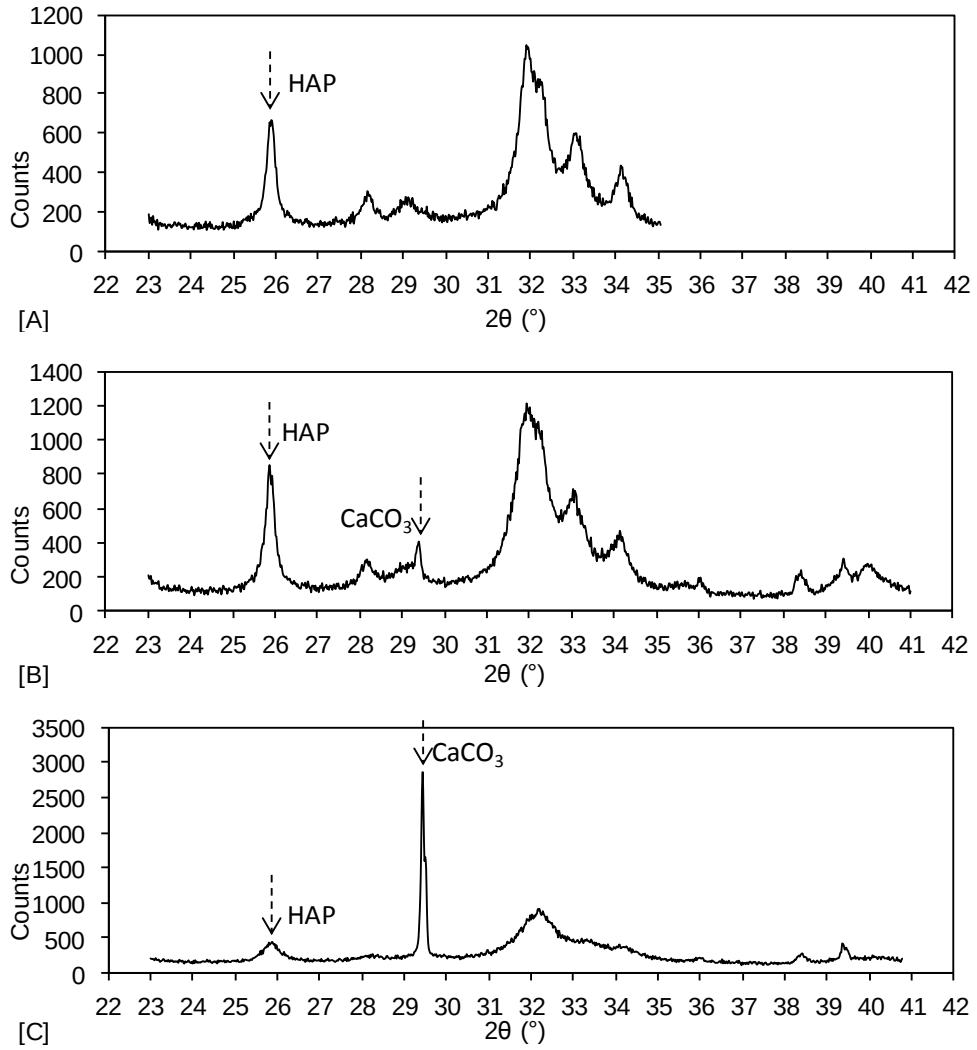

Figure 3.13 : Comparison of HAP / calcite proportions in XRD diffractograms based on intensity of two characteristic peaks. No calcite visible and HAP predominant (A); HAP predominant and calcite present (B); calcite predominant and HAP present (C)

3.4 Toxicity tests

Results of toxicity tests in distilled water and acetic acid are presented in Figure 3.14 and Figure 3.15. Only slags chosen for the column tests were tested (slag #1 and slag #7). Results are compared with Joplin performance goals within these figures.

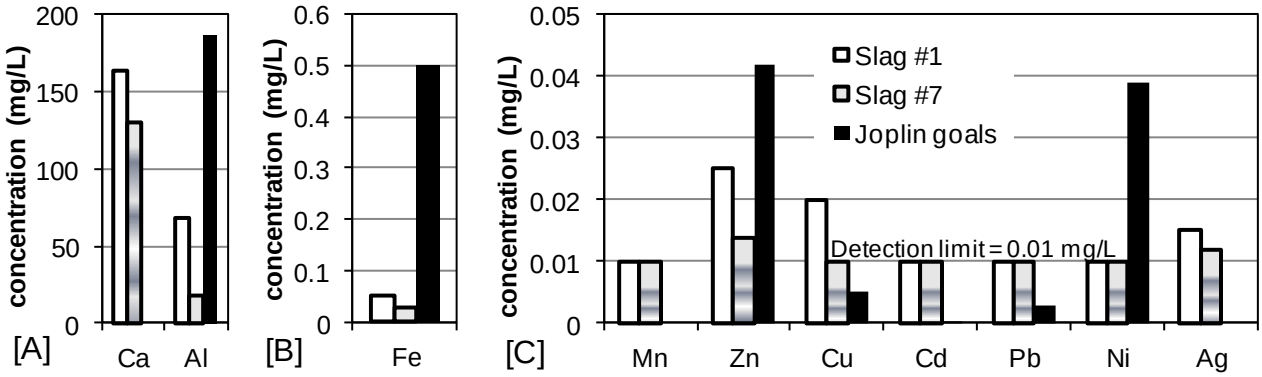

Figure 3.14 : Results of toxicity tests in distilled water for major compounds (A), iron (B) and trace compounds (C)

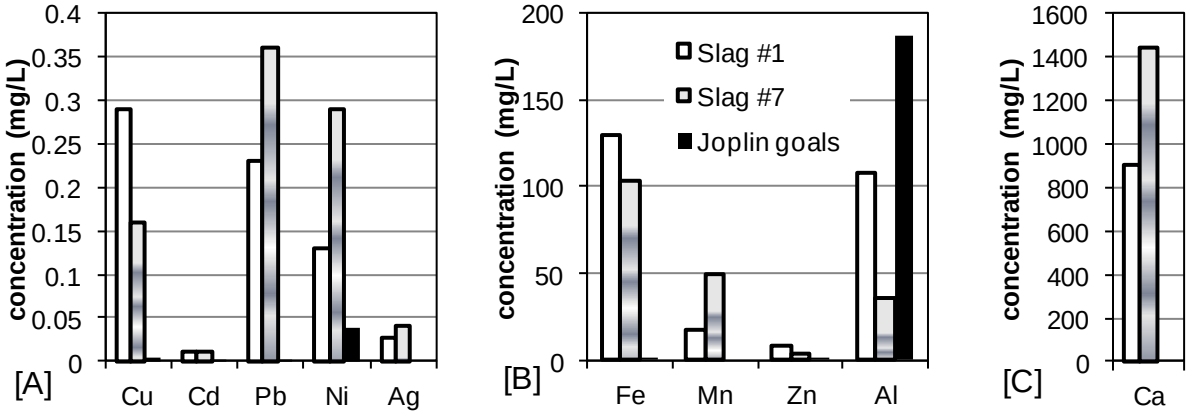

Figure 3.15 : Results of toxicity tests in acetic acid for trace compounds (A), major compounds (B) and calcium (C)

TCLP criterion for Ag, Cd and Pb were respected in the acetic acid extraction fluid, confirming that both slags are not toxic. However, Ba, As, Hg and organic compounds were not analyzed in these tests. They should be tested in a complete TCLP procedure in further work.

The Joplin performance goals were respected in distilled water for both slags, except for Cu. However, several metals (Mn, Cd, Pb, Ni) were present in concentrations lower than the detection limit.

In acetic acid, Joplin performance goals were not respected for several compounds (Cu, Pb, Ni, Fe, Zn).

An interpretation of toxicity tests results regarding the type of extraction fluid, TCLP criterion and Joplin performance goals is presented in section 5.1.

CHAPTER 4 MODEL OF PHOSPHORUS PRECIPITATION AND CRYSTAL FORMATION IN ELECTRIC ARC FURNACE STEEL SLAG FILTERS (ARTICLE)

ABSTRACT. The objective of this study was to develop a phosphorus retention mechanisms model based on precipitation and crystallization in electric arc furnace (EAF) slag filters. Three slag columns were fed during 30 to 630 days with a reconstituted mining effluent at different void hydraulic retention times. Precipitates formed in columns were characterized by X-ray diffraction and transmission electronic microscopy. The proposed model is expressed in the following steps: 1) the rate limiting dissolution of slag is represented by the dissolution of CaO, 2) a high pH in the slag filter results in phosphorus precipitation and crystal growth, 3) crystal retention takes place by filtration, settling and growth densification, 4) the decrease in available reaction volume is caused by crystal and other particulate matter accumulation (and decrease in available reaction time), and 5) the pH decreases in the filter over time if the reaction time is too low (which results in a reduced removal efficiency). Crystal organization in a slag filter determines its phosphorus retention capacity. Supersaturation and water velocity affect crystal organization. A compact crystal organization enhances the phosphorus retention capacity of the filter. A new approach to define filter performance is proposed: saturation retention capacity is expressed in units of mg P/ mL voids.

KEYWORDS. phosphorus, apatite, wastewater treatment, slag, removal mechanisms

4.1 Introduction

Phosphorus is generaly the limiting nutrient in freshwater systems and its discharge from wastewaters favors eutrophication. Phosphorus is typically removed in wastewater treatment plants by chemical precipitation and by biological systems (Metcalf & Eddy, 2003). Stricter regulations for phosphorus discharges to smaller treatment plants creates a need for the development of new and extensive (requiring minimal operation) treatment technologies. Steel slag filters offer a promising treatment system for efficient and economical phosphorus removal used as post treatment units from constructed wetland systems and other small scale wastewater treatment systems (Chazarenc, Brisson & Comeau, 2007; Shilton et al., 2005).

Steel slag is a by-product material from steel mills. The 2010 slag production in United States was estimated at 11 to 15 million metric tons (USGS, 2011). The use of various types and sizes of slag in reactive filters has been studied in batch tests, column tests and field tests (Chazarenc et al., 2008; Pratt & Shilton, 2010; Vohla et al., 2011). Fe-Ti rich slag filters were successfully used in a full-scale application (Shilton et al., 2006). Three potential limitations of slag filters were highlighted by Chazarenc et al (2008): a decrease in removal efficiency after 6 months was reported in a number of studies, filter clogging by physical and chemical solids accumulation, and diverging results in terms of a correlation between phosphorus removal efficiency and filter longevity between authors.

Calcium-rich slags are one type of slag of great interest. Calcium-rich slag filters result in high effluent pH, associated with efficient phosphorus removal (Chazarenc et al., 2008; Vohla et al., 2011). Two main mechanisms were studied in this type of filter: precipitation of phosphate phases and dissolution of slag.

Precipitation of phosphate phases occurs mainly as hydroxyapatite ($Ca_5(PO_4)_3OH$) formation in calcium-rich slag filters (e.g. (Baker et al., 1998; Chazarenc et al., 2008)). Nucleation and crystal growth of hydroxyapatite were proposed to be the limiting steps (Baker et al., 1998) for phosphorus removal. A succession of different phosphorus mineralogical phases on slag particles with time was also reported (Bowden et al., 2009). Some authors suggested that in a high pH environment typical of calcium-rich slag, adsorption is inhibited and precipitation is the main removal mechanism (Baker et al., 1998; Bowden et al., 2009).

Different aspects of slag dissolution were studied by some authors. pH rise was shown to be related to the dissolution of a succession of different complex mineralogical phases containing calcium oxides, such as bredigite ($Ca_{14}Mg_2(SiO_4)_8$) and gehlenite ($Ca_2Al_2SiO_7$) (Kostura et al., 2005). The acid-neutralization capacity of slag was used to study the kinetics of pH rise. The effect of a longer hydraulic retention time on increased retention capacity was observed by some authors (Drizo et al., 2006; Shilton et al., 2005).

The lack of similarity between results obtained under different testing conditions (type of slag, type of wastewater, flow properties, filter geometry) and proposed explanations creates a need to develop a removal mechanism model to predict the performance of calcium-rich slag filters (P removal efficiency and longevity). The objective of this paper was to study phosphorus

retention mechanisms in calcium-rich slag filters using column tests and to propose a phosphorus retention mechanism model.

4.2 Materials and methods

4.2.1 Reactive media and reconstituted effluent

The tested slag was 5-10 mm electric arc furnace (EAF) slag from Contrecoeur, Quebec, Canada. This slag was previously shown to be efficient for phosphorus removal (Drizo et al., 2002; Drizo et al., 2006; Forget, 2001). The slag density is 3.6 g/cm^3 and its Fe_2O_3, CaO, SiO_2 and MgO contents were 33%, 30%, 16% and 12%, respectively.

A reconstituted gypsum mining effluent was used for column tests. Chemical salts were dissolved in distilled water to form three 2-liter concentrated solutions. Solution 1 contained KH_2PO_4, NaF, $(NH_4)_2SO_4$, K_2SO_4, Na_2SO_4 and $NaNO_3$; solution 2 contained $Al_2(SO_4)_3 18H_2O$, $MgSO_4 7H_2O$, $MnSO_4 H_2O$ and $ZnSO_4 7H_2O$ and solution 3 contained $CaCl_2 3H_2O$. These solutions were mixed together in a 200-liter barrel half-filled with distilled water. Then, distilled water was added up to 200 liters. Concentrated NaOH was added for pH adjustment. Flocs formed during pH adjustment were settled and the clear water was analyzed and used from the barrel for testing. The main characteristics of the settled reconstituted water were pH = 6.52, [Ca] = 151 mg/L, [Na] = 146 mg/L, [K] = 52 mg/L, [Mg] = 8 mg/L, [Mn] = 0.72 mg/L, [Zn] = 0.53 mg/L, [Cl] = 197 mg/L, [$S0_4$] = 134 mg S/L, [o-PO_4] = 26 mg P/L and [F] = 6.9 mg/L. Sampling and analyses of the reconstituted effluent were performed for each new 200-liter feed barrel.

4.2.2 Column tests

Three vertical transparent columns of 15 cm in diameter by 17 cm in length were continuously fed by a peristaltic pump with the reconstituted effluent. Void volume hydraulic retention times (HRT_V) of 16.3 h, 3.8 h and 1.5 h were maintained for a duration of 630, 152 and 30 days, respectively. The void volume was defined as that occupied by liquid and air at the beginning of the test. The void volume was determined with a weight method proposed by Chapuis et al. (1989), using the volume of the empty column and the mass and density of the slag in the column. These initial HRT_V corresponded to water velocities of 14, 49 and 152 mm/h, respectively.

The effluent from each column was sampled every two weeks for o-PO_4 and calcium concentration, and for pH. pH determinations were conducted within a half-hour of sampling to minimize interference with atmospheric carbon dioxide.

The precipitate formed in the columns was sampled at the inlet of the columns at the end of the operation of a column, and air-dried. An extra precipitate sample was taken in the column with an HRT_V of 16.3 h during operation after 438 days.

4.2.3 Analytical determinations

Analysis for slag composition was performed by Acme Labs (Vancouver, B.C., Canada) with ICP-emission spectrometry preceded by a $LiBO_2/Li_2B_4O_7$ fusion and dilute nitric digestion. Analyses of o-PO_4 were conducted with a Lachat QuikChem 8500 flow injection analyser, using the ascorbic acid method (APHA et al., 2005). Analyses of Ca were conducted with a AAnalyst 200 flame atomic absorption apparatus, using a standard mass spectrometry method (Centre d'expertise en analyse environnementale du Québec, 2006). Powdered precipitate samples were used for X-ray diffraction (XRD) and transmission electronic microscope (TEM) analyses. XRD analyses were performed with a Philipps X'Pert diffractometer operated at 50 kV and 40 mA, using the Bragg-Brentano geometry and a Cuk_{α} radiation. The mean size of crystal was determined from XRD diffractograms with the Scherrer equation (Cullity, 2001). TEM analyses were performed with a Jeol JEM-2100f field emission gun microscope operated at 200 kV, using bright field imaging technique. Samples were prepared on a typical copper grid covered with Formwar lightly coated with amorphous carbon.

4.3 Results

All columns had an effluent pH between 11.0 and 11.5 at the beginning of the test. A pH decrease in the effluent was observed after 20 and 1 day for columns having initial HRT_V of 3.8 and 1.5 hours, respectively. No pH drop was observed in the column having an initial HRT_V of 16.3 h after 630 days. Calcium concentration at the columns effluent was approximately 200 mg/L when the effluent pH was over 11. The relationship between effluent pH and effluent o-PO_4 concentration is presented in Figure 4.1. The increase in phosphorus concentration at the effluent of these columns was associated with a decrease in effluent pH.

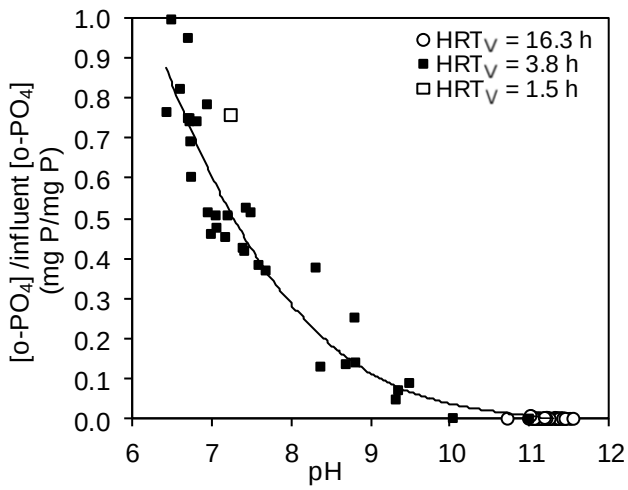

Figure 4.1 : Relationship between effluent pH and normalized effluent o-PO_4 (influent [o-PO_4] = 26 ± 2 mg P/L)

The phosphorus removal within each column is presented with respect to the influent P loading expressed in mg P added / g slag (Figure 4.2A) and mg P added / mL voids (Figure 4.2B). The expression of P removal in mg P / mL voids is proposed to account for P accumulation in the filter voids, as explained in a subsequent section. The saturation retention capacity was defined as the maximum amount of phosphorus removed by a filter and was determined for two of the three columns. Saturation retention capacities were 2.0 and 14.5 mg P/ void mL for columns with HRT_V of 1.5 and 3.8 h, respectively. Saturation was not reached for the column with HRT of 16.3 h but was greater than 23 mg P/ mL void.

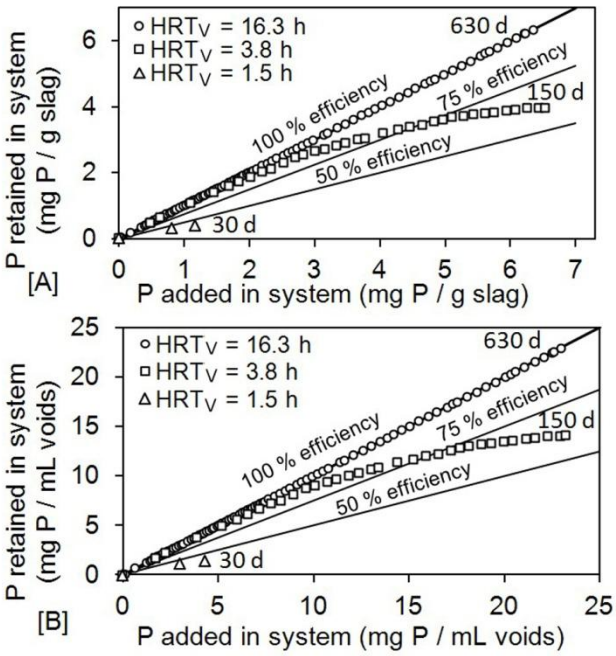

Figure 4.2 : Phosphorus removal efficiency at different HRTV expressed in traditional mg P / g slag (A) and newly proposed mg P / mL voids (B). The duration of the experiment is indicated besides the last data point presented

Results from crystal analyses and observations are presented in Figure 4.3 and Figure 4.4. White precipitate accumulation was visible in all columns. A slowly moving precipitation bed was observed in the column with an HRT_V of 16.3 h and its position is shown in Figure 4.3. Settling of crystals was visible within this column. In the other columns, white precipitates were uniformly distributed within the column and no settling was observed.

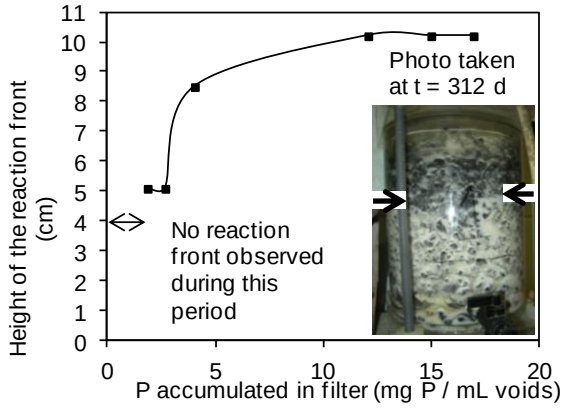

Figure 4.3 : Progression of the precipitate bed within the HRT_V = 16.3 h column. The position of the reaction front was determined visually

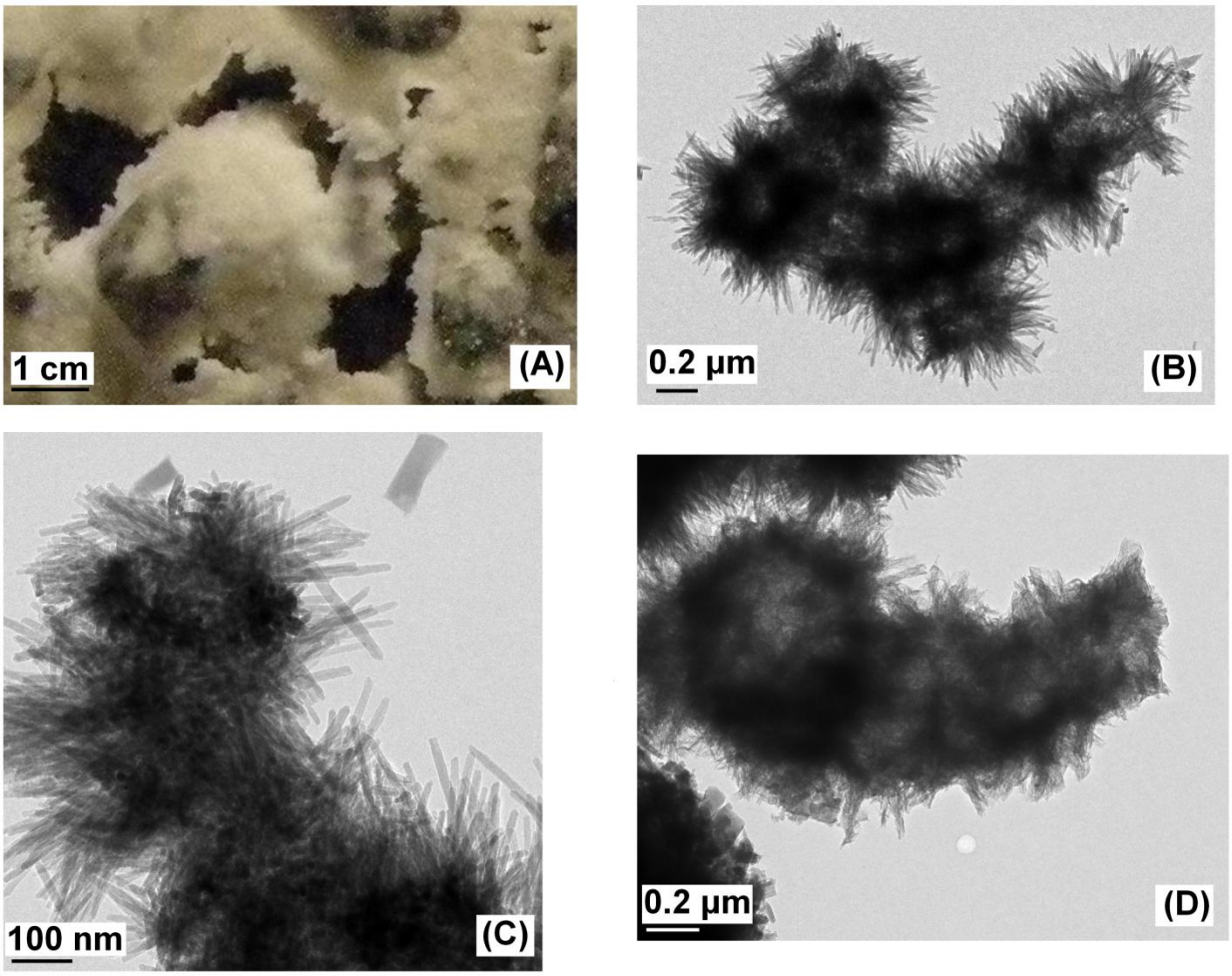

Figure 4.4 : Photo of white crystals (>95% apatite confirmed by X-ray diffraction) formed on cavity wall (A); TEM photo of apatite crystal aggregate (B); TEM photo of acicular apatite crystals (C); TEM photo of a crystal seed with fibrous aspect (D)

Precipitates in columns were sampled and analyzed. It was determined by X-ray diffraction that precipitates were crystalline and that they corresponded to the theoretical hydroxyapatite diffractogram by more than 95%. Mean crystal sizes determined by X-ray diffraction were from 20 to 86 nm in different columns. Apatite crystal shapes seen in transmission electronic microscope (TEM) imagery were either acicular or fibrous crystals. Crystals were organized in agglomerates of one mean crystal size (Figure 4.4). The mean crystal width in one agglomerate was between 5 and 40 nm. Fibrous crystals were smaller than acicular crystals. Crystal formation around filter cavities was visible to the naked eye, as shown in Figure 4.4A. Determination of the crystal size was done using the diffractogram peak at position $2\theta = 26°$.

4.4 Discussion

4.4.1 Slag dissolution and role of pH

Phosphorus treatment in calcium-rich slag filters depends largely on the dissolution of slag in the water to be treated. Dissolution of slag involves complex kinetic reactions of various mineralogical phases such as bredigite ($Ca_{14}Mg_2(SiO_4)_8$) and gehlenite ($Ca_2Al_2SiO_7$) (Kostura et al., 2005). However, dissolution of slag can be approximated by the dissolution of CaO, which results in an increase of calcium and hydroxide (pH) concentration.

A high pH is the major factor that ensures an efficient phosphorus removal. Under basic conditions, phosphorus is precipitated in a variety of metastable calcium phosphates (Lundager Madsen, 2008) that are transformed into hydroxyapatite ($Ca_5(PO_4)_3OH$), a final stable mineralogical phase. A strong link between o-PO_4 concentration and pH in the effluent was observed (Figure 4.1). The hydroxyapatite composition of the precipitate was confirmed by XRD. Particles were efficiently retained in the filter by filtration. Should water velocity in the filter have been too high, precipitates could have leached out of the columns. This phenomenon was observed for columns with HRT_Vs of 1.5 and 3.8 h. When the water velocity was low enough, particles settled in the column as observed in that with an HRT_V of 16.3 h.

4.4.2 Water velocity and crystal behavior in the filter

Columns with longer hydraulic retention times reached greater retention capacities. As column size and geometry were identical, testing different hydraulic retention times meant testing different water velocities. A non linear relationship between P retention capacity and water velocity was observed in this study (Figure 4.5).

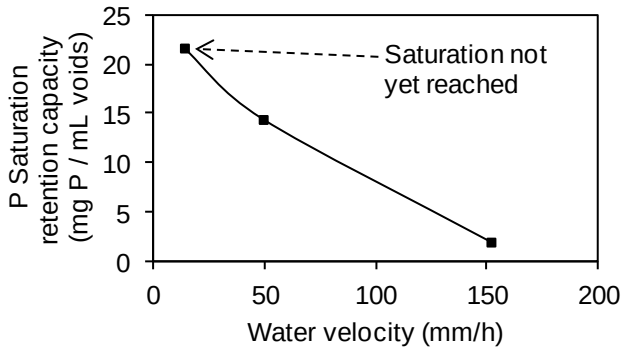

Figure 4.5 : Effect of water velocity on phosphorus retention capacity

XRD analyses indicated that apatite crystals were of different mean sizes for different conditions (different HRT_V and sampling time). The rate of crystal growth appeared to be constant for the conditions tested, independently of water velocity (Figure 4.6). TEM analyses showed that apatite crystals formed acicular agglomerates. Different mean crystal sizes of different agglomerates in the same column were observed. It is suggested that each crystal agglomerate offers a growing hydroxyapatite (HAP) seed. During operation, pre-existing seeds continue to grow while new seeds are formed, resulting in different seed crystal sizes. These results indicate that crystal growth represents a major part of the P removal mechanism in calcium-rich slag filters and that the rate of crystal growth is independent of water velocity. Thus, crystals have a maximum rate of growth that cannot be increased by higher loading rates. If the growing capacity of existing seeds is exceeded by input phosphorus, new seeds will be formed and they will contribute to the phosphorus removal.

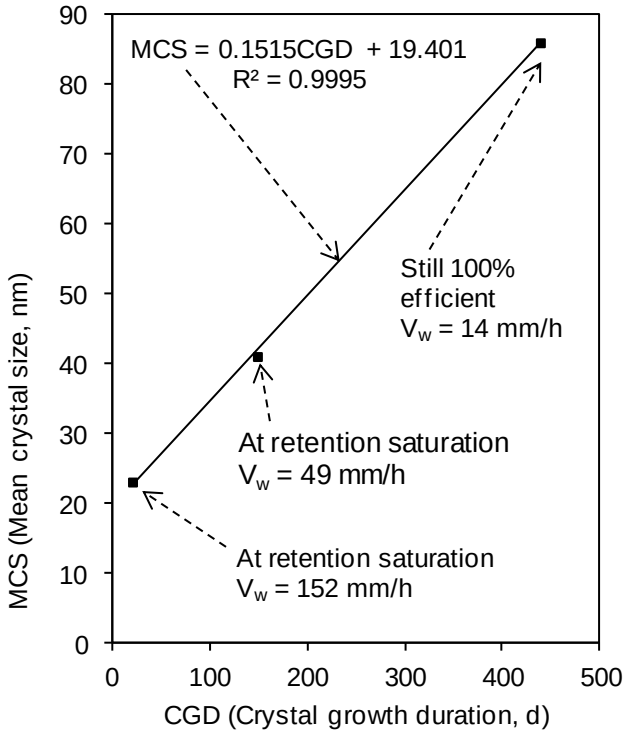

Figure 4.6 : Crystal growth observed in filters (three data points for three different filters). Mean crystal size was determined by XRD and V_w stands for water velocity

While the rate of crystal growth is independent of hydraulic conditions, it is influenced by the chemical composition of the water in contact with HAP crystals. pH has a major impact on the rate of crystal growth, as phosphorus removal is not significantly achieved at pH values under 7 (Figure 4.1). In this study, since the influent composition was constant and completely soluble, it was not possible to assess the influence of phosphorus or other ions concentration on crystal growth rate. However, some authors have shown the influence of hydroxide, phosphorus, calcium and other metallic ions on crystal growth behavior of apatite (Lundager Madsen, 2008; Tsuru et al., 2001). Metals as Zn and Cd were found to be nucleation promoters by precipitation of insoluble compatible metal phases in the apatite seeds and metals as Pb were found to be growth inhibitor of apatite because of adsorption onto crystals (Lundager Madsen, 2008). Hydroxides were shown to act as growth catalysts of apatite while Ca acted as a nucleation catalyst (Tsuru et al., 2001).

A high P retention capacity was favored by two factors, a low water velocity and a large mean crystal size. These two factors also resulted in a more compact organization of crystals. A low water velocity favored settling and the accumulation of crystals at the bottom of a vertical

upflow filter. Large crystal sizes meant that phosphorus was removed by crystal growth on preexisting seeds instead of precipitating in new seeds, resulting in a denser crystal structure and a greater P removal capacity.

4.4.3 Proposed conceptual model

A model for phosphorus removal mechanisms in calcium-rich slag filters is presented on the basis of two main hypotheses:

a) Phosphorus removal is achieved by the formation of hydroxyapatite at a high pH (Baker et al., 1998) which is the result of the rate limiting dissolution of CaO from slag (Kostura et al., 2005). Thus, the HRT_V should be long enough to allow the dissolution of CaO from the specific slag used into the effluent to be treated.

b) The hydroxyapatite crystal state (size, organization) in the filter determines the P retention capacity of the slag filter.

The model is expressed in four steps:

A minimum hydraulic retention time is necessary to kinetically raise the pH up to a value that allows phosphorus precipitation and crystallisation as hydroxyapatite (pH > 10.5 according to this study). This time is dependent on the type of slag and the influent water composition (pH, buffer capacity, concentration of phosphorus, concentration of competitive compounds such as inorganic carbon, organic soluble and particulate matter, inorganic particulate matter, etc). A preliminary treatment (e.g. aeration, settling, filtration) can reduce the concentration of competitive compounds.

Phosphorus precipitates accumulate in the filter by three means: 1- precipitation of new crystals and filtration, 2- settling and 3- crystal growth on preexisting seeds.

The P removal efficiency gradually decreases as explained by two phenomena. First, HRT_V decreases with time because crystal accumulation creates confined cavity volumes and short-circuiting in the filter. If the hydraulic retention time decreases under a critical value, the pH rise and precipitation become kinetically limiting, resulting in a decrease in treatment efficiency. Second, a decrease in P removal efficiency is caused by a decrease in the rate of dissolution of slag. The dissolution rate will decrease because of the complexity of the slag

composition. Some calcium oxides present at the slag surface are readily dissolved. These oxides determine the dissolution rate at the beginning of the filter life. When they become largely dissolved, the dissolution rate will be determined by the slower dissolution of more complex oxides from surfaces still exposed to the flowing liquid.

The volume fraction of confined cavities (degree of short-circuiting) is affected by the accumulation of crystals. A compact accumulation of crystals in voids favours an efficient utilization of the available space and limits short-circuiting. A loose accumulation of crystal in voids, however, creates more confined void spaces that are not any more available for water circulation and favours short-circuiting.

The impact of crystal organization and the effect of water velocity are illustrated in Figure 4.7, where two slag filters with different water velocities are represented. These two filters have the same initial geometry and mass of slag. They also have the same mass of formed crystals, but with different crystal organization. The loose crystal organization creates a large proportion of confined spaces, where flowing water has limited access. When this filter reaches a critical effective volume (i.e. volume available for water circulation and reaction) after which the dissolution of slag becomes kinetically limited, the amount of crystals accumulating in the filter (instead of being washed out) becomes low, resulting in a poor retention capacity. Therefore, the crystal organization behavior in a slag filter is a key concept to describe its retention capacity. Factors that influence crystal accumulation and organization are discussed in the next section.

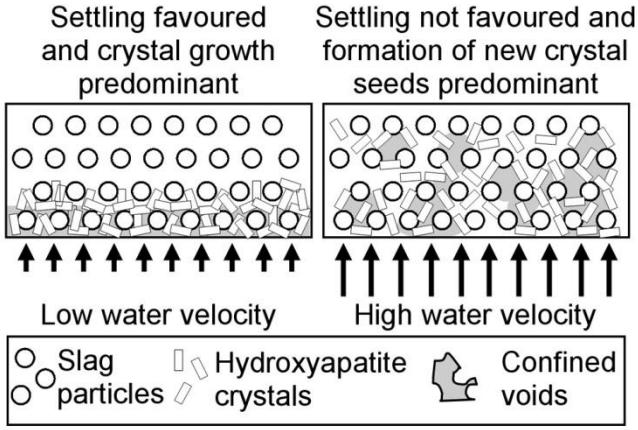

Figure 4.7 : Conceptual representation of a compact (left) and a loose (right) crystal organization in a slag filter. The mass of apatite crystals in the filter is considered identical in both filters

4.4.4 Parameters that influence crystal accumulation and organization

Two main feeding conditions influence crystal accumulation and organization. The first parameter is the composition of the influent solution. First, organic and inorganic particles directly accumulate in the filter. If particles are removed in an upstream treatment, only the dissolved components contribute to accumulation by precipitation. Dissolved components include mainly organic matter, inorganic carbon, phosphorus and cations. This parameter was not directly evaluated in this study, as only one influent was used, containing no organic matter and low soluble inorganic carbon. However, it was shown that the degree of supersaturation influences the crystallization behavior (Aldaco, Irabien & Luis, 2005; Seckler, Bruinsma & van Rosmalen, 1991). A high supersaturation index of crystals favours the formation of new crystal seeds against crystal growth on pre-existing seeds for fluoride precipitates (Aldaco, Irabien & Luis, 2005). Different crystal shapes under different phosphorus concentrations for various calcium phosphate precipitates were observed (Seckler et al., 1991). Other authors have shown that the presence or deficiency in different ions influenced crystal shape, crystal nucleation and crystal growth (Lundager Madsen, 2008; Tsuru et al., 2001; Yousefpour et al., 2006). Further work is needed to assess the contribution to crystal accumulation and organization of organic matter and inorganic carbon.

The composition of the slag also influences crystal accumulation. If the slag leaches metallic ions, they may act as catalysts or inhibitors. Adsorption phenomena onto slag surface may influence the nucleation step of apatite formation. Adsorption bonds between phosphorus and iron present in slag have been reported (Drizo et al., 2002).

Water velocity in the filter is the second main parameter that influences crystal accumulation and organization. A low water velocity allows phosphorus to completely precipitate in a shorter distance than a high water velocity, as illustrated in Figure 4.7. When precipitation and crystallization occur over a short distance, crystals are more likely to be organized in a dense network by growth on existing crystal seeds. When precipitation and crystallization occur over a longer distance, crystals form in a dispersed space and more confined voids are created. Therefore, the hydraulic properties of the filter should be designed to avoid local high velocities at the entrance and to uniformly distribute the influent. Moreover, a low water velocity allows

newly formed seeds to settle, favouring a compact crystal organization. Further work is needed to compare the crystal organization of filters in continuous and intermittent inflow conditions.

The proposed model is expressed in a conceptual mathematical expression for the pH at the effluent of the filter (equation 4.1). k is the kinetic constant of dissolution of slag and it is dependent on the slag type, the influent composition and time. HRT_V is the theoretical initial void volume and it has a constant value. F_c is the crystal accumulation factor, introduced in the mathematical expression to consider the volume occupied by crystal and confined voids. Its value is between 0 (volume completely filled with crystals or confined voids) and 1 (all the volume is available). F_c depends on influent composition, filter geometry, water velocity and time.

$$pH_{effluent}(t) = f(k, HRT_V, F_c) \tag{4.1}$$

Knowing the expressions for f, k and F_c would allow to determine the duration when the effluent pH will be above a critical value such as 10.5 and to estimate the longevity of the filter. Further work is needed to evaluate these expressions and to validate the conceptual equation 1.

4.4.5 A new approach for the expression of phosphorus retention capacity

P retention capacities are usually reported in mg P/g slag (Bowden et al., 2009; Chazarenc et al., 2008; Drizo et al., 2002; Pratt & Shilton, 2010; Vohla et al., 2011). An expression of this type refers to P retention capacity related to the slag itself. In this study, it was shown that the P retention capacity was related to HAP crystal accumulation in the filter voids. Therefore, retention capacities are reported in mg P/ mL voids. These units can be easily converted into g hydroxyapatite / mL voids using the stoichiometric ratio 16.19 g HAP/g P. These last units allow to compare observed P retention capacities with some reference or theoretical P retention values. As an example, the theoretical maximum P retention capacity is between 2.6 and 3.0 g hydroxyapatite / mL voids, which is the range for the density of many natural HAP crystals. This value represents an ultimate upper limit that is impossible to reach, as it would mean that the filter would be completely filled with rock apatite. Another interesting retention capacity value is 1.8 g hydroxyapatite / mL voids, which corresponds to a natural spherical sand density. This value corresponds to an extremely high removal efficiency, as no confined spaces would be created except for the spaces between compacted spheres. Again, this value is not possible to reach because crystals organize in acicular aggregates, which are less compact than sand. The

higher retention capacity obtained in this study was 0.35 g hydroxyapatite / mL voids, which is 4 times lower than a natural sand density. This value is higher than obtained (0.15 g hydroxyapatite / mL voids) in previous experiments conducted with the same media (Drizo et al., 2002).

Crystals were determined to be composed of >95% hydroxyapatite. Retention capacities were converted from mg P / mL voids to mg hydroxyapatite / mL voids using the stoichiometric composition of hydroxyapatite. With real effluents containing organic inorganic matter in both soluble and particulate forms, including inorganic carbon, other compounds would accumulate or form (e.g. calcite precipitates). Therefore, retention capacities would be converted from mg P / mL voids to mg crystal / mL voids using the mean stoichiometric composition of the crystal. The advantage of this approach is to consider the effect of competitive compounds on treatment capacities of slag.

4.4.6 Practical recommendations

In full scale applications, the phosphorus removal performance of a calcium-rich slag filter can be increased by providing an efficient upstream treatment. Components of wastewaters that compete with phosphorus precipitation should be removed prior to slag filtration. A biological treatment (e.g. constructed wetland) reduces the organic matter loading to the slag filter, limiting biofilm formation and solids accumulation that would favor filter clogging. Chemical clogging by carbonate precipitates may happen, particularly at a high HRT (Liira et al., 2009). The formation of carbonate precipitates was not observed in this study because of the composition of the synthetic wastewater that did not contain inorganic carbon. In full-scale applications, the HRT should be high enough to favor compact crystallization and low enough to minimize the precipitation of carbonates. The formation of calcium carbonate in the slag filter can be limited by trapping bicarbonate in an easily cleaned preliminary coarse slag filter and by minimizing exposure to air (instead of CO_2 trapping in a high pH solution). Major cations such as Ca or Mg, if present at high concentration, may limit the dissolution rate of slag and should be removed if possible. Secondary metallic ions may also inhibit or promote the formation of hydroxyapatite. The slag filter effluent should be neutralized prior to discharge by dilution or neutralization by peat (Koiv et al., 2009) or gaseous CO_2 neutralisation (Sawyer, McCarty & Parkin, 2003).

The type of slag for the filter should be selected on the basis of several properties. The slag used in the filter should be a non hazardous material as determined by standard leaching testing such that its effluent should be non toxic to meet discharge criteria and to facilitate final disposal or valorization. It should have a strong mechanical stability to avoid disaggregation and the formation of fines during preparation, which would favor clogging. Its calcium oxide dissolution rate in the effluent to be treated should be sufficient and steady enough to increase the pH even with wastewaters having a high buffering capacity for long-term operation. Factors influencing the dissolution rate should be studied in greater detail, but it should be related, notably, to slag size, precipitates accumulation and CaO and FeO content.

Crystal growth rather than the formation of new crystal seeds should be favored. To promote crystal growth, the water velocity should be kept low enough (high HRT_V) and the configuration of the filter should provide uniform influent distribution (using vertical flow, inlet diffuser, uniform slag size) to avoid high local water velocities and short-circuiting. The minimum HRT_V required to favor crystal growth and long-term operation is related to the hydroxyapatite crystal growth rate, which is related to the composition of the water.

ACKNOWLEDGEMENTS. Technical support from Denis Bouchard of Ecole Polytechnique of Montreal is gratefully acknowledged. Scientific assistance was provided by Shaw Environmental. This project was supported by the Missouri Remediation Trust, the Natural Sciences and Engineering Research Council of Canada and the *Fonds québécois de la recherche sur la nature et les technologies*.

CHAPTER 5 TREATMENT PERFORMANCE OF SLAG FILTERS

This chapter addresses to the first objective of the master project, which is proposing a treatment system for the Joplin mine.

5.1 Selection of media and treatment sequences

The objective of running individual and sequential batch tests was to choose the most promising media and sequences to test in lab-scale filters. Apatite was discarded because its phosphorus removal efficiency was too low compared to slag media. Individual batch tests results indicated that three types of slag were very efficient to raise the pH and, as a result, for phosphorus and metal removal (slags #3, #7 and #10). Slag #1 was efficient for fluoride removal (final fluoride concentration of 0.3 mg/L), but only in WW 1, where its final pH was over 11. In WW 3, its final pH was only 8.5, resulting in a final fluoride concentration of 15 mg/L. Therefore, the fluoride removal seems to be highest at high pH, but only for one type of slag. A question was formulated on the basis of individual batch tests results. Can we increase the fluoride removal capacity of slag #1 by adding an upstream filter to raise the pH? This question led to the sequential batch test program, in which this specific sequence was tested. A first filter resulting in a high pH rise (slags #3, #7 and #10) was followed by a filter with a high fluoride removal efficiency (slag #1). Only the more concentrated WW 3 was used in sequential batch tests because it was not possible to compare efficiently the pH rise capacity using WW 1.

Results of sequential batch tests validated the hypothesis formulated in the last paragraph. Fluoride removal capacity of slag #1 was improved by an upstream pH-rise filter. The most efficient sequence was slag #10-slag #1, but slag #10 was discarded because it was too friable for a filter application. Therefore, the sequence slag #7-slag #1 was chosen for column tests. Single slag systems composed of slag #1 or slag #7 were also tested for comparison purpose.

Environmental safety of slag #1 and slag #7 was assessed from the toxicity test results. These two slags were considered non toxic regarding TCLP criterion. However, TCLP results must be compared to stricter limits because slag will leach directly in the environment in a slag filter application. In distilled water, slags #1 and #7 leaching resulted in concentrations lower than the performance goals for all compounds except for the copper goal for slag #1 (concentration of 0.02 mg/L compared to a goal of 0.005 mg/L). In acetic acid, however, all the

performance goals were exceeded for both slags. In a full-scale application, both situations (leaching in distilled water or acetic acid) may happen. An efficient filter will leach as if it were tested in the distilled water toxicity test. If it is deficient, it will act as if it were tested in acetic acid (the slag is not able any more to raise the acid pH of the WW). The parameter that determines the most the leaching behavior of slag is pH. As long as the pH remains high, metals will not be leached. Therefore, filters should be replaced before their treatment capacity is reached (i.e. the effluent pH drops) to minimize metal leaching. As long as they are used with a high effluent pH, slag #1 and #7 are environmentally safe, except for copper leaching of slag #1. In further work, all trace compounds (heavy metals) should be monitored in column tests to assess the leaching behavior of the filter within time and confirm its environmental safety.

5.2 Efficiency and longevity of filters

The column tests experimental setup is represented in Figure 5.1. Results of column tests (set 1) showed that the efficient treatment of a multi-component WW is possible. The treatment performance of upstream columns is shown in Table 5.1Figure 5.4. The best global removal efficiency in WW 3, which corresponds to a concentrated WW, was obtained by the sequence slag #1 – slag #1. This sequence achieved global removals of 98.8 %, 94.8 %, 94.4 % and 98.6 % for P, F, Mn and Zn, respectively, after 169 days of operation. However, a decrease in pH and removal efficiency was observed in the upstream column after 30 days, limiting its use as a long-term treatment system. The sequence slag #7 – slag #7 resulted in a lower fluoride removal efficiency, but in a greater longevity as the pH decrease in the upstream column was observed after 70 days of operation. The global removal of sequence slag #7 – slag #7 after 179 days of operation was 99.9 %, 85.3 %, 98.0 % and 99.3 % for P, F, Mn and Zn, respectively.

Table 5.1 : Contaminant retention for Joplin column tests

Column	**Reached retention capacity (mg contaminant/g media)**					**WW type**	**HRT_V (h)**	**slag type**
	P	**F**	**Mn**	**Zn**	**Al**			
11A	0.737	0.16	0.010	0.011	0.050	1	14.2	7
12A	8.26	2.30	0.053	0.241	0.369	3	17.2	7
13A	4.54	2.46	0.026	0.183	0.387	3	14.5	1
14A	2.62	0.301	0.035	0.048	0.227	1	4.8	7
15A	8.11	2.21	0.054	0.244	0.516	3	19.2	7

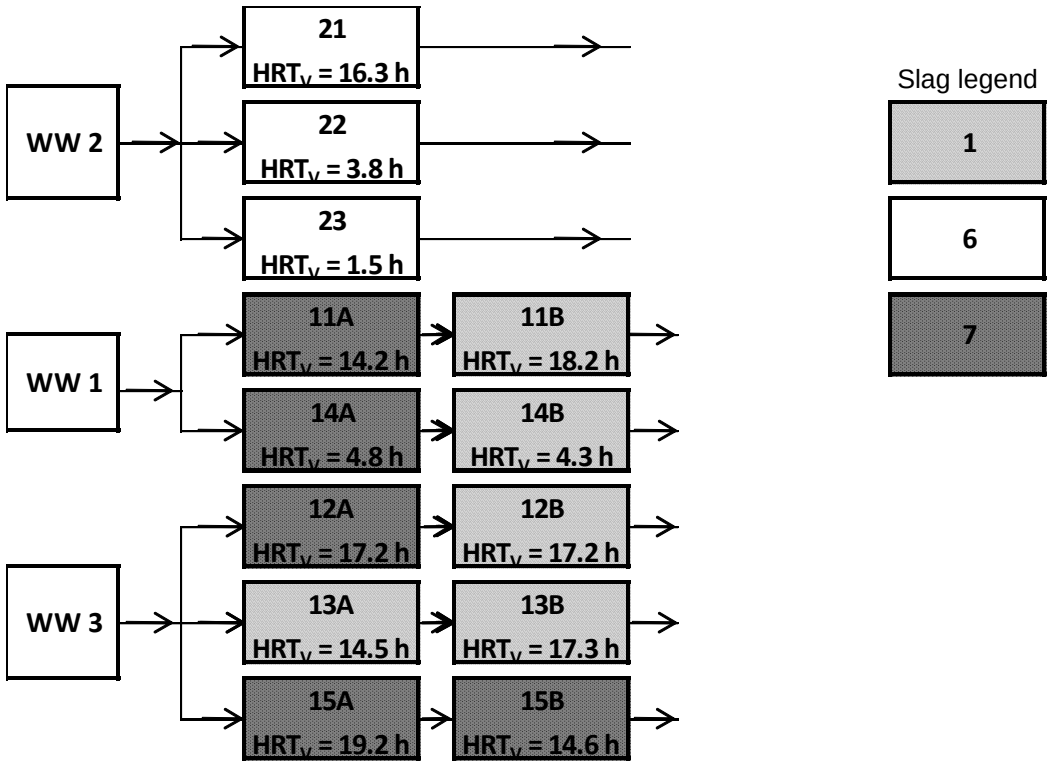

Figure 5.1 : Column tests experimental setup

The effect of lowering the HRT_V was evaluated within WW 1, which represents a relatively dilute wastewater. The efficiency was affected at an HRT_V of 4.8 h as the pH dropped slowly from 11.5 to 9 after 150 days of operation while it remained above 11 at an HRT_V of 14.2 h. The effect of lowering the HRT_V within WW 3 was not tested due to time availibility, but it would probably result in a shorter longevity.

5.2.1 Phosphorus removal

The retention capacities reached by upstream columns are presented in **Erreur ! Source du renvoi introuvable.** and summarized in Table 5.1 for all contaminants. The highest value obtained for phosphorus was 8.26 mg P/g media with EAF slag from Fort Smith. This value is higher than typical retention capacities obtained in column tests or field tests for EAF slag, which are between 1 and 2.5 mg P/g media (Chazarenc et al., 2008; Vohla et al., 2011). However, retention capacities at saturation could not be extrapolated from Figure B.1 because all columns were still efficient at the end of operation. Columns 12A and 15A, both filled with Fort Smith slag and fed with identical conditions, had similar removal efficiency curves (Figure B.1). Both columns had a pH drop after 70 days and erratic pH profile after this time.

A strong link between pH rise and phosphorus removal was observed (Figure 5.2). A pH higher than 9 reduced the phosphorus concentration to less than 1 mg P/L. When the effluent pH was higher than 11, the effluent phosphorus concentration was between 0.01 and 1.0 mg P/L while an effluent pH between 6 and 9 resulted in a partial phosphorus removal.

Different logarithmic regressions were obtained for the pH-o-PO_4 relation between pH 6 and pH 9 (Figure 5.2B). These variations may be caused by different initial water compositions. WW 2 and WW 3 have different chemical equilibrium caused by different contaminant concentrations and the absence or presence of the carbonate system. Moreover, different precipitation behaviors could explain the different relationships between columns 13A and 15A, that were fed with the same solution. Fluoride removal was more efficient in column 13A than in column 15A. The formation of fluoroapatite (and competition with the formation of hydroxyapatite) has an effect on pH and o-PO_4 concentration. Finally, the column 13A relationship was less spread than that of columns 22 and 15A. This variation is caused by the different pH drop observed in operation. Column 13A had a smooth pH drop that generated sub-steady state conditions for chemical equilibrium. Columns 22 and 15A had erratic pH drops, preventing the solution to reach chemical equilibrium.

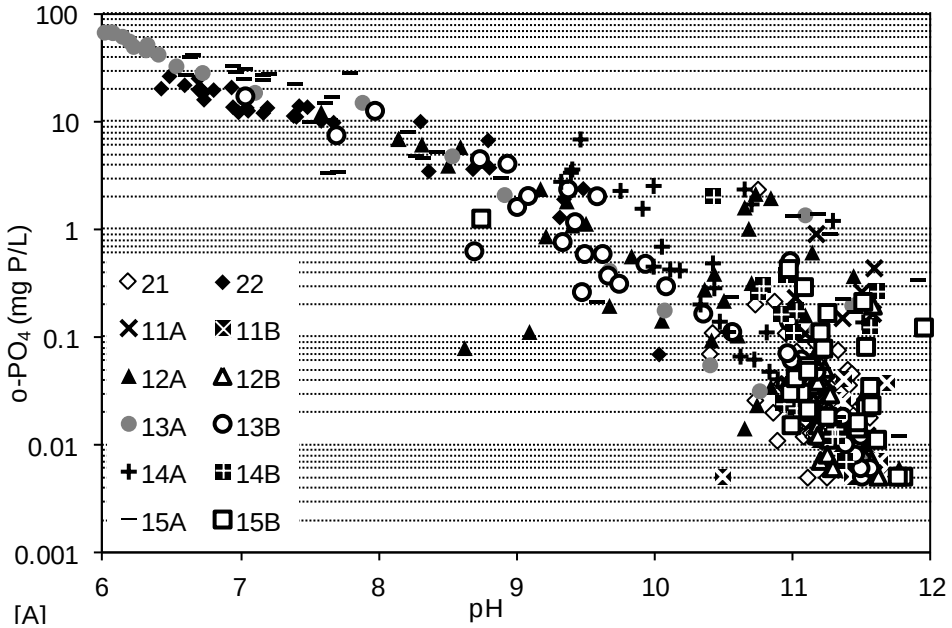

Figure 5.2: Relationship between effluent Relationship between effluent o-PO_4 concentration and pH ([A] in logarithm scale, [B] in arithmetic scale)

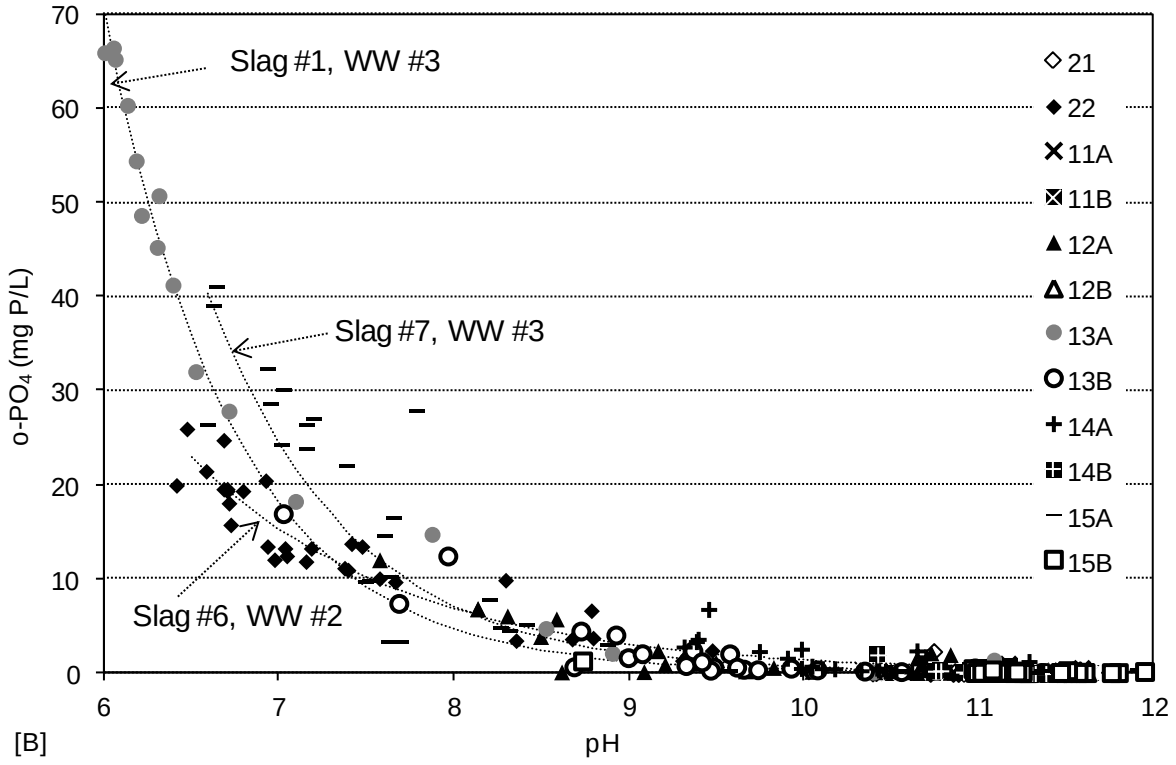

Figure 5.2 (suite): Relationship between effluent o-PO_4 concentration and pH ([A] in logarithm scale, [B] in arithmetic scale)

5.2.2 Fluoride removal

Fluoride removal was linked with pH. The removal was poorer when pH was lower for all columns (Figure 5.3). The composition of WW had an influence on fluoride removal. The mean fluoride removal at full efficiency was 10% within WW 1 and 85% within WW 3 when slag #7 was used (Figure B.2). Fluoride removal is increased when the fluoride/phosphorus ratio of the WW is low, favouring the precipitation of fluoroapatite. Fluoroapatite has the same molecular structure as HAP, but precipitation of HAP is probably favoured by the constant dissolution of slag that adds hydroxide ions in water. The fluoride/phosphorus mass ratio is 0.88 in WW 1 and 0.33 in WW 3. In comparison, the stoichiometric fluoride/phosphorus mass ratio of fluoroapatite is 0.20.

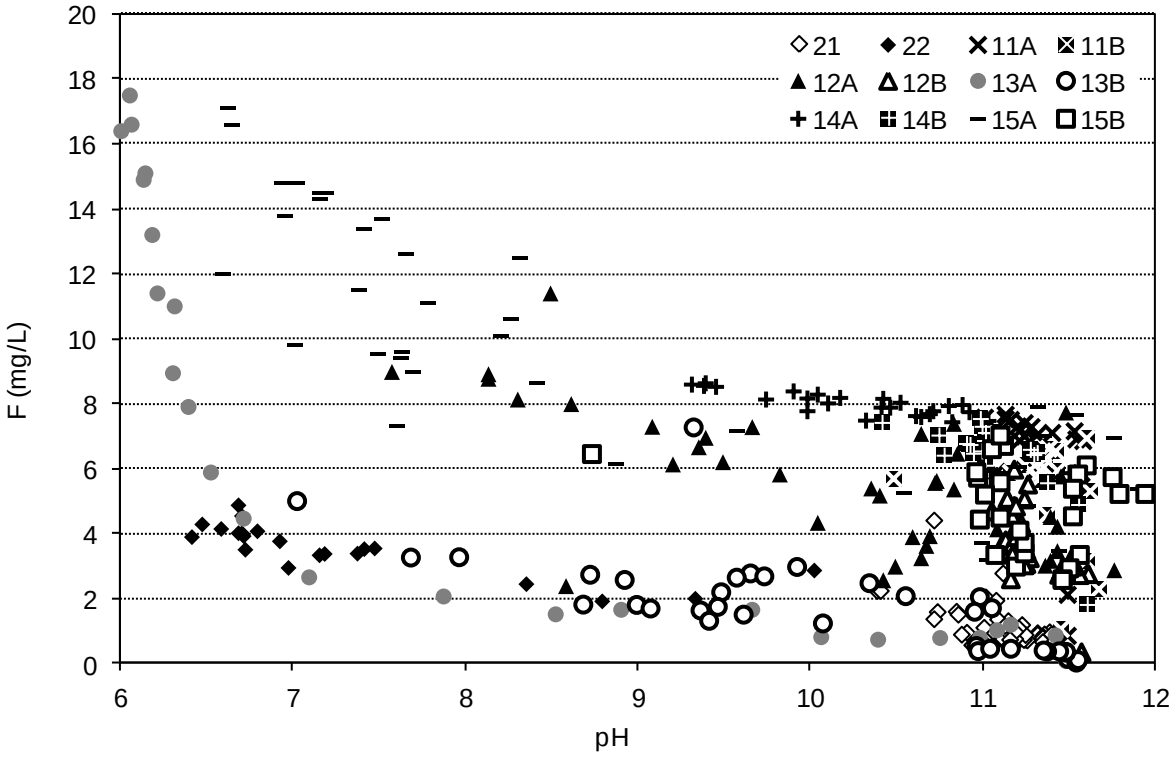

Figure 5.3 : Relationship between fluoride and pH in column effluent

Fluoride removal performances and mechanisms observed in this study are quite different than what was tested with other kinds of WW containing both phosphorus and fluoride. Fluoride removal from electronics WW by CaF_2 precipitation was observed (Yang et al., 2001). This author noted that phosphorus is competitive to fluoride precipitation and that addition of CaF_2 seeds increases the selective precipitation of fluoride, which is optimized at pH below 9. Grzmil and Wronkowski (2006) performed selective precipitation of phosphorus and fluoride (by CaF_2) from a phosphoric acid production WW by stages, using different pH and chemical additives. These authors reached final concentrations of 5-10 mg P/L and 8-18 mg F/L from initial concentrations of 200 mg F/L and 200-400 mg P/L. Selective precipitation of phosphorus from semiconductor WW containing fluoride was performed using magnesium salts (Warmadewanthi & Liu, 2009). The initial WW contained 936 mg F/L, 118 mg P/L and other compounds. It seems that in high fluoride concentration, precipitation of CaF_2 is favoured. It was also observed by Yehia and Ezzat (2009), who observed respectively precipitation of FAP and CaF_2 at low and high concentrations on apatite media. Combined removal of phosphorus and fluoride by slag filters has the advantage of reaching low fluoride concentration and being simple and economic. However, processes of selective precipitation of phosphorus or fluoride allow recovery of

relatively pure phases, even if they involve the use of chemical additives and mechanical maintenance.

The slag composition had an influence on fluoride removal. The mean fluoride removal at full efficiency was >90% within slag #1 and 75% within slag #7 when columns were fed with WW 3 (Figure B.2). HAP and FAP have the same molecular structure; they differ by the OH or F ion that places itself within the hexagonal pattern. It is possible that a solid solution of HAP and FAP is precipitated and that slag #1 has a specific characteristic that catalyzes the formation of FAP. It may be the leaching of some trace metallic compounds that affects the presence of fluoride in nucleation and growth processes. Slag #1 did not contain a specific mineralogical phase that could be directly related to fluoride removal (Table 2.4).

In sequential batch tests, the sequence #7-#1 increased the fluoride removal efficiency of slag #1. In column test, this effect was not observed: column 12B did not add significant fluoride removal to the effluent of column 12A (Figure 3.5). This is explained by the phosphorus need to remove efficiently fluoride. As the effluent of column 12A does not contain phosphorus, no additional fluoride removal is possible. In sequential batch tests, slag #1 used as a post-treatment of slag #7 achieved fluoride removal because there was still phosphorus in the solution.

A particular behavior was observed in column 21. Its fluoride removal efficiency increased with time, starting at 50% and progressing slowly up to 80% (Figure B.2). This phenomenon could be caused by increased adsorption of fluoride on freshly formed apatite that favours the direct crystallization of FAP instead of HAP. It was previously shown that apatite has strong fluoride adsorption potential (Bellier, Chazarenc & Comeau, 2006; Harouiya et al., 2011; Yehia & Ezzat, 2009). The increase of fluoride removal efficiency should not be explained by ionic exchange between hydroxides in HAP and F ions because fluoride migration within apatite crystal occurs only over 1100 K (Jay et al., 2012). Below that temperature, fluoride movement in apatite is limited to atomic vibration. Fluoride removal efficiency of columns fed with WW 1 and WW 3 did not increase with time. It is possible that fluoride adsorption on apatite is limited by the presence of carbonate precipitates (see section 5.2.5 for crystal growth and calcite formation). As column 21 was fed with WW 2, which was prepared with distilled water, no carbonate precipitates were formed in that column.

5.2.3 Metals removal

Metal removal efficiency was linked with pH as did phosphorus removal (Figures B.3 to B.5). The mean removal efficiency at full efficiency of slag #1 and slag #7 was 75% for Mn and >90% for Zn. Mn was not removed if the pH is lower than 6 (Figure 3.2 and Figure 3.6). Slag #1 and slag #7 showed initial Al leaching (concentration at effluent up to 70 mg/L), but Al removal was >90% after that time.

5.2.4 Performance goals

Treatment results of the selected treatment system (two successive Fort Smith EAF filters operated at total HRT_V of 34 h) are presented in boxplots and compared with performance goals and actual effluent concentrations of the lime treatment plant in Figure 5.4. The main performance goal, which was for phosphorus removal, was not reached. However, the Joplin criterion for phosphorus discharge is very strict (0.5 µg P/L). A conventional chemical precipitation system can reach 0.5 mg P/L with significant chemical addition and filtration (Metcalf & Eddy, 2003). It can reach 0.02 mg P/L with a two-stage filtration system combined with recirculation (Metcalf & Eddy, 2003). Reverse osmosis allows effluent concentrations of 0.1-1 mg P/L (Metcalf & Eddy, 2003). Thus, slag filters efficiency for phosphorus removal is comparable with complex and expensive treatment systems. Moreover, slag filters were more efficient than the actual lime treatment plant. Considering the economical simplicity of slag filters, their performances for phosphorus removal could be considered acceptable for the present application. If the Quebec regulations were applicable, treatment results would meet requirements of the most severe phosphorus discharge criterion of 0.1 mg P/L (Figure 5.4). Results obtained in that study could certainly be applied to other similar mining site remediation projects.

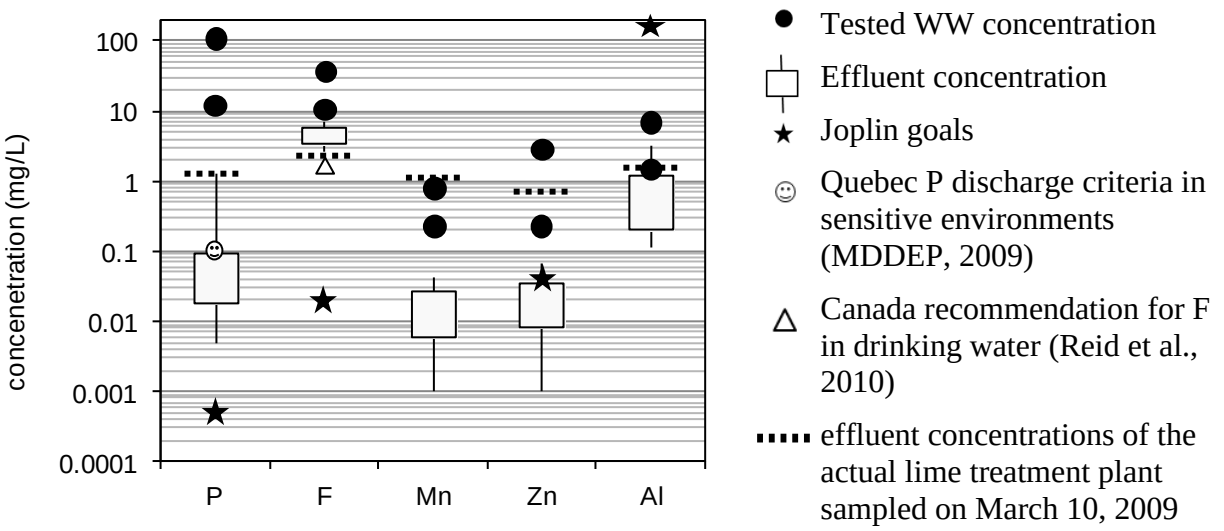

Figure 5.4 : Effluent concentrations of an efficient slag filter (two successive Fort Smith EAF slag filters operated at total HRT_V of 34 h) compared with Joplin project performance goals, actual effluent concentrations of the lime treatment plant and selected regulations

The fluoride performance goal of 2 μg/L was not reached. The effluent fluoride concentration was between 2 mg/L and 7 mg/L. However, such effluent concentrations are low compared to other types of WW containing fluoride (Aldaco, Irabien & Luis, 2005; Grizmil & Wronkowski, 2006; Warmadewanthi & Liu, 2009; Yang et al., 2001). It is the same order of magnitude than the Canada recommendation for fluoride in drinking water (Reid et al., 2010). Moreover, fluoride removal was a secondary objective in the Joplin project, the priority being phosphorus removal. Considering the preceding circumstances, fluoride treatment performances of slag filters are considered acceptable given the relative mechanical and operational complexity of the technologies currently in use. The performance goals for the studied metals (Mn, Zn and Al) were reached. Slag filters were significantly more efficient than the lime treatment plan for metals removal.

5.2.5 Crystal growth

As mentioned in Chapter 4, phosphorus removal in slag filters takes place by HAP precipitation and crystallization, preceded by dissolution of calcium oxides that can be simplified by CaO dissolution. Efficient HAP formation needs calcium present in the initial WW or dissolved from the slag. It was previously shown that a lack of calcium limits the formation of

HAP (Barca et al., 2012). The relationship between soluble calcium and effluent pH observed in this study is shown in Figure 5.5. Between pH 6 and 10, calcium concentration is independent of pH. Calcium concentration increases with a pH over 10. It suggests that calcium is consumed as it is released from slag until all phosphorus is precipitated, with a pH over 11. In the concentrated WW (WW 3), the calcium concentration was even below its initial value in neutral pH, meaning that calcium release from slag was not enough for complete precipitation of HAP.

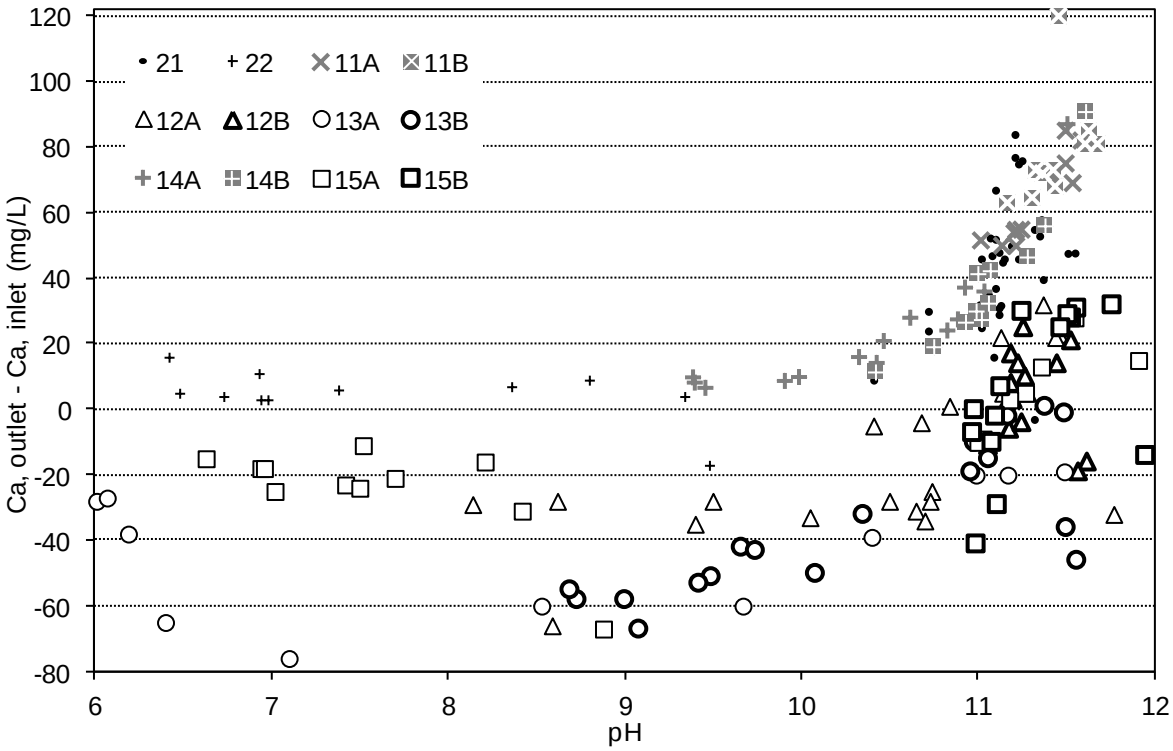

Figure 5.5 : Relationship between calcium and pH at columns' effluent. Ca, inlet refers to the initial concentration in WW (WW 1, 2 or 3). Ca, outlet refers to the concentration at each column's effluent

Crystal growth in filters was investigated using crystal size determination. A qualitative interpretation of HAP growth in upstream filters is presented in Figure 5.6. Growth rates were dependent of the WW composition. For the same slag media (slag #7), the growth rate was smaller in WW 1 (diamonds) than in WW 3 (triangles), suggesting that a higher phosphorus concentration results in a higher HAP growth rate. As efficient crystal growth increases the retention capacity of slag filters, the high initial phosphorus concentration of WW 3 may explain high retention capacities obtained in that study compared with typical low phosphorus

concentration experiments. However, it was previously shown that highly saturated WW favours nucleation instead of crystal growth (Seckler et al., 1991), resulting in an inefficient crystal organization. Similar growth rates were observed in WW 2 and WW 3 even if their phosphorus concentrations were different (crosses and triangles in Figure 5.6). Direct comparison of crystal growth in WW 2 and WW 3 may not possible as their carbonate compositions and slag media are different. Carbonates may act as a HAP growth inhibitor (Valsami-Jones, 2001). Moreover, crystal data is insufficient to assess precisely quantitative growth rates.

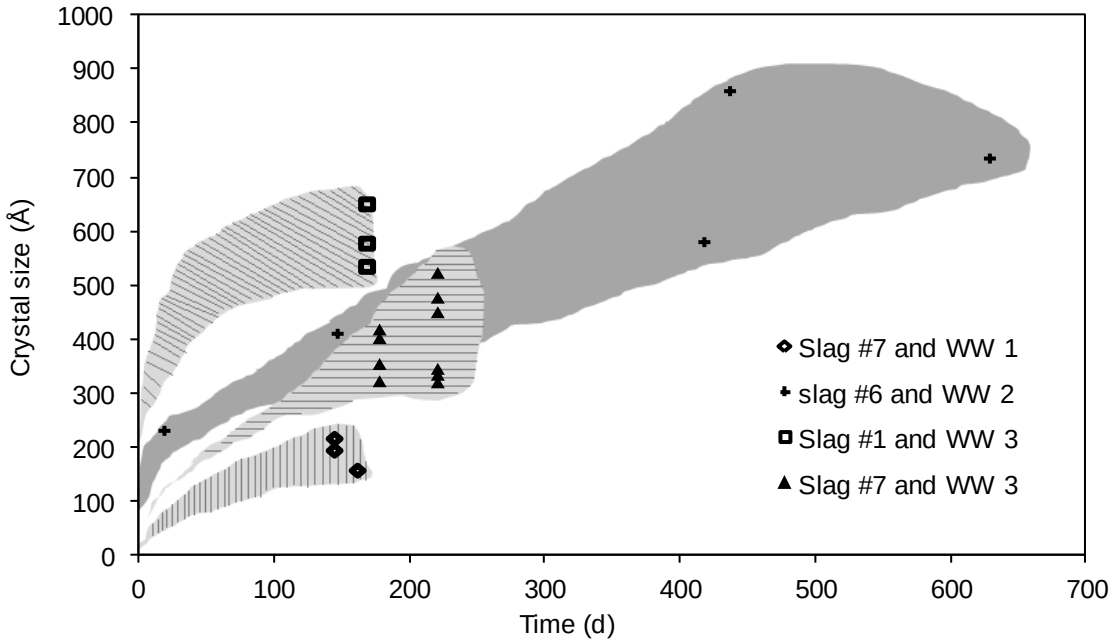

Figure 5.6 : Hydroxyapatite growth in upstream filters

Crystal-size-time curves had fan shapes. It suggests that new crystal seeds are constantly formed while older seeds continue to grow. It results in a distribution of crystal sizes, older seeds being larger and younger seeds being smaller. Moreover, the HAP composition of crystal was observed in a very early stage. HAP was the main mineralogical phase after 30 d in column 23. Thus, primitive calcium-phosphate precipitates that are either amorphous or meta-stable mineralogical phases (Bowden et al., 2009; Lundager Madsen, 2008) were rapidly transformed in HAP. At this early time, HAP diffractogram was rough, indicating a small-size and disorganized mineralogical phase. HAP diffractograms became neater with evident peaks as columns were operated, indicating and increase in crystal organization and quality.

HAP crystal growth was also dependent on pH. With regards to saturation, HAP has three stability zones related to phosphorus concentration and pH (Kim et al., 2006). The first one (low pH and low phosphorus concentration) corresponds to soluble HAP. The second one (high pH and high phosphorus concentration) involves direct precipitation and crystal growth of HAP. The last zone is an intermediary meta-stable zone (high phosphorus concentration and neutral pH) where HAP may remain supersaturated. In that meta-stable zone, specific conditions such as HAP crystal seeds are necessary for HAP precipitation and crystallization, otherwise HAP remains in solution. This phenomenon was observed in column 13A, where crystal seeds were formed in the first 30 days of operation at pH over 9. In the following period (pH = 6 between t = 50 d and t = 150 d), crystal growth occurred. This neutral-conditions HAP growth had the highest growth rate observed (squares in Figure 5.6).

Results of this study highlight the importance of calcite formation in slag filters as a competitive reaction to HAP formation. Calcite formation was observed in the filters of set 1, which were fed with WW containing inorganic carbon. The amount of calcite present in interstitial precipitate was evaluated with the arbitrary HAP/$CaCO_3$ ratio (section 3.3.3). For the same feeding solution (WW 1), crystals in column with HRT_V of 14 h had a mean HAP/$CaCO_3$ ratio of 0.64 when crystals in column with HRT_V of 4.8 h had a mean HAP/$CaCO_3$ ratio of 0.33. Thus, calcite formation was more important when the HRT_V was higher, meaning that calcite grows faster than HAP. Calcite crystals were effectively bigger than HAP crystals (Figure 5.7).

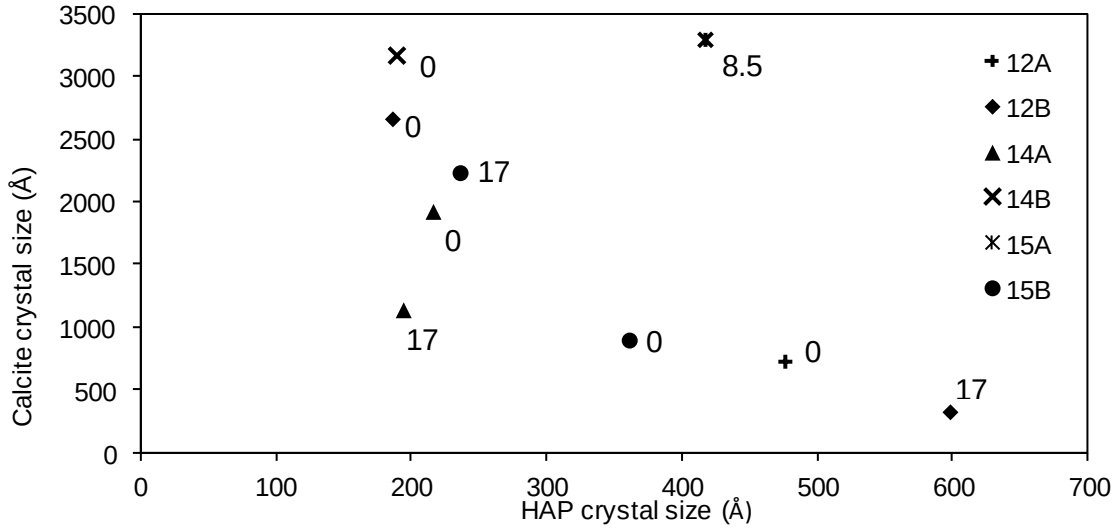

Figure 5.7 : Comparison of HAP and calcite crystal sizes. For each point, sizes are computed from the same diffractogram. The height of the sample in the column is given at the right of each point (cm)

These observations, which agree to what was noted by Liira et al. (2009), highlights the importance of HRT_V optimization. A high HRT_V favours compact precipitation and increases the crystal retention capacity, but calcite grows faster than HAP, resulting in a bigger proportion of calcite. As calcite crystals occupy void space that is not any more available for HAP formation and growth, an efficient filter should be operated to minimize calcite formation. In summary, choosing the HRT_V of a slag filter is a compromise between a long retention time for efficient crystal accumulation and a short retention time for limiting calcite formation. When phosphorus concentration of the WW was high (ie. WW 3), the importance of competitive calcite formation was decreased. Calcite was less present in precipitates from WW 3-fed columns.

CONCLUSION AND RECOMMENDATIONS

This master project had two main objectives. The first one was to propose and test a treatment system for the mining leachate of the Joplin abandoned mining site, located in Missouri. The proposed system, which is based on steel slag filters, has to be economical and more efficient than the actual liming treatment plant. The second objective was to propose a new phosphorus mechanisms retention model for steel slag filters. Both objectives were met: an efficient slag filter was operated for 172 days in the laboratory and a new model based on crystal formation and accumulation was proposed in an article published in the journal *Environmental Science & Technology*.

Three experimental phases were conducted. First, individual batch tests resulted in a comparative list of 10 types of slag that could be economically transported to treat the mine effluent. Two slags were selected as the most efficient for phosphorus, metals and fluoride removal. Second, different treatment sequences were compared on the basis of sequential batch tests. Third, two sets of column tests were conducted in the laboratory. The first set was operated using the mining site conditions to characterize the performance and longevity of the proposed system. The second set was operated to develop the phosphorus retention mechanisms model.

The proposed system consisted of two successive Fort Smith EAF slag filters with a total HRT_V of 34 h. This filter gave very high removal efficiency for phosphorus, manganese, zinc, aluminum and fluoride for at least 172 days. On the basis of this proposed system, recommendations were formulated for the implementation of a pilot test at the mining site.

A model based on HAP crystal formation and accumulation in steel slag filters was proposed. It was shown that phosphorus retention capacity at saturation is related with water velocity. Water velocity affects HAP crystal organization (compact or loose), which determines the filter retention capacity. HAP growth rate was shown to be independent of water velocity. A preliminary mathematical expression for pH rise in filters was proposed.

RECOMMENDATIONS FOR THE TREATMENT SYSTEM AT THE JOPLIN SITE

Several recommendations for the Joplin mining site restoration are drawn from this master's project. The forthcoming steps are column and pilot tests to be conducted directly on the Joplin mine site. The use of filters made of EAF slag from Fort Smith is recommended, as this type of slag allows the most durable pH rise. This study showed that two successive Fort Smith filters with a total HRT_V of 34 h resulted in a very high removal efficiency during at least 172 d. The longevity of the system could be increased by adding downstream filters. The use of EAF Blytheville slag is not recommended because its longevity is too short, even if it has a higher fluoride removal capacity than the Fort Smith slag.

- The recommended system does not meet all of the very stringent performance goals formulated at the beginning of the project. However, it provides significant phosphorus removal, which is the main objective. Several specific recommendations are formulated for future tests:
- A real mining effluent with variable characteristics should be used. It would allow a better appreciation of the influence of composition on treatment capacity. This is especially important for fluoride, which removal depends on the influent composition, as stated in section 5.2.2. Fluoride removal is likely to be affected by influent varying concentrations.
- The effect of wastewater temperature on filters efficiency should be assessed. The wastewater is subject to seasonal changes of temperature.
- The effect of different feeding regimes (continuous, batch feedings, resting periods, etc.) should be assessed.
- Slag may have composition variability that affect pH rise behavior and trace compounds release. The slag variability should be characterized with batch tests similar to these used in that project.
- All metals of concern should be monitored, including heavy metals such as arsenic, cadmium, chromium, copper, lead and mercury.

- Different HRT_V should be tested and tests should be operated until the treatment efficiency is greatly diminished. This would allow to optimize the size of the final system and reduce its replacement frequency. Suggested HRT_V to test are 10, 20 and 30 h.
- Mixes of Fort Smith slag with a small amount of Blytheville slag should be tested. This may favor fluoride treatment without affecting the pH rise capacity of the Fort Smith slag.

RECOMMENDATIONS FOR FUTURE WORK

A preliminary model for phosphorus removal mechanisms in slag filters was proposed in this master's thesis. This model is intended to be improved to lead to better performance modelling and prediction. Supplementary work is needed for this:

A precise characterization of slag dissolution kinetics is needed. The slag dissolution rate is probably changing with time, as readily available calcium oxides are dissolved. The exact mineralogical phases present in slag responsible for CaO dissolution should be assessed. Slag may be exhausted by highly concentrated WW that have acidity and buffering capacity. The validity of measuring slag dissolution kinetics in batch tests should be confirmed by kinetic tests in column experiments. Quantitative evaluation of all these parameters will lead to formulation of dissolution kinetic constants and pH-rise modelling in several situations (different composition of WW, exhausting of slag, etc.)

An in-depth study of crystal characteristics is needed, including shapes, organization, nucleation and growth. These parameters may be influenced by WW composition, presence of organic matter, slag surface characteristics, hydrodynamics or other unknown factors. A complete literature review of HAP crystal growth in related domains (crystallography, mineralogy, ceramics, biocompatibility of implants, etc.) is needed and additional experiments adapted to high pH environments should be conducted. Secondary crystal phases such as calcite and their interaction with HAP should be characterised. The influence of direct contact of the filter with atmospheric inorganic carbon on calcite growth rate must be studied.

The model needs to be completed with concepts of permeability and diffusion in granular media (Courcelles et al., 2011). HAP growth in slag filters complicates permeability theory because it involves three components: water, slag grains, HAP crystals and solid particles from the wastewater. Traditional permeability laws are applicable when media grains are close to spherical grains, which is not the case with acicular HAP crystals and other particulates present in wastewater (organic matter). An exhaustive literature review of permeability theory, including three-phase seepage (petroleum applications; water, gas and media grains) and unsaturated flows is needed to find an applicable permeability model. This model will probably have to include diffusion at the molecular scale to consider pH-rise in crystal agglomerations.

The preceding research needs (slag dissolution kinetics, HAP crystal characteristics, permeability model in slag filters) are essential to complete the model for phosphorus removal mechanisms in steel slag filters. The last step would be the formulation of equations and numerical modelling, calibrated with experimental tests.

REFERENCES

Aldaco, R., Irabien, A., & Luis, P. (2005a). Fluidized bed reactor for fluoride removal. *Chemical Engineering Journal, 107*(1-3), 113-117.

American Public Health Association, American Water Works Association & Water Environment Federation. (2005). *Standard methods for the examination of water and wastewater* (21st ed.). Washington, D. C.

Anjab, Z. (2009). Development of a steel slag bed for phosphorus removal of fishfarm wastewater. Unpublished Master Thesis (in French), Ecole Polytechnique of Montreal, Montreal.

ASTM. (2006). *Standard test method for permeability of granular soils (constant head).* ASTM D2434-68.

Aubertin, M., Bussière, B., Aachib, M., Chapuis, R. P., & Crespo, J. R. (1996). Numerical modelling of unsaturated flow in multilayer soil covers. *Hydrogeology* (1).

Baker, M. J., Blowes, D. W., & Ptacek, C. J. (1998). Laboratory development of permeable reactive mixtures for the removal of phosphorus from onsite wastewater disposal systems. *Environmental Science and Technology, 32*(15), 2308-2316.

Barca, C., Gérente, C., Meyer, D., Chazarenc, F., & Andrès, Y. (2012). Phosphate removal from synthetic and real wastewater using steel slags produced in Europe. *Water Research, 46*(7), 2376-2384.

Beh, C. L., Chuah, L., Choong, T. S. Y., Kamarudzaman, M. Z. B., & Abdan, K. (2010). Adsorption Study of Electric Arc Furnace Slag for the Removal of Manganese from Solution. *American Journal of Applied Sciences, 7*(4), 442-446.

Bellier, N., Chazarenc, F., & Comeau, Y. (2006). Phosphorus removal from wastewater by mineral apatite. *Water Research, 40*(15), 2965-2971.

Bowden, L. I., Jarvis, A. P., Younger, P. L., & Johnson, K. L. (2009). Phosphorus removal from waste waters using basic oxygen steel slag. *Environmental Science and Technology, 43*(7), 2476-2481.

Brient, S. (2012). *Dephosphatation of a fish farm wastewater with extensive steel slag fiters (in French).* Unpublished Master Thesis, Ecole Polytechnique of Montréal, Montréal.

Chapuis, R. P., Baass, K., & Davenne, L. (1989). Granular soils in rigid-wall permeameters. Method for determining the degree of saturation. *Canadian Geotechnical Journal, 26*(1), 71-79.

Chazarenc, F., Brisson, J., & Comeau, Y. (2007). *Slag columns for upgrading phosphorus removal from constructed wetland effluents.* Paper presented at the Wetland Systems for Water Pollution Control X, 12 Caxton Street, London, SW1H 0QS, United Kingdom.

Chazarenc, F., Kacem, M., Gerente, C., & Andres, Y. (2008, November 1 - November 7). *'Active' filters: a mini-review on the use of industrial by-products for upgrading phosphorus removal from treatment wetlands.* Paper presented at the 11th Int. Conf. on Wetland Systems for Water Pollution Control, Indore, India.

Chen, N., Zhang, Z., Feng, C., Li, M., Chen, R., & Sugiura, N. (2010). Removal of fluoride from aqueous solution by adsorption onto Kanuma mud. *Water Science and Technology, 62*(8), 1888-1897.

Claveau-Mallet, D., Wallace, S., & Comeau, Y. (2012). Model of phosphorus precipitation and crystal formation in electric arc furnace steel slag filters. *Environmental Science and Technology, 46*(3), 1465-1470.

Courcelles, B., Modaressi-Farahmand-Razavi, A., Gouvenot, D., & Esnault-Filet, A. (2011). Influence of precipitates on hydraulic performance of permeable reactive barrier filters. *International Journal of Geomechanics, 11*(2), 142-151.

Cullity, B. D. (2001). Diffraction III: Real Samples. In *Elements of x-ray diffaction* (3rd ed.). Upper Saddle River, NJ: Prentice Hall.

Demers, I., Bussière, B., Aachib, M., & Aubertin, M. (2011). Repeatability evaluation of instrumented column tests in cover efficiency evaluation for the prevention of acid mine drainage. *Water, Air, and Soil Pollution, 219*(1-4), 113-128.

Drizo, A., Comeau, Y., Forget, C., & Chapuis, R. P. (2002). Phosphorus saturation potential: A parameter for estimating the longevity of constructed wetland systems. *Environmental Science and Technology, 36*(21), 4642-4648.

Drizo, A., Forget, C., Chapuis, R. P., & Comeau, Y. (2006). Phosphorus removal by electric arc furnace steel slag and serpentinite. *Water Research, 40*(8), 1547-1554.

Environmental Health & Safety Online. *The EPA TCLP: Toxicity Characteristic Leaching Procedure and Characteristic Wastes (D-codes).* Accessed on April 19, 2012, retreived from http://ehso.com/cssepa/TCLP.htm

Forget, C. (2001). *Dissolved phosphorus removal from fish farm effluents by reactive granular media.* Unpublished Master Thesis (in French), Ecole Polytechnique of Montreal, Montreal.

Grzmil, B., & Wronkowski, J. (2006). Removal of phosphates and fluorides from industrial wastewater. *Desalination, 189*(1-3 SPEC. ISS.), 261-268.

Harouiya, N., Rue, S. M., Prost-Boucle, S., Lienar, A., Esser, D., & Molle, P. (2011). Phosphorus removal by apatite in horizontal flow constructed wetlands for small communities: pilot and full-scale evidence. *Water Science and Technology, 63*(8), 1629-1637.

Huang, Y.-H., Shih, Y.-J., & Chang, C.-C. (2011). Adsorption of fluoride by waste iron oxide: The effects of solution pH, major coexisting anions, and adsorbent calcination temperature. *Journal of Hazardous Materials, 186*(2-3), 1355-1359.

Huifen, Y., Wen, M., Weina, Z., & Zhiyong, W. (2011). *Steel slag as multi-functional material for removal of heavy metal ions in wastewater.* Paper presented at the 2011 International Conference on Computer Distributed Control and Intelligent Environmental Monitoring, CDCIEM 2011, February 19, 2011 - February 20, 2011, Changsha, Hunan, China.

Jay, E. E., Rushton, M. J. D., & Grimes, R. W. (2012). Migration of fluorine in fluorapatite - a concerted mechanism. *Journal of Materials Chemistry, 22*(13), 6097-6103.

Kim, E.-H., Yim, S.-B., Jung, H.-C., & Lee, E.-J. (2006). Hydroxyapatite crystallization from a highly concentrated phosphate solution using powdered converter slag as a seed material. *Journal of Hazardous Materials, 136*(3), 690-697.

Koiv, M., Liira, M., Mander, U., Motlep, R., Vohla, C., & Kirsimae, K. (2010). Phosphorus removal using Ca-rich hydrated oil shale ash as filter material - The effect of different phosphorus loadings and wastewater compositions. *Water Research, 44*(18), 5232- 5239.

Koiv, M., Vohla, C., Motlep, R., Liira, M., Kirsimae, K., & Mander, U. (2009). The performance of peat-filled subsurface flow filters treating landfill leachate and municipal wastewater. *Ecological Engineering, 35*(2), 204-212.

Kostura, B., Kulveitova, H., & Leko, J. (2005). Blast furnace slags as sorbents of phosphate from water solutions. *Water Research, 39*(9), 1795-1802.

Liira, M., Koiv, M., Mander, U., Motlep, R., Vohla, C., & Kirsimae, K. (2009). Active filtration of phosphorus on Ca-rich hydrated oil shale ash: Does longer retention time improve the process? *Environmental Science and Technology, 43*(10), 3809-3814.

Lu, H., Wang, B., & Ban, Q. (2010). Defluoridation of drinking water by zeolite NaP1 synthesized from coal fly ash. *Energy Sources, Part A: Recovery, Utilization and Environmental Effects, 32*(16), 1509-1516.

Lundager Madsen, H. E. (2008). Influence of foreign metal ions on crystal growth and morphology of brushite (CaHPO4, 2H2O) and its transformation to octacalcium phosphate and apatite. *Journal of Crystal Growth, 310*(10), 2602-2612.

Mbonimpa, M., Aubertin, M., Aachib, M., & Bussière, B. (2003). Diffusion and consumption of oxygen in unsaturated cover materials. *Canadian Geotechnical Journal, 40*(5), 916-932.

MDDEP. (2006). *Metals determination: method by mass spectrometry with argon plasma ionizing source (in French).* Centre d'expertise en analyse environnementale du Québec. MA. 200 – Mét 1.1.

MDDEP. (2009). Réduction du phosphore dans les rejets d'eaux usées d'origine domestique - Position du MDDEP. Retreived from http://www.mddep.gouv.qc.ca/eau/eaux-usees/reduc-phosphore/index.htm

Metcalf & Eddy. (2003). *Wastewater engineering: treatment and reuse* (4th ed.). New York: McGraw-Hill.

National Slag Association. (2009). General information about National Slag Association. Accessed on March 16th, 2012. Retreived from http://www.nationalslag.org/nsageneral.htm

Neculita, C.-M., Zagury, G. J., & Bussière, B. (2007). Passive treatment of acid mine drainage in bioreactors using sulfate-reducing bacteria: Critical review and research needs. *Journal of Environmental Quality, 36*(1), 1-16.

Pratt, C., & Shilton, A. (2010). Active slag filters-simple and sustainable phosphorus removal from wastewater using steel industry byproduct. *Water Science and Technology, 62*(8), 1713-1718.

Proctor, D. M., Fehling, K. A., Shay, E. C., Wittenborn, J. L., Green, J. J., Avent, C., et al. (2000). Physical and chemical characteristics of blast furnace, basic oxygen furnace, and

electric arc furnace steel industry slags. *Environmental Science and Technology, 34*(8), 1576-1582.

Reid, D., Boettger, B., Somers, G., Philip, K., White, K., MacDonald, J., Deshpande,, S., Robert, C., Ferris, S., Khan, H., Workman, P., Brooks, P., Fleming, D. & Cooper, J. (2010). *Recommandations pour la qualité de l'eau potable au Canada - tableau sommaire*. Santé Canada, Comité fédéral-provincial-territorial sur l'eau potable, retrieved from http://www.hc-sc.gc.ca/ewh-semt/alt_formats/hecs-sesc/pdf/pubs/water-eau/2010-sum_guide-res_recom/sum_guide-res_recom-fra.pdf

Renman, A., Renman, G., Gustafsson, J. P., & Hylander, L. (2009). Metal removal by bed filter materials used in domestic wastewater treatment. *Journal of Hazardous Materials, 166*(2-3), 734-739.

Sawyer, C. N., McCarty, P. L., & Parkin, G. F. (2003). *Chemistry for Environmental Engineering and Science* (5th ed.). Boston: McGraw-Hill.

Seckler, M. M., Bruinsma, O. S. L., & van Rosmalen, G. M. (1991). Crystallization of calcium and magnesium phosphates in a fluidized bed. *Crystal Properties and Preparation, 36*(38), 263-272.

Sheng-Yu, L., Jin, G., Bin, Q., & Yijin, Y. (2009). *Adsorption behaviors of heavy metal ions by steel slag-an industrial solidwaste.* Paper presented at the 2009 3rd International Conference on Bioinformatics and Biomedical Engineering (iCBBE 2009), 11-16 June 2009, Piscataway, NJ, USA.

Shilton, A., Pratt, S., Drizo, A., Mahmood, B., Banker, S., Billings, L., et al. (2005). 'Active' filters for upgrading phosphorus removal from pond systems. *Water Science and Technology, 51*(12), 111-116.

Shilton, A. N., Elmetri, I., Drizo, A., Pratt, S., Haverkamp, R. G., & Bilby, S. C. (2006). Phosphorus removal by an 'active' slag filter-a decade of full scale experience. *Water Research, 40*(1), 113-118.

Smyth, D. J. A., Blowes, D. W., Ptacek, C. J., Baker, M. J., & McRae, C. W. T. (2002). *Steel production wastes for use in permeable reactive barriers (PRBs).* Paper presented at the Proceedings of the Third International Conference on Remediation of Chlorinated and Recalcitrant Compounds, May 20, 2002 - May 23, 2002, Monterey, CA., United states.

Tsuru, K., Kubo, M., Hayakawa, S., Ohtsuki, C., & Osaka, A. (2001). Kinetics of apatite deposition of silica gel dependent on the inorganic ion composition of simulated body fluids. *Nippon Seramikkusu Kyokai Gakujutsu Ronbunshi/Journal of the Ceramic Society of Japan, 109*(1269), 412-418.

United States Department of the Interior. (2011). *Mineral commodity summaries 2011: U. S. Geological Survey.* , retrieved from http://minerals.usgs.gov/minerals/pubs/mcs/2011/mcs2011.pdf

USEPA (1992). *Toxicity characteristic leaching procedure.* Method 1311. Retreived from http://ehso.com/cssepa/TCLP_from%20EHSOcom_Method_1311.pdf

Valsami-Jones, E. (2001). Mineralogical controls on phosphorus recovery from wastewaters. *Mineralogical Magazine, 65*(5), 611-620.

Vohla, C., Koiv, M., Bavor, H. J., Chazarenc, F., & Mander, U. (2011). Filter materials for phosphorus removal from wastewater in treatment wetlands-A review. *Ecological Engineering, 37*(1), 70-89.

Wang, L.-H., & Lin, C.-I. (2010). The removal of heavy metal ions from spiked aqueous solutions using solid wastes-Comparison of sorption capability. *Journal of the Taiwan Institute of Chemical Engineers, 41*(5), 585-590.

Warmadewanthi, & Liu, J. C. (2009). Selective precipitation of phosphate from semiconductor wastewater. *Journal of Environmental Engineering, 135*(10), 1063-1070.

Xu, X., Li, Q., Cui, H., Pang, J., Sun, L., An, H., et al. (2011). Adsorption of fluoride from aqueous solution on magnesia-loaded fly ash cenospheres. *Desalination, 272*(1-3), 233-239.

Xue, J., & Ma, Y. (2009). *Removal of high fluoride from drinking water treated by new type fly ash filter material.* Paper presented at the 3rd International Conference on Bioinformatics and Biomedical Engineering, iCBBE 2009, June 11, 2009 - June 13, 2009, Beijing, China.

Yang, M., Zhang, Y., Shao, B., Qi, R., & Myoga, H. (2001). Precipitative removal of fluoride from electronics wastewater. *Journal of Environmental Engineering, 127*(10), 902-907.

Yehia, A., & Ezzat, K. (2009). Fluoride ion uptake by synthetic apatites. *Adsorption Science and Technology, 27*(3), 337-347.

Yousefpour, M., Afshar, A., Yang, X., Li, X., Yang, B., Wu, Y., et al. (2006). Nano-crystalline growth of electrochemically deposited apatite coating on pure titanium. *Journal of Electroanalytical Chemistry, 589*(1), 96-105.

Zhou, Y.-F., & Haynes, R. J. (2010). Sorption of heavy metals by inorganic and organic components of solid wastes: Significance to use of wastes as low-cost adsorbents and immobilizing agents. *Critical Reviews in Environmental Science and Technology, 40*(11), 909-977.

APPENDIX A – INDIVIDUAL BATCH TEST RESULTS

In a 1 liter Erlenmeyer flask, a 35 g sample of slag (ID from 1 to 10) or apatite (ID Ap1) is shaken 48 h in 700 mL of WW solution (WW 1 or WW 3). Parameters are measured at time 0, 24 h and 48 h (pH, o-PO_4, F, Ca, Mn, Zn and Al). Note: n.a. for not available.

Table A.1 : Individual batch tests results (tests in WW 1)

ID	pH (-)			[o-PO_4] (mg P/L)			[F] (mg/L)		
	t=0	t=24h	t=48h	t=0	t=24h	t=48h	t=0	t=24h	t=48h
1	6.9	11.3	11.5	10.6	0.008	0.027	9.1	1.3	0.2
	6.9	11.3	11.5	10.6	0.006	0.006	9.1	1.1	0.3
2	7.1	8.2	8.8	11.2	8.46	4.32	9.3	8.6	8.1
	7.1	8.2	8.9	11.2	8.87	3.82	9.3	8.9	8.4
3	7.1	11.5	11.8	11.2	0.025	0.011	9.3	6.7	5.5
	7.1	11.3	11.7	11.2	0.011	0.009	9.3	7.4	6.4
4	7.1	8.0	9.1	11.2	11.0	4.55	9.3	9.1	8.5
	7.1	7.9	8.9	11.2	10.9	5.71	9.3	8.7	9.0
5	6.9	9.9	10.9	10.6	0.744	0.026	9.1	7.8	7.5
	6.9	9.9	10.8	10.6	0.754	0.033	9.1	8.0	7.9
6	7.0	8.9	10.3	10.7	6.00	0.153	9.0	8.7	7.7
	7.0	9.0	10.3	10.7	6.16	0.172	9.0	8.3	7.8
7	7.0	11.5	11.6	10.7	0.02	0.006	9.0	6.5	6.2
	7.0	11.5	11.6	10.7	0.008	0.005	9.0	n.a.	5.9
8	7.0	9.2	10.7	10.7	4.23	0.051	9.0	7.7	8.2
	7.0	9.1	10.1	10.7	3.81	0.142	9.0	7.6	7.8
9	6.7	8.8	10.4	10.7	5.73	0.127	9.1	8.9	8.3
	6.7	8.8	10.5	10.7	5.82	0.056	9.1	8.8	8.4
10	6.7	11.8	11.9	10.7	0.016	0.007	9.1	7.6	8.0
	6.7	11.8	11.9	10.7	0.007	0.006	9.1	7.1	7.3
Ap1	6.9	7.0	6.9	10.6	8.72	8.1	9.1	6.5	5.8
	6.9	7.2	7.1	10.6	8.62	8.31	9.1	7.4	7.0

Note: precision for pH and F is ± 0.1
Note: precision for P is ± 0.001 below 1 mg P/L, ±0.01 between 1 and 10 mg P/L and ± 0.1 over 10 mg P/L

In a 1 liter Erlenmeyer flask, a 35 g sample of slag (ID from 1 to 10) or apatite (ID Ap1) is shaken 48 h in 700 mL of WW solution (WW 1 or WW 3). Parameters are measured at time 0, 24 h and 48 h (pH, o-PO_4, F, Ca, Mn, Zn and Al). Note: n.a. for not available.

Table A.2 : Individual batch tests results (tests in WW 1)

ID	**[Ca] (mg/L)**			**[Mn] (mg/L)**			**[Zn] (mg/L)**		
	t=0	**t=24h**	**t=48h**	**t=0**	**t=24h**	**t=48h**	**t=0**	**t=24h**	**t=48h**
1	31.7	92.5	60.9	0.279	0.016	0.031	0.095	0.001	0.005
	31.7	92	60.2	0.279	0.021	0.037	0.095	0.001	0.001
2	32.1	60	66.1	0.16	0.24	0.12	0.03	0.01	0.005
	32.1	58.9	59.4	0.16	0.28	0.11	0.03	0.01	0.003
3	32.1	87.5	152.3	0.16	0.01	0.01	0.03	0.01	0.005
	32.1	76.4	129	0.16	0.01	0.01	0.03	0.01	0.005
4	32.1	46.4	47.2	0.16	0.61	0.08	0.03	0.01	0.002
	32.1	46.8	48.5	0.16	0.59	0.12	0.03	0.004	0.011
5	31.7	38.6	69.6	0.279	0.027	0.01	0.095	0.001	0.061
	31.7	36.4	69.6	0.279	0.03	0.01	0.095	0.001	0.001
6	33.0	40	74.6	0.32	0.02	0.01	0.104	0.01	0.003
	33.0	42.7	55.5	0.32	0.03	0.01	0.104	0.002	0.001
7	33.0	100.5	123	0.32	0.01	0.01	0.104	0.005	0.005
	33.0	n.a.	133.4	0.32	n.a.	0.01	0.104	n.a.	0.005
8	33.0	35.7	56.8	0.32	0.02	0.018	0.104	0.002	0.001
	33.0	41.5	49.5	0.32	0.03	0.017	0.104	0.001	0.001
9	32.9	45.8	63.8	0.17	0.03	0.02	0.094	0.001	0.004
	32.9	41.9	69.5	0.17	0.03	0.02	0.094	0.001	0.004
10	32.9	148	175	0.17	0.01	0.02	0.094	0.009	0.004
	32.9	144	163	0.17	0.01	0.02	0.094	0.001	0.003
Ap1	31.7	33.1	32.9	0.279	0.093	0.03	0.095	0.001	0.001
	31.7	30.1	31.9	0.279	0.102	0.03	0.095	0.001	0.001

Note: precision for Ca, Mn and Zn is ± 0.01

In a 1 liter Erlenmeyer flask, a 35 g sample of slag (ID from 1 to 10) or apatite (ID Ap1) is shaken 48 h in 700 mL of WW solution (WW 1 or WW 3). Parameters are measured at time 0, 24 h and 48 h (pH, o-PO_4, F, Ca, Mn, Zn and Al).

Table A.3 : Individual batch tests results (tests in WW 3)

ID	**pH (-)**			**[o-PO_4] (mg P/L)**			**[F] (mg/L)**		
	t=0	**t=24h**	**t=48h**	**t=0**	**t=24h**	**t=48h**	**t=0**	**t=24h**	**t=48h**
1	5.7	6.8	8.3	101	67.6	11.1	31.1	22.7	13.8
	5.7	7.1	9.3	101	80	1.42	31.1	19.0	15.5
2	5.7	6.6	7.3	101	81.9	48.1	31.1	23.5	18.2
	5.7	6.7	7.3	101	81.8	46	31.1	23.7	18.1
3	5.6	6.6	11.2	113	94.1	0.022	32.1	25.8	20.7
	5.6	6.5	11.4	113	72	0.009	32.1	26.2	23.0
4	5.8	6.9	7.7	96.8	83.2	32	16.4	15.2	11.4
	5.8	6.9	7.5	96.8	83	41.6	16.4	15.0	11.8
5	5.7	6.7	7.1	101	85.8	61.2	31.1	24.6	21.1
	5.7	6.6	7.1	101	88.8	60.8	31.1	25.0	21.1
6	5.8	6.9	7.3	96.8	82.6	51.7	16.4	16.0	13.8
	5.8	6.9	7.6	96.8	82.4	32.6	16.4	15.3	14.8
7	5.6	7.6	11.0	115	25.5	0.131	29.9	19.4	22.3
	5.6	7.9	11.4	115	12.1	0.015	29.9	14.9	24.9
8	5.6	6.2	7.2	115	14.4	48.3	29.9	26.4	22.0
	5.6	6.2	7.1	115	109	44.9	29.9	26.3	23.0
9	5.6	6.2	7.3	115	108	38.3	29.9	26.4	23.5
	5.6	6.1	7.2	115	108	42.4	29.9	26.2	23.6
10	5.6	11.3	11.8	113	0.057	0.006	32.1	25.2	25.5
	5.6	11.1	11.7	113	0.01	0.005	32.1	23.6	25.2
Ap1	5.6	5.7	5.9	113	109	95.4	32.1	16.2	9.8
	5.6	5.6	5.7	113	104	97.2	32.1	16.0	9.5

Note: precision for pH and F is ± 0.1
Note: precision for P is ± 0.001 below 1 mg P/L, ±0.01 between 1 and 10 mg P/L, ± 0.1 between 10 and 100 mg P/L and ± 1 over 100 mg P/L

In a 1 liter Erlenmeyer flask, a 35 g sample of slag (ID from 1 to 10) or apatite (ID Ap1) is shaken 48 h in 700 mL of WW solution (WW 1 or WW 3). Parameters are measured at time 0, 24 h and 48 h (pH, o-PO_4, F, Ca, Mn, Zn and Al).

Table A.4 : Individual batch tests results (tests in WW 3)

ID	**[Ca] (mg/L)**			**[Mn] (mg/L)**			**[Zn] (mg/L)**			**[Al] (mg/L)**		
	t=0	**t=24h**	**t=48h**	**t=0**	**t=24h**	**t=48h**	**t=0**	**t=24h**	**t=48h**	**t=0**	**t=24h**	**t=48h**
1	150	145	78	1.08	0.79	0.02	2.96	0.042	0.019	2.98	0.1	0.14
	150	139	80.8	1.08	0.39	0.01	2.96	0.008	0.013	2.98	0.1	1.29
2	150	168	147	1.08	1.34	0.23	2.96	0.029	0.028	2.98	0.1	0.19
	150	174	153	1.08	1.37	0.19	2.96	0.021	0.018	2.98	0.1	0.14
3	201	210	188	0.73	0.55	0.02	0.321	0.001	0.001	0.8	0.1	0.1
	201	186	199	0.73	0.55	0.01	0.321	0.001	0.001	0.8	0.1	0.1
4	146	167	115	0.69	0.91	0.04	1.807	0.025	0.011	1.25	0.25	0.26
	146	165	126	0.69	0.9	0.05	1.807	0.015	0.001	1.25	0.25	0.1
5	150	166	150	1.08	0.76	0.11	2.96	0.027	0.015	2.98	0.11	0.17
	150	165	147	1.08	0.83	0.18	2.96	0.061	0.013	2.98	0.08	0.18
6	146	174	140	0.69	0.45	0.03	1.807	0.016	0.001	1.25	0.27	0.1
	146	171	121	0.69	0.44	0.05	1.807	0.009	0.001	1.25	0.29	0.1
7	199	142	187	0.78	0.09	0.74	0.251	0.001	0.001	0.94	0.1	0.4
	199	124	210	0.78	0.02	0.03	0.251	0.001	0.001	0.94	0.1	7
8	199	203	156	0.78	0.5	0.01	0.251	0.013	0.001	0.94	0.1	0.1
	199	204	161	0.78	0.72	0.23	0.251	0.017	0.001	0.94	0.1	0.1
9	199	206	158	0.78	0.75	0.29	0.251	0.05	0.001	0.94	0.1	0.1
	199	208	162	0.78	0.66	0.31	0.251	0.05	0.001	0.94	0.1	0.1
10	201	183	233	0.73	0.02	0.02	0.321	0.001	0.001	0.8	0.1	0.5
	201	168	228	0.73	0.02	0.01	0.321	0.001	0.009	0.8	0.1	0.79
Ap1	201	204	187	0.73	0.54	0.56	0.321	0.001	0.012	0.8	0.1	0.11
	201	190	182	0.73	0.58	0.59	0.321	0.033	0.017	0.8	0.4	0.22

Note: precision for Ca, Mn , Zn and Al is ± 0.01

APPENDIX B – RETENTION CAPACITY OF FILTERS

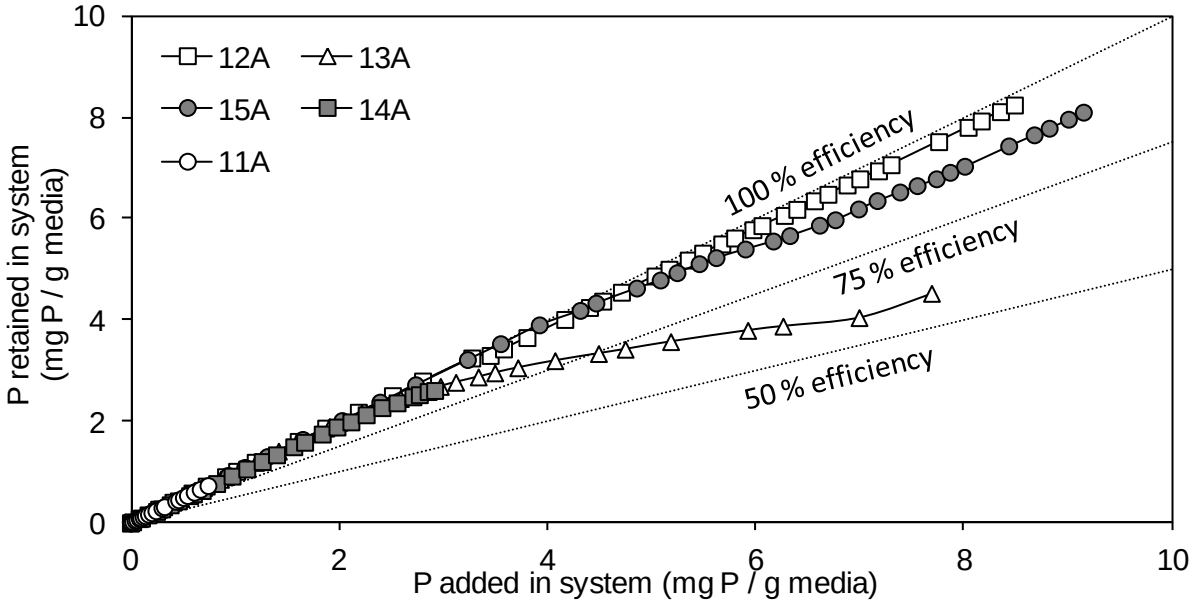

Figure B.1 : Phosphorus retention capacities of upstream filters (set 1 only)

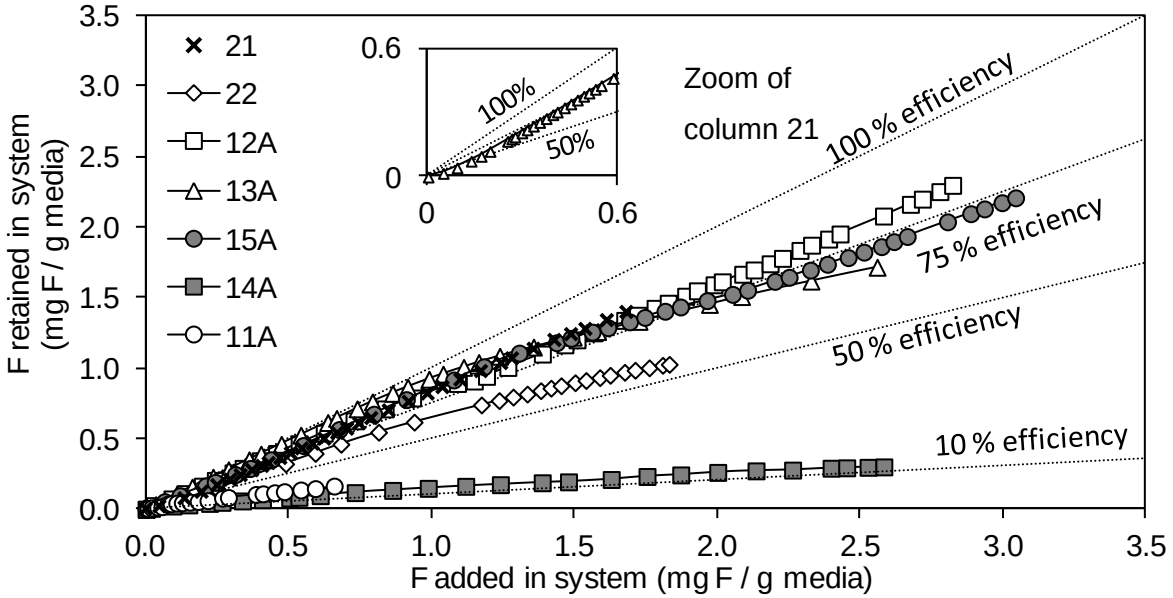

Figure B.2 : Fluoride retention capacities of upstream filters

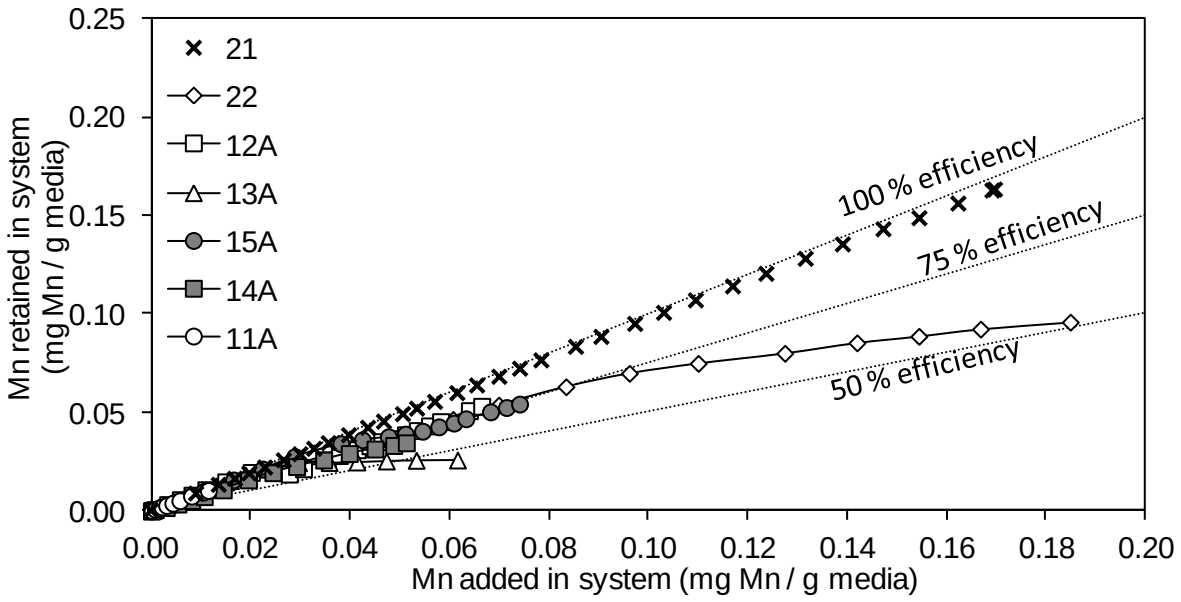

Figure B.3 : Manganese retention capacities of upstream filters

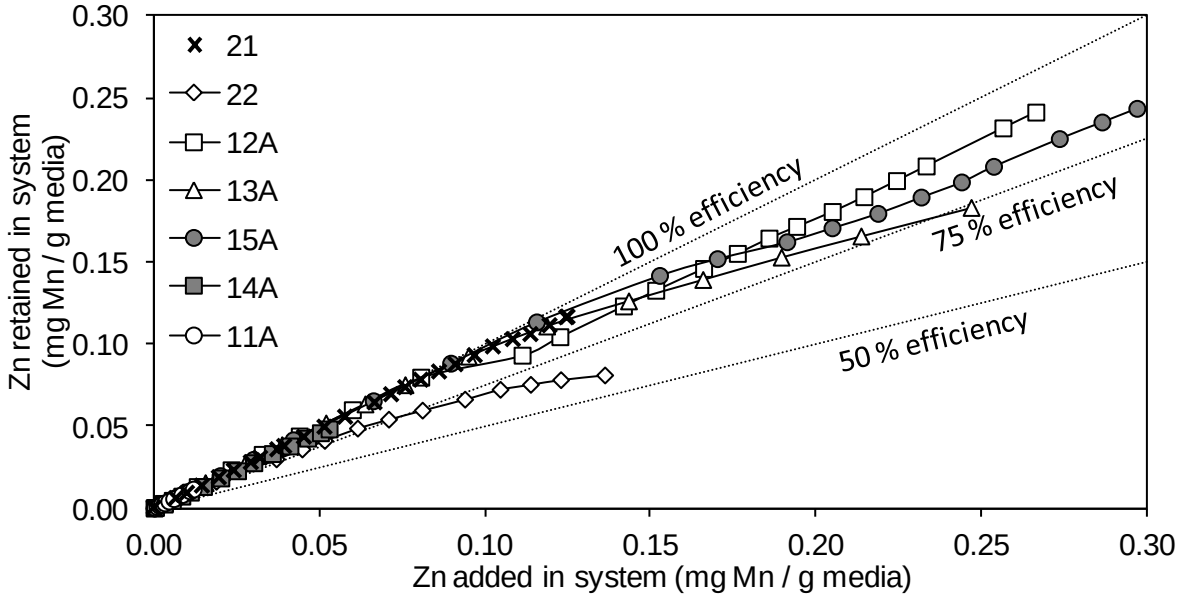

Figure B.4 : Zinc retention capacities of upstream filters

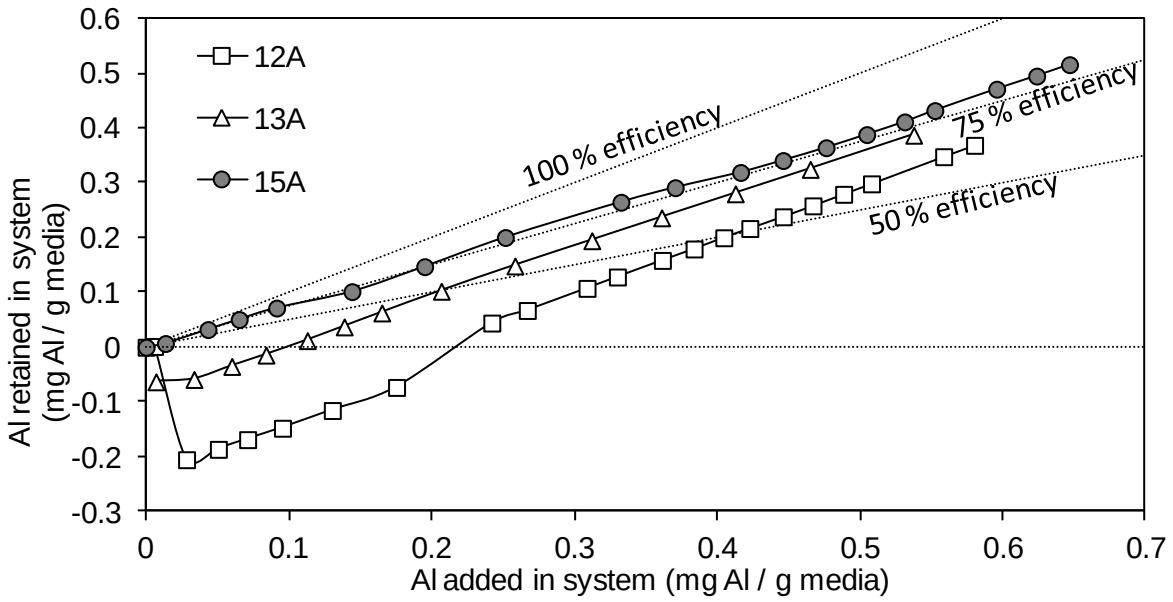

Figure B.5 : Aluminum retention capacities of upstream filters